EFFECT OF ELECTRODES MATERIAL ON THE DEGRADATION OF p-CRESOL IN ELECTROCHEMICAL PROCESS

BY

MUFID MAHMOUD ABU-EIDEH

A Thesis Presented to the

DEANSHIP OF GRADUATE STUDIES

KING FAHD UNIVERSITY OF PETROLEUM & MINERALS

DHAHRAN, SAUDI ARABIA

In Partial Fulfillment of the
Requirements for the Degree of

MASTER OF SCIENCE

In

CIVIL ENGINEERING

May 2010

KING FAHD UNIVERSITY OF PETROLEUM & MINERAL
DHAHRAN 31261, SAUDI ARABIA

DEANSHIP OF GRADUATE STUDIES

This thesis, written by **Mufid Mahmoud Abu-Eideh** under the direction of his thesis advisor and approved by his thesis committee, has been presented to and accepted by the Dean of Graduate Studies, in partial fulfillment of the requirements for the degree of **MASTER OF SCINCE IN CIVIL ENGINEERING.**

Thesis Committee:

Dr. Bukhari, A. A.
Chairman

Dr. Al-Malack, M. H.
Co-Chairman

Dr. Vohra, M. S.
Member

Dr. Al-Gahtani, H. J.
Chairman, Department of Civil Engineering

Dr. Al-Suwaiyan, M. S.
Member

Dr. Zummo, S. A.
Dean, College of Graduate Studies

Dr. Abu Zaid, N. S.
Member

16/6/10
Date

Dedication

I thank God, who helped me to complete this work by strengthening me in my efforts, knowledge, ability and pursuit. And I am thankful to my beloved mother and my wife who always enriched my good efforts with great support, and have been a powerful source of inspiration to me in my life, in general, and in my completing this thesis in particular.

ACKNOWLEDGEMENT

Acknowledgement is due to King Fahd University of Petroleum and Minerals for support of this research. I acknowledge, with deep gratitude and appreciation, the inspiration, encouragement, valuable time and guidance given to me by the Committee Chairman, Dr. Alaadin Al-Bukhari, whose expertise, knowledge, and patience, added considerably to my graduate experience. My special thanks are due to my Committee Members, Dr. Muhammad H. Al-Malack, Dr. Nabil Said Abu Zaid, Dr. M. S. Vohra, and Dr. M. Al-Suwaiyan for their kind help and guidance during this research work. I would also like to thank Dr. M. Balluch for his genuine support and guidance.

A word of thanks is inevitable to Dr. Muhammad H. Al-Malack, my Professor and Co-advisor, whose sincere advice, motivation and encouragement helped me to tackle many obstacles during my M. Sc. Program. I am deeply indebted to Dr. Husain Al-Gahtani, Chairman of the Civil Engineering Department for his continuous support and able guidance. Appreciation also goes out to Dr. Ahsan Shemsi, Mr. A. I hteram, Mr. T. Zaidi, Mr. H. Al-Muhnna, and Mr. Nazir of the Center for Environment & Water (Research Institute, KFUPM) for all of their laboratory and technical assistance throughout my research and graduate program. Special thanks to my colleagues at KFUPM, Mr. Bushra Osman Ibrahim, and Mr. A. Lattife for their continuous help and wonderful company and some memories that will last a lifetime.

Finally, I would also like to thank my family and Mr. Abdul-Rahman Alshaiji (Ameron Co., Saudi Arabia) for the support they provided me through my entire life and in particular for their great moral support during my study.

TABLE OF CONTENTS

Page

LIST OF TABLES

LIST OF FIGURES

THESIS ABSTRACT

TITLE OF STUDY: Effect of electrodes material on the degradation of p-Cresol in electrochemical processes.

MAJOR FIELD: Environmental Engineering

DATE OF DEGREE: May 2010

SUBMITTED BY: Mufid Mahmoud Abu-Eideh

Many researches have been conducted regarding the degradation of p-Cresol using electrochemical oxidation process, and that method has recently achieved considerable success. This is mainly due to its higher removal efficiency and lower cost compared to other treatment methods. However, the process has experienced some difficulties, mainly due performance of the electrode material used in the process. The main objective of this study is to investigate the degradation of p-Cresol in industrial wastewater by electrochemical process, using 4 types of electrodes (stainless steel, aluminum. Graphite and diamond), synthetic industrial wastewater was used on this study with deionized water as a base solvent. In final stage raw water used as base solvent of the synthetic wastewater to study the effect of the electrodes material on the process (one experiment for each electrode). And finally the polarization effect of the electrodes on the process was studied. A lab-scale experimental reactor was used to carry out the electrochemical oxidation of p-Cresol. The results showed that 20 mA/sq cm was found to be the optimum current realized in this Study, There were considerable difference among the electrodes in their effectiveness And performance, It was found that the highest removal of p-Cresol was achieved by Diamond, graphite, followed by stainless steel while aluminum electrode doesn't show Any removal. The optimum polarity time is 30 seconds, in addition polarization increases the removal percentage, and reduces time of treatment. It was found that the commercial aluminum electrodes is not suitable to remove p-Cresol. The findings of this study are expected to contribute in solving the p-Cresol degradation problem and enhancing the environmental efforts to remove p-Cresol from the Industrial wastewater.

ملخص الرسالة

الاسم :مفيد محمود حسن أبوعيدة
عنوان الرسالة : تأثير مواد ألأقطاب على أزآلة البارا كريسول بأستخدام طريق عملية الأكسدة الكهروكيميائية.
الدرجة : الماجستير
التخصص الرئيسى : الهندسة البيئية.
تاريخ التخرج : ما يو - 2010

أجريت العديد من الأبحاث العلمية لإزالة الباراكريسول باستخدام عملية الأكسدة الكهروكيميائية ، والتي حققت نجاحا كبيرا فى الآونة الأخيرة، ولكن مع ذلك النجاح الذى حققتة، فإن العملية واجهت بعض الصعوبات أهمها مادة القطب الكهربائي المستخدم في عملية إزالة الباراكريسول.

الأهداف الرئيسية لهذه الدراسة هي البحث عن تأثير أربعة أنواع من الأقطاب المختلفة من القرافيت والحديد المقاوم للصدأ والدايموند والألمنيوم على عملية أكسدة الباراكريسول باستخدام الأكسدة الكهروكيميائية. في هذه الدراسة ، تم إستخدم خلية كهروكيميائية بنطاق مختبرى للقيام بعملية الأكسدة الكهروكيميائية للباراكريسول.و من أهداف الدراسة البحث عن تأثير عملية عكس إتجاة التيار الكهربائي بين الأقطاب على أكسدة الباراكريسول وملاحظة أداء الأقطاب الأربعة عند استخدام المياة الخام بدلا من المياة المقطرة أثناء عملية الأكسدة.

أظهرت الدراسة أن أفضل أزالة للباراكريسول ذي تركيز 75 جزء في المليون كانت عند إستخدام تيار كهربائي بكثافة 20 مللي أمبير / سم مربع و 4000 جزء في المليون للمحلول الالكتروليتي (كلوريد الصوديوم) كانت للدايموند ومن ثم القرافيت ثم الحديد المقاوم للصدأ بينما لم تنجح أكسدة الباراكريسول عند إستخدام الألمنيوم, كما أظهرت الدراسة أن عملية عكس اتجاة التيار الكهربائي بين الأقطاب عند كل 30 ثانية عملت علي زيادة سرعة الأكسدة للباراكريسول. وعندما تم إستبدال المياة المقطرة بالمياة الخام لم تلاحظة أي تغيرات فعلية في عملية أكسدة الباراكرسول بأستخدام القرافيت وا لدايموند بينما تراجعت عملية إزالة الباراكرسول عند إستخدام اقطاب الحديد المقاوم للصدأ.
ومن المتوقع ان تسهم نتائج هذه الدراسة في حل مشكلة إزالة الباراكرسول، وتعزيز الجهود البيئية لإزالتة من مياه الصرف الصحي والصناعى.

ماجستير الهندسة
جامعة الملك فهد للبترول والمعادن
الظهران – المملكة العربية السعودية
مايو - 2010

CHAPTER 1

INTRODUCTION

Industries require constant improvement due to rigorous regulations and environmental laws, and enhancements in the current technologies. Exploration of new technologies and their various combinations with existing ones are studied therefore various types of effluents with contaminants such as p-Cresol. Phenolics compounds used widely in industry were over time intentionally or inadvertently released into the environment in large quantities. Widespread contamination of water by p-Cresol has been recognized as an issue of growing importance in recent years, and p-Cresol has been listed as a priority pollutant by the U.S. Environmental Protection Agency (EPA) (Lin and Tseng, 1999). Wastewater containing phenolics has malodorous odor, high toxicity, bioaccumulation carcinogenic potentials, is of considerable health concern, even at low concentration. As the accumulation of these aromatic compounds in the environment has become a serious problem, it is imperative to develop effective methods to remove these contaminants from effluents before their being discharge to the receiving environment (Cong et al., 2005).

Many technologies have been investigated for removing and degradation of organic compounds in wastewater. These include adsorption (Rengaraj et al., 2002),

biodegradation (Miland et al., 1996), UV/Fe+3 (Zhou et al., 2001), extraction by liquid membrane (Lin et al., 2004) and oxidation (Comninellis and Pulgarin, 1991; Tahar and Savall, 1998; Polcaro et al., 1999; Tahar and Savall, 1999, Awad and Abuzaid, 2000, Idris and Saed, 2003).

Recently, advanced oxidation processes (AOPs) have attracted the attention of many Researchers as they can be used to effectively treat wastewater containing organics (de Lucas et al., 2008, Zhang and George, 2005). Another common type of treatment method for degrading organics such as p-Cresol is the electrochemical method, which have been widely studied (Brillas et al., 1995; Tahar and Savall, 1998; Houk et al., 1998; Polcaro et al., 1999; Cong et al., 2004; Siddiqui, 2006).

Electrochemical oxidation has been applied to many kinds of wastewater (Naumczyk et al., 1996; Simonsson, 1997). It is presented as an effective, selective, economical, and clean alternative for dealing with wastewaters bearing high loads organic compounds. By means of electrochemical oxidation, pollutants in wastewater can be completely mineralized by electrolysis using high oxygen over-voltage anodes (Xuejun Chen et al., 2005).

Electrochemical oxidation reactions of organic species are a promising method for wastewater treatment (Houk, et al., 1998; Tahar and Savall, 1998; Brillas, et al., 1998). This technique depends mainly on the type of anode used (Vercesi, et al., 1991; Rao, et

al., 2001) but also on the properties of the wastewater (Rodrigo et.al, 2001, Wanga, et al., 2006).

The higher degradation of organic material in the initial phase that could not continue at later stages was attributed to a reaction taking place at the surface of the cathode that has a significant role in the electrochemical degradation process. It was suspected that this hindrance was due to gradual accumulation of high amount of salts present in the raw water used as the base of synthetic wastewater (Siddiqui, 2006). More research has been undertaken with the aim of gaining a better insight into this process and, consequently, to develop a less expensive application. These studies concluded that the electrochemical generation of oxidants used for the recovery or treatment of wastewaters from industrial plants by electrochemical oxidation processes is playing an ever increasing role due to their reliable operating conditions and ease of handling (Fryda et al., 2005).

The influence of operational parameters such as temperature, pH, initial substance concentration, current density, and electrode material on the performance of the electrochemical oxidation process was thoroughly investigated (Zhang and George, 2005).

The main objective of this study is to investigate the degradation of p-Cresol in industrial wastewater by electrochemical process, using four types of electrodes

(stainless steel, aluminum, graphite and diamond); Deionized water was used as a base solvent to prepare synthetic industrial wastewater. In the final stage, raw water was used to study the effect of the electrodes material on the process (one experiment for each electrode). Finally, the effect of electrodes polarization on the process was studied.

CHAPTER 2

LITERATURE REVIEW

The first part of this chapter discusses the composition, basic characteristics, uses, health hazards, environmental impact of the p-Cresol, treatment and analysis methods used for the p-Cresol degradation, and detection and quantification in order to establish background information about this pollutant. The rest of the chapter provides a short review and description for mechanisms of passivation of various electrodes investigated in this study.

2.1. P-CRESOL

Cresols are organic compounds which are methyl phenols. They are a widely occurring natural and manufactured group of aromatic organic compounds which are categorized as phenols' (sometimes called *phenolics*). Depending on the temperature, cresols can be solid or liquid because they have melting points not far from room temperature. Like other types of phenols, they are slowly oxidized by long exposure to air and the impurities often give cresols a yellowish to brownish red tint. Cresols have an odor characteristic similar to that of other simple phenols, reminiscent to some of a "medicine" smell.

In its chemical structure, a cresol molecule has a methyl group substituted onto the benzene ring of a phenol molecule. There are three forms of cresols that are slightly different in their

chemical structure: ortho-cresol (o-cresol), meta-cresol (m-cresol), and para-cresol (p-Cresol). These forms occur separately or as a mixture. The word tri-cresol can be used as a synonym for cresol where it means a mixture of o-, m- and p-Cresols.

P-Cresol is a natural product present in many foods, crude oil, and coal tar, and is also detected in animal and human urine. In addition to its industrial uses, p-Cresol is also used as an antiseptic and disinfectant because of its bactericidal and fungicidal properties. As a metabolite of toluene, p-Cresol is a known toxin associated with toxicity of its precursor mole (Wojnárovitset al., 2004). The term *p-Cresol* is usually used to describe any compound that contains a hydrocarbon derivative containing an (OH) and (CH3)group bound to an aromatic ring (see figure 2.1) (American Chemical Society, 2009). As reported by Arslan et al. (2005), p-Cresol is a class of organic compounds, (4-methylpHenol) with formula (CH3) C6H4 (OH).

2.1.1. BASIC CHARACTERISTICS

P-Cresol is colorless in pure form; or pinkish liquid. It has a burning taste and a distinct aromatic, acrid odor. It can be tasted and smelled at levels lower than those that are associated with harmful effects i.e. 0.004 milligrams per cubic meter (mg/m^3).(US Agency for Toxic Substances and Disease Registry, 2009).

Its molecular weight is 108.14 g/mol and its melting point and boiling point are 35.5 C and 201.9 C respectively. The commercial product is a liquid with relative

density (20 / 4 ° C) 1.0178 (1.0341), refractive index of 1.5312 (1.5395), flash point of 86.1 ° C (closed cup), self-ignition point of 559 ° C, limited solubility in water (1.9 g/100 ml), miscibility with alcohol, benzene, ether, glycerol, petroleum, and solubility in vegetable oils and glycol.

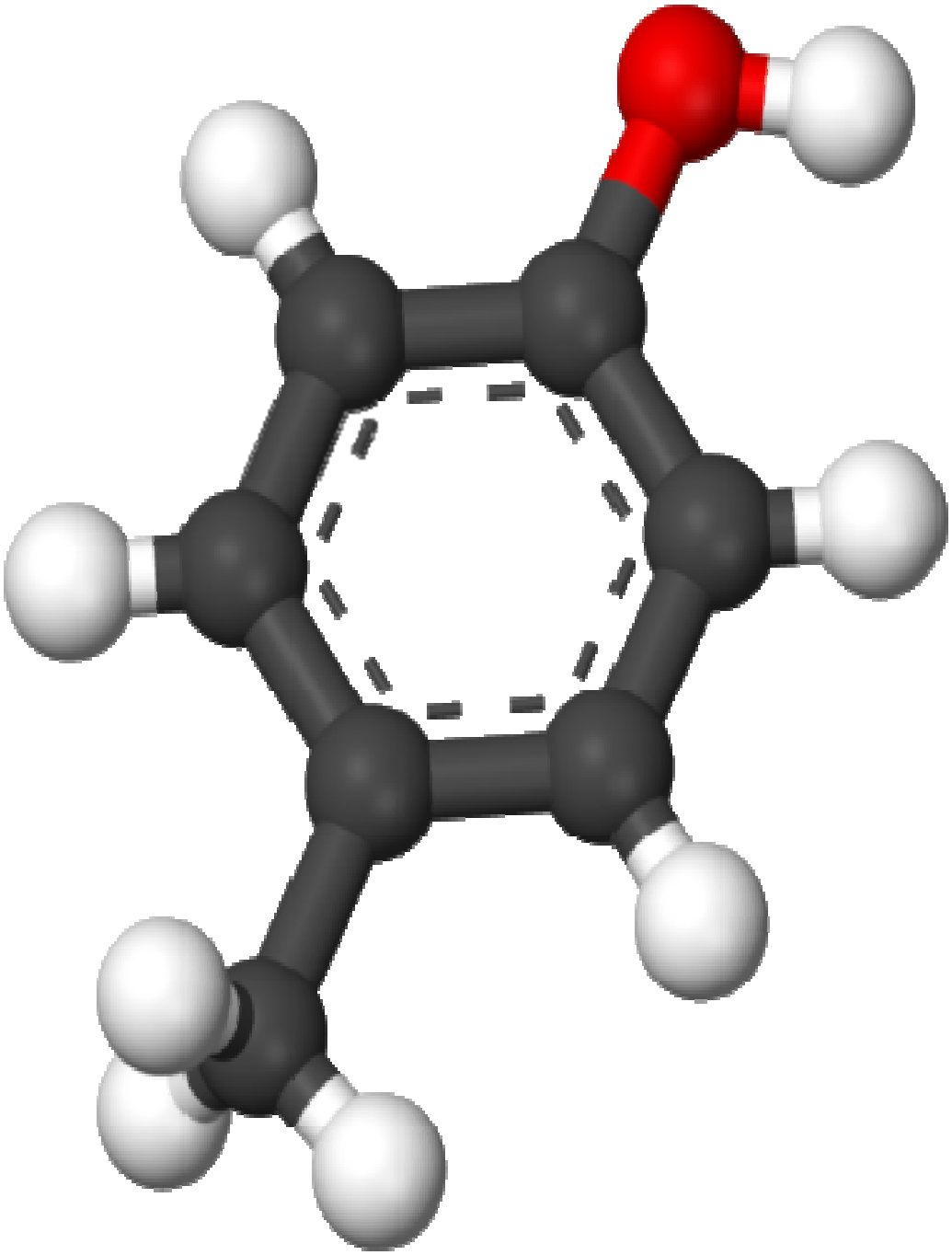

Figure (2.1): 3D Representation of P-Cresol Structure

In p-Cresol the OH radicals produced by water electrolysis attacked p-Cresol to form hydroxylated p-Cresol derivatives, that were then transformed into one-ring aromatic compounds. These compounds undergo ring breakage, which leads to the formation of aliphatic acids that are eventually mineralised by electrolysis to CO2. (Santos et al., 2006).

The OH radical induces oxidation of p-Cresol to p-methylphenoxyl radical (Wojnaravits and Foldik, 2004). P-Cresol shows much higher acidity; it even reacts with aqueous NaOH to lose H^+, whereas alipHatic alcohols do not. However, many carboxylic acids are more acidic than p-Cresol (McMurry, 2008 and Silva, 2009).

2.1.2. MAJOR SOURCES AND USES

Cresols are toxic to plants, animals, and humans. The major sources of cresols are wastewaters from oil refineries, petrochemicals, coal conversion plants, coal tar distillation and phenol-production industries, discharges pose significant threat to the environment. Cresol compounds (mixtures of the ortho-, meta- and para-isomers) can be obtained from coal tar and petroleum or synthesized by sulfonation or oxidation of toluene (HSDB, 1995). Crude cresol (commercial grade) contains approximately 20% o-cresol, 40% m-cresol, and 30% p cresol.

.

Cresols have a wide variety of uses including the manufacture of synthetic resins, tricresyl pHospHate, salicylaldehyde, coumarin, and herbicides. Cresols also serve as components of degreasing compounds in textile scouring and paintbrush cleaners as well as fumigants in pHotograpHic developers and explosives. Cresols also function as antiseptics, disinfectants, and parasiticides in veterinary medicine.

P-Cresol is found naturally in animal wastes and decomposition of organic wastes and also is obtained from coal tar or crude petroleum. It was first isolated in 1834 from coal tar and this remained the main source of p-Cresol until the First World War. The first synthetic method was then devised and all of the commercial p-Cresol today is synthetic (Harrison, 2009).

The primary use of p-Cresol is to sterilize as disinfectant, deodorizers, and pesticide cleaner. Its solution is used as a household cleaner for disinfection, and in construction, automotive, and appliance industries. Other uses of p-Cresol are in the manufacture of medicine and antiseptic. (US Agency for Toxic Substances and Disease Registry, 1998).

P-Cresols are frequently found in various industrial effluents and reported in hazardous waste sites. The major sources of phenolic wastes are oil refineries, coal gasification and liquification plants, chemical plants, resin and paint

industries. p-Cresol is also found in waste water and other compounds containing one or more hydroxyl groups attached to an aromatic ring.

As little as 0.002 milligrams per cubic meter (mg/m^3) of p-Cresol will impart objectionable taste and odors to drinking water. The exposure to p-Cresol is highly irritating to the skin, eyes, and mucous membranes in humans.

2.1.3. HEALTH HAZARDS

Brief exposure to 6 mg cresol/m3 resulted in irritation of the throat and nose, nasal constriction, and dryness in 8 of 10 subjects (Uzhdavini *et al.*, 1972). Chemical burns may result from exposure to cresols (Pegg and Campbell, 1985). The lungs of humans exposed to cresols have shown signs of empHysema, edema, bronchopneumonia, and small hemorrhages (Clayton and Clayton, 1982). Skin contact has resulted in the development of white patches and blistering, eventually turning brown or black (Lefaux, 1968). Other reported effects include turbidity, inflammation, and fatty degeneration of the liver, nepHritis, and hemorrhage of the epicardium and endocardium. Infant fatally which occurred at exposure ~20 ml of a 90% cresol solution dermally showed widespread edema of the internal organs, especially the brain and kidney (Green, 1975). The liver showed signs of centrilobular and midzonal necrosis.

Chronic systemic poisoning by any route of exposure may produce symptoms of vomiting, dyspHagia, salivation, diarrhea, loss of appetite, headache, fainting, dizziness, and mental disturbances (Sittig, 1981). Skin rash and discoloration may also result from prolonged or repeated exposure of the skin. Death may result from severe damage to the liver and kidneys. Ingestion of *p-Cresol* can cause death (Monma-Ohtaki et al., 2002), and acute exposure can lead to a number of toxic effects such as uremia (De Smet et al., 2003) and hepatotoxicity (Kamijo et al., 2003). Acute animal tests in rats, mice, and rabbits have shown p-Cresol to have high acute toxicity from oral exposure (U.S. Department of Health and Human Services, 2009). P-Cresol is among the list of priority organic pollutants proposed by the US Environmental Protection Agency "EPA" (Yan et al., 2006). EPA has established a provisional Reference Concentration for p-Cresol of 0.006 milligrams per cubic meter (mg/m^3) based on no effects in rats, mice, or monkeys. The provisional RfC is a value that has had some form of Agency review, but it does not appear on IRIS (US Environmental Protection Agency, 2009).

The World Health Organization (WHO) prescribed 1 μg/L as the maximum permissible concentration of total p-Cresol in drinking water. (Kumaran and Paruchuri, 1996; Nuhoglu and Yalcin, 2005). P-Cresol is toxic to aquatic organisms, however due to scarcity of exposure data, firm conclusions cannot be drawn with regard to the extent of the risk for either aquatic or terrestrial ecosystems (Zhang and George, 2005).

However, in view of the derived environmental concern level for water, it is reasonable to assume that aquatic organisms may be at risk in any surface or sea waters that are contaminated with p-Cresol (World Health Organization, 1994). Elimination of p-Cresol is, therefore, a necessity to preserve the environmental quality. Yet, p-Cresol is considered to be one of the major and most difficult pollutants in wastewater to be removed by water treatment processes.

2.1.4. TREATMENT METHODS

Cresols are extensively used in the manufacture of resin, sebacic acid, herbicide, pharmaceuticals, tricresylic acid, pesticides, and surfactants, Therefore, the removal of p-Cresol from wastewaters is of significant importance. The processes used for the removal of cresols from industrial effluents are classified into two types: destructive processes (that lead to the degradation of cresols, converting them into other compounds) and nondestructive processes (that allow the separation of cresols from the aqueous effluent and posterior recovery).

Methods used in destructive processes are incineration, electro chemical oxidation, thermal decomposition, photo-degradation, and anaerobic biodegradation. The methods used in non destructive processes are liquid-liquid

extraction, membrane separation, absorption, ion exchange, and mixed processes involving liquid-liquid extraction adsorption.

Treatment of wastewater containing high concentration of p-Cresol is difficult with traditional wastewater treatment methods that normally include a biological treatment step. Therefore, the most efficient way to treat p-Cresol is degrading it by a specific method directly at the point of discharge before sending it to a common wastewater treatment facility. The methods proved effective for this purpose are Fenton (Chedeville and Bayraktar, 2005), O_3/UV, O_3/H_2O_2, wet air oxidation and electro oxidation using Ti/SnO_2-Sb anode (Li et al., 2005).

Extensive research had been conducted to remove p-Cresol and its derivatives. Current treatment processes include carbon adsorption, solvent extraction, biodegradation, advanced oxidation and electrochemical processes. The selection of a proper treatment mainly depends on the treatment efficiency, reliability, ease of control and economics (Dane et al., 2007).

Carbon adsorption and solvent extraction can effectively remove p-Cresol from aqueous solutions, but the high cost of carbon regeneration and extraction solvent has hindered the large scale application (Azni et al., 2003).

Advanced oxidation processes (AOPs) include ultraviolet (UV) pHotolysis (Sun et al., 2006), direct ozonation (Staehelin et al., 1985), high-energy electron irradiation (Nickelson et al., 1993), supercritical oxidation (Krajnc et al., 1997; Thornton et al., 1992), and ultrasonification (Petrier et al., 1994). Over the past decade, another AOP utilizing a pulsed corona discharge in gas or liquid pHase has been used in removing and degrading organic contaminants from aqueous solutions (Clements et al., 1987; Joshi et al., 1995) in laboratory scale experimental setups. All of these advanced oxidation methods suffer high operational costs.

On the other hand, biological treatment methods are not quite as effective as anaerobic process, since it cannot effectively remove p-Cresol from the liquid pHase (Yan et al., 2007).

Electrochemical methods for water treatment have attracted wide attention and are recognized to be advantageous due to high efficiency, ease of control, and low costs (Zhang and George, 2005). The destruction of p-Cresol using electrochemical methods has been reported (Sathish et al., 2005).

The influence of operational parameters such as temperature, pH, initial substance concentration, current density, and electrode material on the performance of the electrochemical oxidation process was thoroughly investigated (Zhang and

George, 2005). Evaluation of reaction products, electrode fouling and current efficiency were also carried out (Zhang and George, 2005).

Recently, electrochemical oxidation has been intensively studied for the degradation of p-Cresol in aqueous solutions (Brillas et al., 1995; Tahar and Savall, 1998; Houk et al., 1998; Polcaro et al., 1999; Hayashi et al., 2003; Cong et al., 2004; Siddiqui, 2006).

In recent years, there has been increasing interest in developing electrochemical methods for purifying waters containing organic contaminants (Wang and Farrell, 2004). A relevant study was carried out to remove pHenol from simulated petrochemical wastewater using electrochemical treatment (Siddiqui, M., A., 2006). The degradation of pHenol was found to be considerably affected by the base solvent of simulated wastewater, the raw water, and electrode material. The study recommended investigating the effect of electrode material on the degradation of p-Cresol.

2.2. ELECTROCHEMICAL OXIDATION PROCESS

Many organic contaminants do not only give a characteristic taste and odor to water even at low concentrations, but also have bactericidal properties. So, treatment of wastewater

containing high concentration of organics is difficult with traditional wastewater treatment methods that commonly include a biological treatment step. Therefore, the most efficient way to treat organics is degrading them by a specific method directly at the point of discharge before sending the contaminants to a common wastewater treatment facility. The methods proved effective for this purpose are Fenton (Chedeville and Bayraktar, 2005), O_3/UV, O_3/H_2O_2, wet air oxidation and electro oxidation using Ti/SnO_2-Sb anode (Li et al., 2005).

Current treatment processes include carbon adsorption, solvent extraction, biodegradation, advanced oxidation and electrochemical processes. The selection of proper treatment mainly depends on the treatment efficiency, reliability, ease of control and economics (Dane, T., and Adalqisa, R. D., 2007).

Electrochemical methods for water treatment have attracted wide attention and recognized to be advantageous due to high efficiency, ease of control, and low costs (Zhang and George, 2005). The destruction of organics using electrochemical methods has been reported (Marappan Sathish and Ram Prasad Viswanath, 2005). The influence of operational parameters such as temperature, pH, initial substance concentration, current density, and electrode material on the performance of the electrochemical oxidation process has been thoroughly investigated (Zhang and George, 2005). Evaluation of reaction products, electrode fouling and current efficiency were also carried out (Zhang and George, 2005).

Electrochemical oxidation has been proven to be effective in water treatment, such as for drinking water supply for small or medium size communities (Jiang, 2002). Recently, rlectrochemical exidation has been studied for the degradation of p-Cresol in aqueous solutions (D, Rajkumar and K, Palanivelu, 2003).

In recent years, there has been increasing interest in developing electrochemical methods for purifying waters containing organic contaminants (Wang and Farrell , 2004). Electrochemical oxidation processes are expected to remediate the soluble pHase of pollutant. The method of electrochemical oxidation for treatment of the organics contained in wastewater has become a research focus in recent years because of its improved effects over traditional chemical, physical and biological methods. (Hongzhu Ma and Lin Gu, 2006).

The advantages of electro-oxidation include high particulate removal efficiency, compact treatment facility, relatively low cost, and possibility of complete automation. For elimination of organic contaminants from aqueous solutions by electrochemical oxidation at stainless steel oxide electrodes, which is usually used for wastewater treatment, electro-oxidation involves the generation of in-situ coagulants by electrically dissolving iron ions from electrodes (Chen, 2003). The metal ions generation takes place at the anode, while hydrogen gas is released from the cathode. The electrodes can be arranged in a mono-polar mode. A concise description of some types of electrochemical reactions

along with important side reactions expected to influence the removal mechanism, and the use of four types of electrode material will be discussed in the following sections.

2.2.1. SIMPLE REDOX REACTIONS

A simple redox reaction is one that involves a change in the electrical charge of a charge carrier, usually a simple or complex ion in the solution, by its taking away, an electron from the electrode (reduction), or its giving an electron to the electrode (oxidation). The same carrier may be present in solution in two states of charge. The higher, more positive charge is called the oxidized state, and the lower, less positive charge is called the reduced state (John et al., 2002).

For example, when ferric and ferrous ions are both present in solution in significant quantity, and when electron exchange with the electrode is sufficiently fast, redox equilibrium is established at the electrode, giving it a well-defined potential, or reversible redox potential (Encyclopædia Britannica, 2009).

2.2.2. REACTIONS THAT PRODUCE GASES

When hydrogen ions in solution react with electrons ejected from a metal, hydrogen atoms are formed at the surface, where they combine among themselves or with other hydrogen ions and electrons to give gaseous hydrogen molecules. If

all the reactions are fast enough, equilibrium is attained between hydrogen ions and gaseous hydrogen (Encyclopædia Britannica, 2009).

A metal in contact with solution at which such a situation exists is called the reversible hydrogen electrode, and its electrical potential is arbitrarily taken to be zero; every other electrode can thus be compared with it as it represents the basis for constituting the hydrogen scale of relative electrode potentials. Similarly, negative hydroxyl ions in solution (OH^-) can be made to give up electrons to a metal and, in a series of reactions; the final one is the formation of gaseous oxygen. Chlorine is another gaseous product; it evolves upon electrochemical oxidation of chloride ions in concentrated solutions of neutral and acid salts (Petrucci et al., 2004).

2.2.3. REACTION THAT DEPOSIT AND DISSOLVE METAL

When a metal ion is reduced and discharged as a neutral atom, or species, it tends to build into the metal lattice of the electrode. Thus, metals can be deposited at electrodes. Conversely, if electrons are taken away from the metal electrode by applying positive potentials to it, the metal ions thus formed can cross the double layer of electric charge at the interface, undergo hydration (combination with water), and enter the solution. The metal electrode thus dissolves. Many metals

establish well-defined electric potentials when they are in contact with their own ions in solution (Bard et al., 2008).

2.2.4 OXIDATION AND REDUCTION OF ORGANIC COMPOUNDS

A reaction of the oxidation and reduction of organic compounds can also occur at electrodes. Such reactions, however, are mostly irreversible in the literal sense that they lead to products that cannot easily be converted back into the original substance. Exceptions are some oxygen- and nitrogen-containing compounds (quinones, amines, and nitrous compounds) that can give fairly well-defined reversible potentials (McMurry, 2008).

2.2.5. STAINLESS STEEL ELECTRODES APPLICABILITY

The electrochemical oxidation technique depends mainly on the type of anode used (Vercesi et al., 1991; Rao et al., 2001) but also on the properties of the wastewater (Rodrigo et al., 2001; Wanga et al., 2006).

For elimination of p-Cresol from aqueous solutions by electrochemical oxidation at stainless steel oxide electrodes, which is commonly used for wastewater treatment, electro-oxidation involves the generation of an in-situ coagulants by electrically dissolving iron ions from electrodes (Chen, 2003). The metal ions

generation takes place at the anode, while hydrogen gas is released from the cathode.

The chemical reactions taking place at the anode are given as follows.

For iron

$$Fe - 2e \rightarrow Fe^{2+} \quad (2.1)$$

At alkaline conditions;

$$Fe^{2+} + 3OH^{-} \rightarrow Fe(OH) \quad (2.2)$$

At acidic conditions;

$$4Fe^{2+} + O_2 + 2H_2O \rightarrow 4Fe^{3+} + 4OH^{-} \quad (2.3)$$

In addition, there is oxygen evolution reaction;

$$2H_2O - 4e \rightarrow O_2 + 4H^{+} \quad (2.4)$$

The reaction at the cathode is;

$$2H_2O + 2e \rightarrow H_2 + 2OH^{-} \quad (2.5)$$

2.3. MECHANISM OF PASSIVATION

Under normal conditions of pH and oxygen concentration, passivation is seen in such materials as aluminum, iron, zinc, magnesium, copper, stainless steel, titanium, and silicon. Ordinary steel can form a passivating layer in alkali environments, as rebar does in concrete. The conditions necessary for passivation are recorded in Pourbaix diagrams.

The electrochemical passivation processes occur in some compounds, metals dissolving in solutions (chromates, molybdates) form non-reactive and low solubility films on metal surfaces.

2.3.1. STAINLESS STEEL PASSIVATION

Stainless steel has excellent characteristics of unique intensity, higher wear than other steels resistance, superior antiseptic property and not being apt to rust, etc. So it is widely used in the chemical industry, machinery for food industry, electromechanical industry, environmental protection industry, and domestic electric appliances industry. Three oxidation states of iron (0, +2 and +3) are represented on the figure (2.2) Pourbaix diagram. The stability regions for the oxidized iron states are shown only within the stability region of H2O equilibrium between species separated by vertical lines are dependent on pH only.

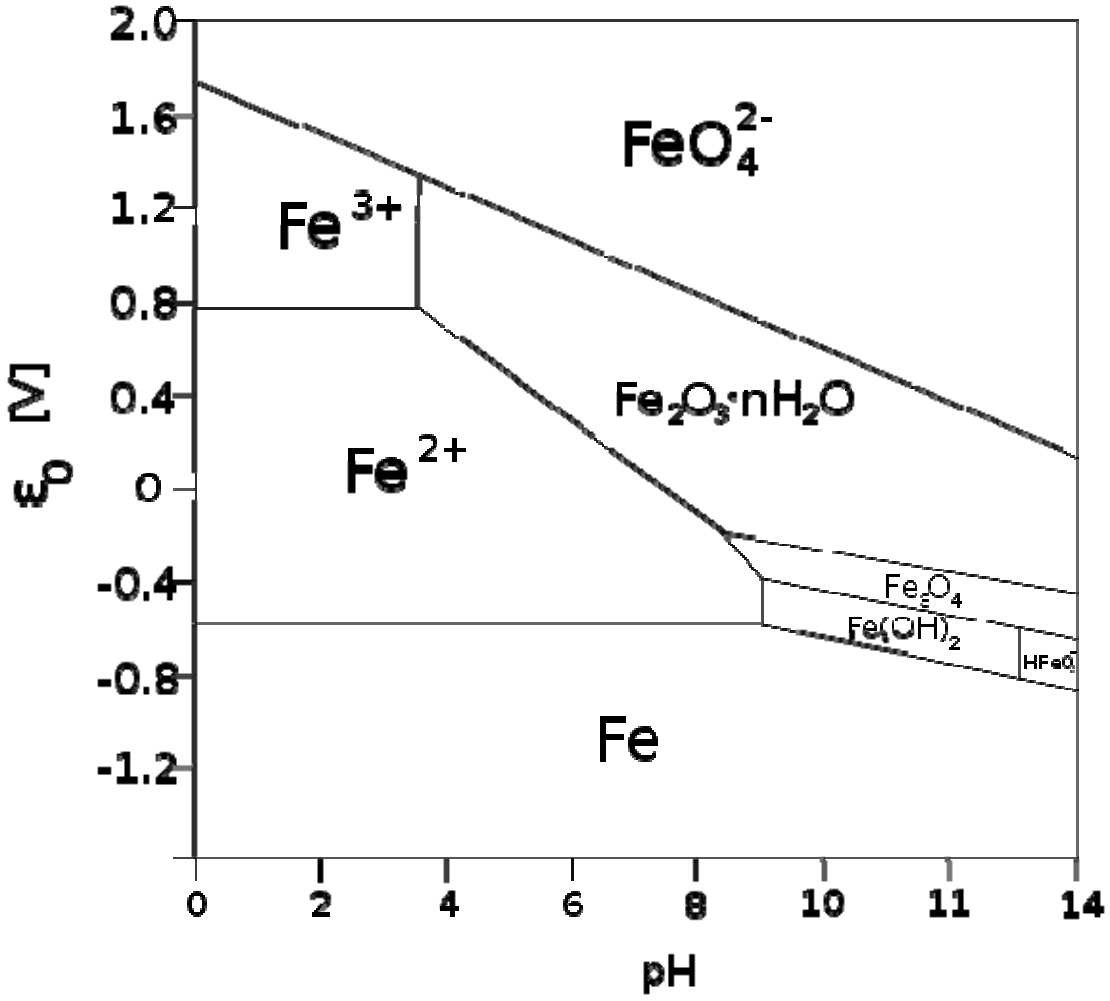

Figure (2.2): Pourbaix Diagram of Iron

2.3.2. ALUMINUM PASSIVATION

Aluminum is the 3rd most widely used element in the metal industry. Aluminum is a light weight metal with good ductility and mall ability. It is a good conductor of the electricity. Aluminum is susceptible to corrosive attack in atmospheric air as well from exposure to oxidizing agents. To prevent the unequal oxidation of the aluminum a process is adopted called Anodizing. Hard anodizing is forming a hard (thick) layer of the aluminum oxide over the surface. This prevents further oxidation.

2.3.3. GRAPHITE PASSIVATION

Graphite is a layered compound. In each layer, the carbon atoms are arranged in a hexagonal lattice with separation of 0.142 nm, and the distance between planes is 0.335 nm. (CRC Press, 2001) The two known forms of graphite, alpha (hexagonal) and beta (rhombohedral), have very similar physical properties (except that the grapheme layers stack slightly differently). (Cousins, 2003). The hexagonal graphite may be either flat or buckled. Another form called cubic may have also been discovered. Graphites that naturally occur have been found to contain up to 30% of the beta form, when synthetically-produced graphite only contains the alpha form. The alpha form can be converted to the beta form through mechanical treatment and the beta form reverts to the alpha form when it is heated above 1000 °C. The layering contributes to its lower density. The acoustic and thermal

properties of graphite are highly anisotropic, since phonons propagate very quickly along the tightly-bound planes, but are slower to travel from one plane to another.

Graphite can conduct electricity due to the vast electron delocalization within the carbon layers. These valence electrons are free to move, so are able to conduct electricity. However, the electricity is only conducted within the plane of the layers.

2.3.4. DIAMOND PASSIVATION

In mineralogy, diamond is the allotrope of carbon where the carbon atoms are arranged in an isometric-hex octahedral crystal lattice. After graphite, diamond is the second most stable form of carbon.

Other specialized applications for diamond also exist or are being developed, including its usage as semiconductors. Some blue diamonds are natural semiconductors, in contrast to most other diamonds, which are excellent electrical insulators. The conductivity and blue color originate from a boron impurity. Boron substitutes for carbon atoms in the diamond lattice, donating a hole into the valence band.

Substantial conductivity is commonly observed in nominally unduped diamond, grown by chemical vapor deposition. This conductivity is associated with hydrogen-related species adsorbed at the surface, and it can be removed by annealing or other surface treatments.

The electrochemical properties of diamond provide a wide range of applications due to the extreme electrochemical window (> 3V) for almost any reaction at the surface, before hydrogen forms at the cathode and oxygen at the anode. The chemical inertness of the diamond is another key factor offering the opportunity to use such electrodes (anodes as well as cathodes) in very aggressive media, thus increasing significantly their lifetime also in fluoridric media.

2.4. RAW WATER SPECIES

The raw water used in the final stage of this study is from a ground water source. Ground waters are usually of higher quality than surface sources. However, they can contain traces of agricultural chemicals and a few may contain toxic chemicals, which occur naturally in some aquifers. Even if the water leaves the source in a relatively clean state, it may get contaminated as it travels through pipes, which could be quite old. It is almost impossible for the water not to become contaminated by something undesirable (Arik, and Philippe, 2001).

2.5. EFFECT OF CHEMICAL SPECIES ON PASSIVATION PHENOMENA

The total dissolved solids present in raw water cause interference in the redox reactions occurring in the electrochemical oxidation process. The complex matrix of total dissolved solids present in raw water has a major role to play in efficiency of the organic degradation process. They also have impact on the removal of phenol when raw water is used as base solvent (Siddiqui, M., A., 2006).

The higher degradation of organic contaminants in the initial phase, that could not continue at later stages was attributed to a reaction taking place at the surface of the cathode that has a significant role in the electrochemical degradation process. It was suspected that this hindrance was due to gradual accumulation of a high amount of salts present in the raw water used as the base of synthetic wastewater (Siddiqui, M., A., 2006).

Later, it was found that the relatively higher removal of organic contaminants in the initial stage of experiments, which fails to persist during treatment for longer time periods, is not linked only to the coating formed on the cathode. It may be a complex reaction between chemical species of raw water and the ions released during electrolysis, that yields such results. The exact mechanism responsible for the observed results was proposed for further research (Siddiqui, M. A., 2006). In cases where the source of the raw water is ground water, the major cations that can be found are [Na^{+}], [Mg^{++}], and [Ca^{++}], and the anions are [SO_4^{--}] and [HCO_3^{-}].

Calcium (Ca^{2+}) and Magnesium (Mg^{2+}) salts are represented by calcium sulfate and magnesium sulfate, which are usually used in electrochemical processes as additional electrolytes to accelerate the ionization process (Pacheco and Lopes, 2007).

Generally, the Sodium (Na^{+}) species present in raw water are sodium chloride or sodium bicarbonate. Because of pH ranges that occur in natural waters, the alkalinity is usually found in the form of the bicarbonate ion, HCO_3^{-1}. In fact, at pH 7.5 or below, the bicarbonate ion is essentially the sources of all the alkalinity.

CHAPTER 3

OBJECTIVES

As discussed in the previous chapters, when electrochemical treatment was used to remove organic material from wastewaters such as p-Cresol, the degradation of organic material was found to be acutely affected by the types of electrode material. The chemical species present in the synthetic industrial wastewater may hinder the degradation process, as the salts of the chemical species (when raw or deionized water is used as base solvent) gradually accumulate on the electrode surface. The main objective of this study is to investigate the degradation of p-Cresol in industrial wastewater by electrochemical process, using 4 types of electrodes (stainless steel, aluminum, graphite and diamond electrodes). Synthetic industrial wastewater will be used on this study with deionized water as a base solvent. The specific objectives are:-

1. To identify the best type of electrode which can be used in industrial wastewater treatment and give the maximum removal of p-Cresol.
2. To investigate the effect of the electrode polarization on the process by introducing polarization instrument.
3. To optimize the current density, by investigate four levels of current density in order to maintain the optimum p-Cresol removal efficiency.
4. To investigate the effect of the electrodes material on the process when raw water is used as a base solvent.

CHAPTER 4

METHODOLOGY

This chapter discusses the apparatus, materials, methods, and analysis techniques used in this study to carry out the laboratory investigations required to achieve the objectives of this research.

4.1. PREPARATION OF SYNTHETIC WASTEWATER

The typical raw water characteristics mentioned in table 4.1 were used at final the stage of this study. Deionized water was used as a base solvent to prepare all combinations of p-Cresol.

4.2. LAB-SCALE EXPERIMENTAL SETUP

The experiments of the electrochemical oxidation for p-cresol were carried out in a reactor made of Plexiglas (flaker) with a volume of 1000 ml and filled with 750 ml solutions containing p-cresol and 4 g/L NaCl as the electrolyte. Four types of circular electrodes, graphite, diamond, stainless steel and aluminum of diameter 100 mm were used as both anode and cathode. The electrodes were connected to a DC power supply and polarization device, with galvanostatic operational options for controlling the current

density, a distance of 20 mm between anode and cathode was maintained for all the experiments, and a magnetic stirrer apparatus was used to mix the contents during experimental runs, as shown in Figure (4.1)

The typical raw water characteristics used at final stage to investigate the effect of the electrodes material on the processes shown in table (4.1.) below.

TABLE (4.1): CHARACTERISTICS OF RAW WATER AT KFUPM (BLD. 26)

Cation	Concentration(mg/l)
Na^{+}	585.62
K^{+}	47.18
Ca^{2+}	307.56
Mg^{2+}	92.74
Fe^{3+}	0.531
Anion	**Concentration(mg/l)**
HCO^{-}_{3}	1543.3
Cl^{-}	601.04
F^{-}	0.60
SO^{2-}_{4}	302
NO_{3}^{-}	2.79
Br^{-}	4.06
pH	7.45
Total Organic Carbon (TOC)	2.908
Total Dissolved Salts (TDS)	490.0

Sources: [l]Laboratory Tests (2009) the Center for Environment & Water, Research Institute, KFUPM

Note: The Total Alkalinity is represented as bicarbonate [HCO_3^-] because the pH is less than 7.5.

4.3. PREPARATION OF ELECTRODES

The anode and cathode were manufactured from same type of material. All electrodes were prepared with circular shape of diameter 100mm and had the same surface area. Commercial SS-316L and SS-304L stainless steel sheets were used to prepare the stainless steel electrode material with 2 mm thickness, commercial aluminum grade metals were used to prepare aluminum electrodes, diamond and graphite electrodes were procured commercially, also with 100mm diameter.

4.4. DESIGN OF EXPERIMENTS

There were three phases of experimental design, the first phase investigated optimizing the current density, the second phase investigated the polarity effect (current reversal) and the third phase investigated use of raw water with 4 types of electrodes.

In the first phase, 16 experiments with different settings were performed for optimizing current density by using 20, 15, 10 and 5 mA/cm2 Current density.

In the second phase, 12 experiments were conducted at four levels of polarity time (0, 30, 45, and 60 seconds).

In the third phase, four experiments were conducted to determine optimum removal current using raw water as base solvent with (NaCl) 4000 mg/L, for contact time 60 minutes. The initial concentration of p-Cresol was 75 ppm.

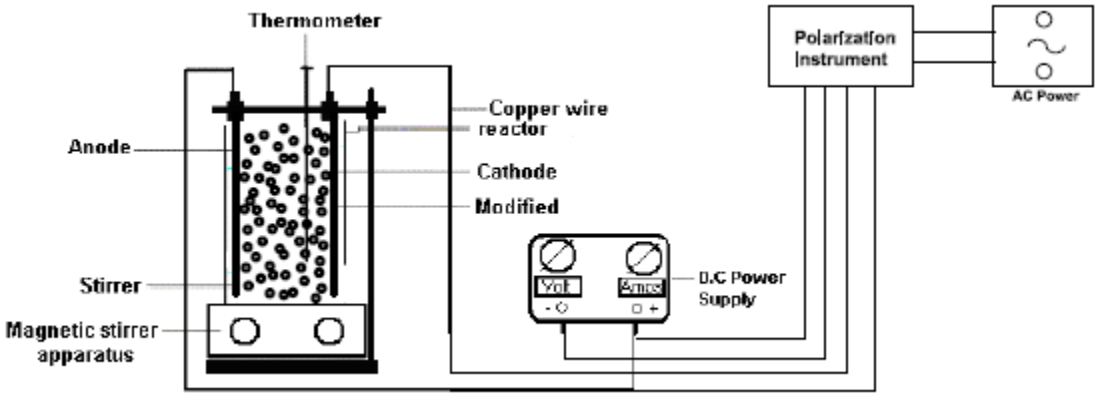

Figure (4.1): Schematic Illustration of Experimental Setup

TABLE (4.2): DESIGN OF EXPERIMENTS, DISSOLVED ELECTRODE

Exp. No.	p-Cresol (mg/l)	Current Density mA/cm^2	Contact Time (min)	NaCl Conc. (mg/l)
Stainless Steel Electrode Current Density Investigation				
DEIONIZED WATER AS BASE SOLVENT				
1	75	20	60	4000
2	75	15	60	4000
3	75	10	60	4000
4	75	5	60	4000
Aluminum Electrode Current Density Investigation				
DEIONIZED WATER AS BASE SOLVENT				
5	75	20	60	4000
6	75	15	60	4000
7	75	10	60	4000
8	75	5	60	4000

TABLE (4.3): DESIGN EXPERIMENTS: INERT ELECTRODES

Exp. No.	p-Cresol (mg/l)	Current Density mA/cm^2	Contact Time (min)	NaCl Conc. (mg/l)
GrapHite Electrode Current Density Investigation				
DEIONIZED WATER AS BASE SOLVENT				
9	**75**	**20**	**60**	**4000**
10	**75**	**15**	**60**	**4000**
11	**75**	**10**	**60**	**4000**
12	**75**	**5**	**60**	**4000**
Diamond Electrode Current Density Investigation				
DEIONIZED WATER AS BASE SOLVENT				
13	**75**	**20**	**60**	**4000**
14	**75**	**15**	**60**	**4000**
15	**75**	**10**	**60**	**4000**
16	**75**	**5**	**60**	**4000**

TABLE (4.4): DESIGN OF EXPERIMENTS, POLARITY STAINLESS STEEL ELECTRODE

Exp. No.	p-Cresol (mg/l)	Current Density mA/cm^2	Contact Time (min)	Polarization Period (sec)	NaCl Conc. (mg/l)
Stainless Steel Electrode Polarity Investigation					
DEIONIZED WATER AS BASE SOLVENT					
17	75	Opt.	60	0	4000
18	75	Opt.	60	30	4000
19	75	Opt.	60	45	4000
20	75	Opt.	60	60	4000

TABLE (4.5): DESIGN EXPERIMENTS, POLARITY ALUMINUM ELECTRODE

Exp. No.	p-Cresol (mg/l)	Current Density mA/cm^2	Contact Time (min)	Polarization Period (sec)	NaCl Conc. (mg/l)
Aluminum Electrode Polarity Investigation					
DEIONIZED WATER AS BASE SOLVENT					
21	**0**	**Opt.**	**60**	**0**	**4000**
22	**75**	**Opt.**	**60**	**30**	**4000**
23	**75**	**Opt.**	**60**	**45**	**4000**
24	**75**	**Opt.**	**60**	**60**	**4000**

TABLE (4.6): DESIGN OF EXPERIMENTS, POLARITY GRAPHITE ELECTRODE

Exp. No.	p-Cresol (mg/l)	Current Density mA/cm^2	Contact Time (min)	Polarization Period (sec)	NaCl Conc. (mg/l)
GrapHite Electrode Polarity Investigation					
DEIONIZED WATER AS BASE SOLVENT					
25	0	Opt.	60	0	4000
26	75	Opt.	60	30	4000
27	75	Opt.	60	45	4000
28	75	Opt.	60	60	4000

TABLE (4.7): DESIGN OF EXPERIMENTS, POLARITY DIAMOND ELECTRODE

Exp. No.	p-Cresol (mg/l)	Current Density mA/cm^2	Contact Time (min)	Polarization Period (sec)	NaCl Conc. (mg/l)
Diamond Electrode Polarity Investigation					
DEIONIZED WATER AS BASE SOLVENT					
29	0	Opt.	60	0	4000
30	75	Opt.	60	30	4000
31	75	Opt.	60	45	4000
32	75	Opt.	60	60	4000

TABLE (4.8): DESIGN OF EXPERIMENTS, ELECTRODES WITH RAW WATER

Exp. No.	p-Cresol (mg/l)	Current Density mA/cm^2	Contact Time (min)	Polarization Period (min)	NaCl Conc. (mg/l)
RAW WATER Effect on Each Electrode					
RAW WATER AS BASE SOLVENT					
33	75	Opt.	60	Opt.	4000
34	75	Opt.	60	Opt.	4000
35	75	Opt.	60	Opt.	4000
36	75	Opt.	60	Opt.	4000

4.5. SAMPLE COLLECTION

In all the experiments, nine samples were collected over a period of one hour at selected time intervals (0, 2, 5, 10, 15, 20, 30, 45, and 60 minutes).

4.6. TESTING OF CONTAMINANTS

Initially, a Shimadzu UV-Spectrophotometer was used to analyze the p-Cresol in the samples. Later, after some experiments in which color interferences happened, high performance liquid chromatography (HPLC) was employed. In addition, a scanning electron microscope was used to scan the surface of electrodes (aluminum / stainless steel). The following methods and apparatuses were used to analyze the treated samples.

4.6.1. UV-SPECTROPHOTOMETER

A Shimadzu UV-Spectrophotometer was used to detect the concentration of p-Cresol in the samples. The device was set in quantization mode; a calibration curve was generated from standard solutions of p-Cresol and used to calculate the concentrations of p-Cresol in the all samples; the peak at 270 nm was used for this purpose. More details about establishing the calibration curve are included in section 4.7. Only stainless steel and aluminum electrodes experiments were analyzed by this instrument. Due to color interferences, HPLC was used instead for other experiments.

4.6.2. HIGH PERFORMANCE LIQUID CHROMATOGRAPHY (HPLC)

The HPLC apparatus consisted of a waters 551 pump including an injector fitted with a 10 μL loop, and a chrome-A-scope rapid scanning UV-Diode Array Detector with computerized integration software. The column used was c-18-Reverse phase RP18; dimensions were 250 mmx4.6 mm packed with 5 – micrometer particles of econosil . The mobile phase was methanol with 0.02M sodium di-hydrogen orthophosphate (NaH_2 $PO_4.2H_2O$) buffer of pH 4 (48:52). The flow rate was 10 μL /min and the UV detection of 270 nm.

Under these conditions the column back pressure was 13.8 MP. The volume of the sample injected was 10 μL and running time for each sample was 12 minutes and p-cresol retention time varied between 8-10 minutes.

4.6.3. SCANNING ELECTRON MICROSCOPE

The scanning electron microscope (SEM) is a type of electron microscope that images the sample surface by scanning it with a high-energy beam of electrons in a Raster scan pattern. The electrons interact with the atoms that make up the sample producing signals that contain information about the sample's surface topography, composition and other properties such as electrical conductivity.

The scanning electron microscope was used to scan the surface of stainless steel and aluminum electrodes to investigate the causes of not removing p-Cresol and the deterioration of electrodes after use.

4.6.4. CHEMICAL OXYGEN DEMAND (COD)

Chemical oxygen demand (COD) was determined with Method 5220 C, Closed Reflux, Titrimetric method (Standard Methods for the Examination of Water and Wastewater, 19th edition 1995). This method was used to confirm the calibration curve of uv-spectrometer and to confirm the (HPLC) results of the water treated by graphite, diamond and stainless steel electrodes at optimum current density of 20 mA/cm^2.

4.7. STANDARD CURVE FOR P-CRESOL

Different concentrations of p-Cresol solutions were prepared for calibrating the UV-Vis spectrophotometer. The data are presented in Table A1 in the appendix for the calibration curve of P-Cresol (Figure 4.2). It is seen that the coefficient of determination, R^2, is 0.9981. This means the variability of the data is insignificant. This may occur because of the number of dilutions prepared for the standard solution. The equation of the best-fitted line is $Y = 0.01481X + 0.0306$. Here, Y is the absorbance and X is the concentration of p-Cresol in (mg/l) . Chemical oxygen demand COD test also was

examined for the same samples (dilutions) to confirm the quality of the calibration curve of p-Cresol (Figure 4.2).

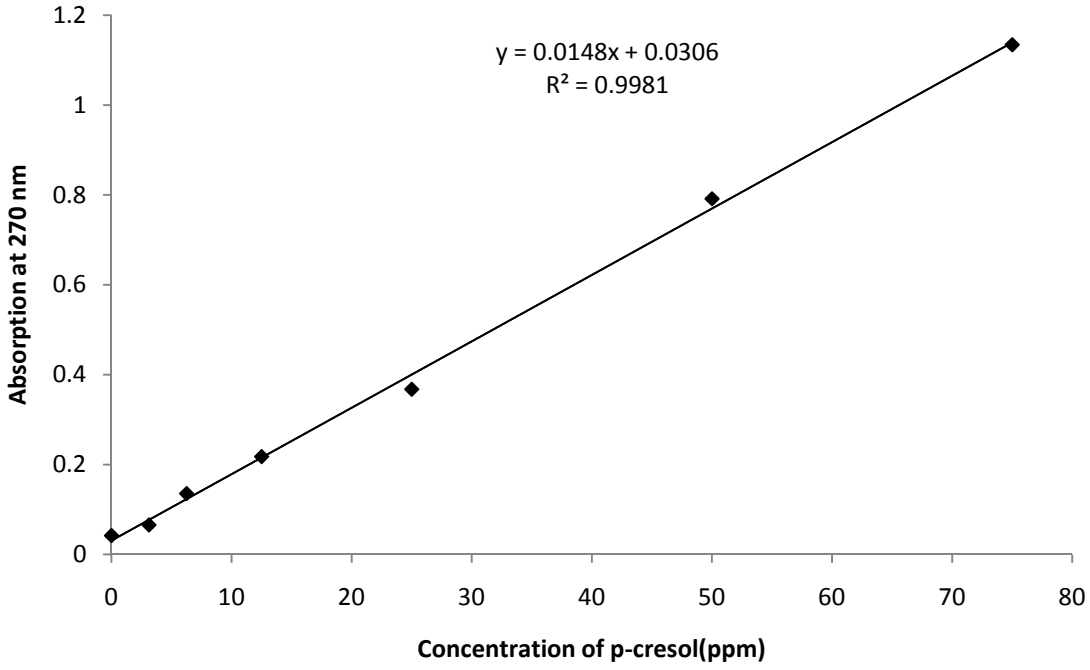

Figure (4.2): Standard Curve for p-Cresol at 270 nm

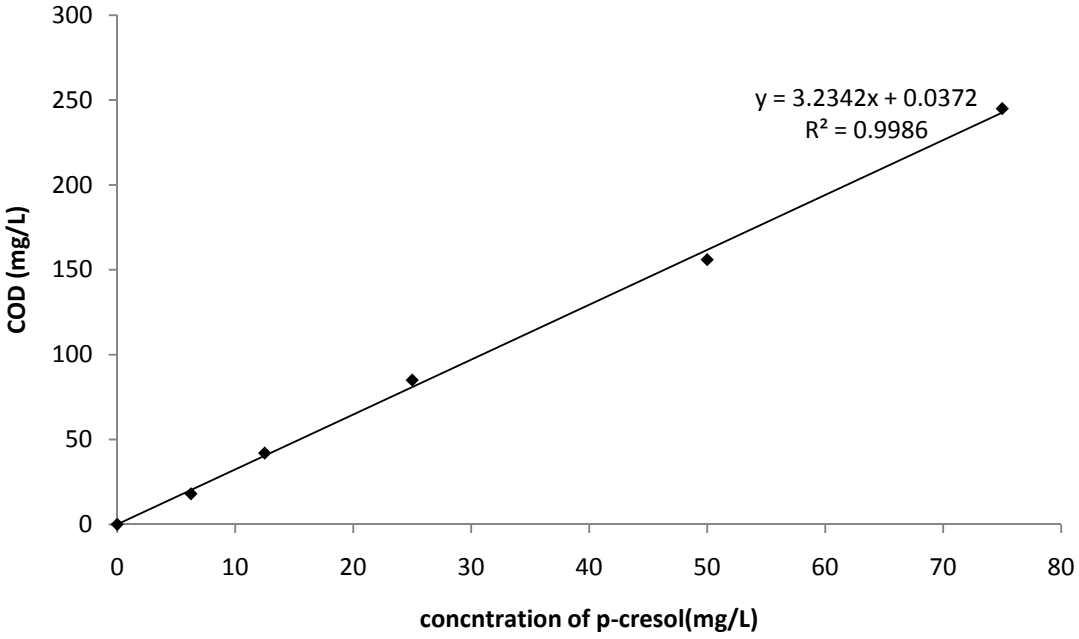

Figure (4.3): Chemical Oxygen Demand (COD) Curve for p-Cresol

CHAPTER 5

RESULTS AND DISCUSSION

5.1. INTERFERENCES IN P-CRESOL ANALYSIS

In the first phase of the study to investigate the optimum current removal of p-Cresol, four experiment for each metal electrode (stainless steel and aluminum) were conducted at 20 ,15,10 and 5 mA/cm2 .The UV-spectrophotometer was used to analyze the treated samples. The results of the analysis are shown in the Appendix. (Tables A4 to A12).

The UV-spectrophotometer apparatus reads substantial values of absorbance along with the color interference at 270 nm wavelength. Therefore it is impossible to identify the amount of p-Cresol in a treated sample due to the color interference.

Table A4 to A12 shows the presence of absorbance for treated samples. Some of the treated samples have an absorbance higher than the reference sample, due to the color interference. Due to the drawback of color interference in the UV-spectrophotometer meter, high performance liquid chromatography was employed to analyze all samples in this study.

This study confirms that the UV-Spectrophotometer does not qualify to quantify the p-Cresol due to color interference. The standard calibration curve of p-Cresol analyzed by (HPLC) is shown in (Figure 5.1). The equation of the best-fitted line is Y = 4709.8X + 802.62. Here Y is the area under the chromatogram of p-Cresol in (microvolt ampere/cm2) and X is the concentration of p-Cresol in (mg/l) and R^2 is 0.999.

.

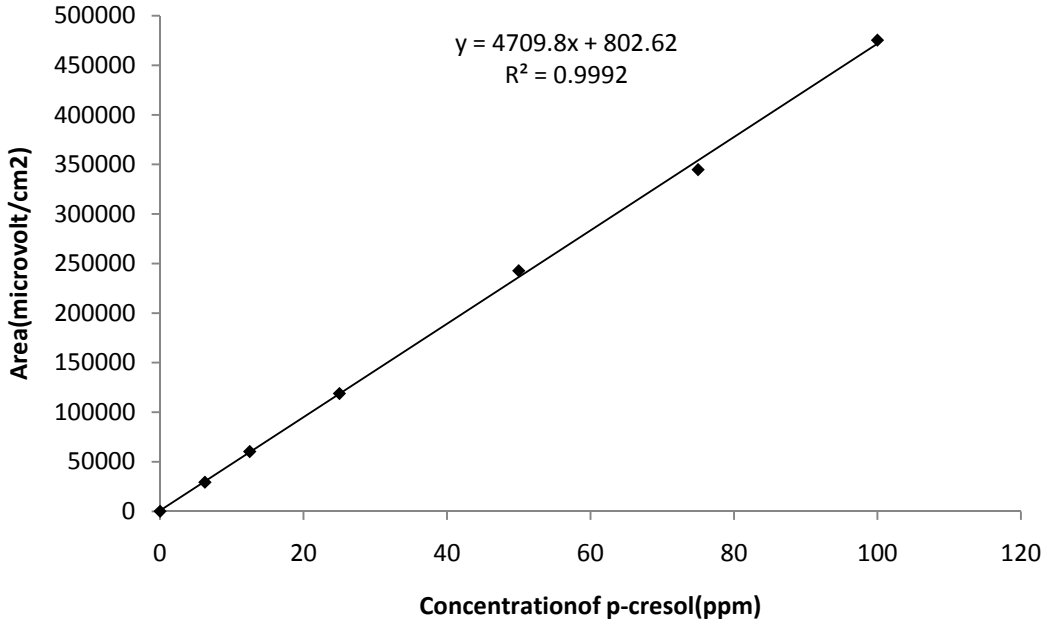

Figure (5.1): (HPLC) Calibration Curve for p-Cresol

5.2. CURRENT DENSITY INVESTIGATION FOR p-Cresol

In this investigation, it was confirmed that the current density considerably affects the p-Cresol degradation process when different current densities were used. Four experiments were performed to identify the optimum current density of each electrode for p-Cresol removal. During these experiments, initial concentration were 75 mg/l for the p-Cresol and optimum electrolyte of 4000mg/l for electrolyte ,different current densities, i.e. 20, 15.10 and 5 mA/cm^2were used .

A control experiment was conducted for each test in this investigation (for more details see tables A28 to A37 and figures A29 to A39 in the appendix). The results show that the optimum p-Cresol removal was observed at 20 mA/cm^2 current density (figure 5.8). The figure shows that as the current density increased, p-cresol oxidation increased except for the aluminum electrode. The increase in p-cresol oxidation can be attributed to the fact that more current density results in more ionization in the water matrix, which leads to more reactions and, consequently, more p-cresol conversion.

In this investigation, it was proven that the material used for electrodes significantly affect the p-Cresol degradation in the electrochemical oxidation process when synthetic refinery and petrochemical wastewater are used with different electrodes and different current densities ranging from 5 mA/cm^2 to 20 mA/cm^2.

5.2.1. CURRENT INVESTIGATION OF GRAPHITE ELECTRODE

Four experiments were conducted by using graphite anode & graphite cathode. Current densities were 20, 15, 10 and 5 mA/cm^2. The residual of p-cresol decreased gradually at 20ma/cm2 current density and complete removal of p-cresol achieved at 20 minutes, while at 15mA/cm2 it took 30 minutes, at10 mA/cm2 it needed 60minutes and finally at 5 mA/cm2, the residual of p-cresol is 30.7% at 60 minutes interval time. (Please refer Fig.5.2) below. For further details refer (Appendix Table A12.).Aluminum electrode didn't show any removal for p-cresol. The increase in p-cresol oxidation can be attributed to the fact that more current density results in more ionization in the water matrix, which leads to more reactions and consequently, more p-cresol conversion. It is noted from the study that the increase in current density had increased the percent of p-cresol removal and decreased the time of treatment required.

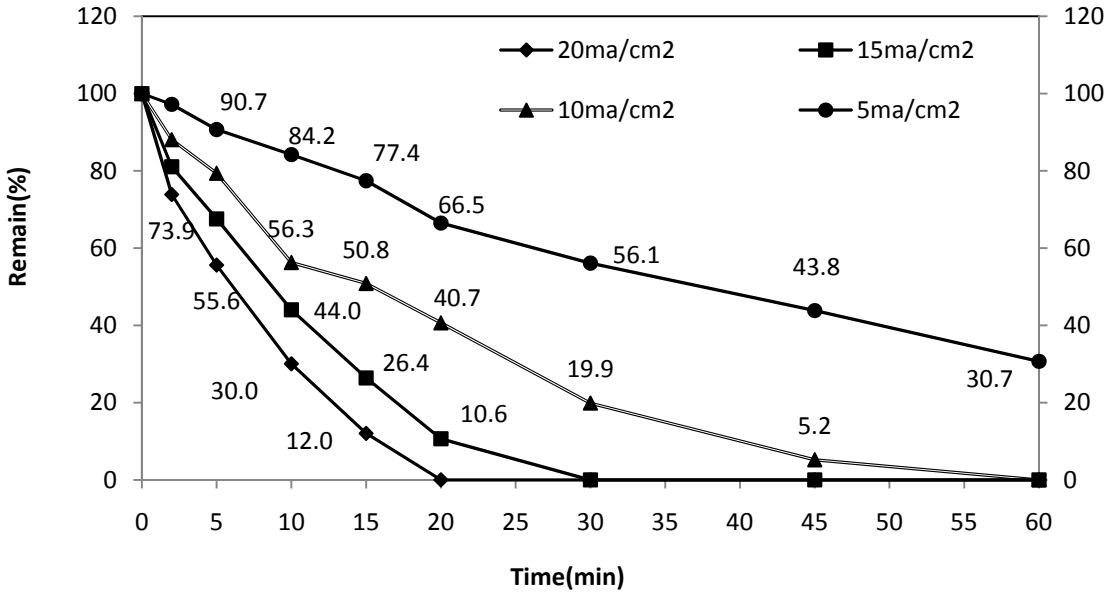

Figure (5.2): Effect of current density by using graphite electrode on the degradation of p-Cresol at 75 ppm initial concentration and a current density of 20, 15, 10, and 5mA/cm^2

5.2.2. CURRENT INVESTIGATION OF DIAMOND ELECTRODE

Four experiments were conducted by using Diamond anode and Cathode. Current densities were 20, 15, 10, and 5 mA/cm^2. The residual of p-cresol decreased sharply at $20ma/cm^2$ current density until disappear completely at 10 minutes, while at $15mA/cm^2$ it took 15 minutes, at 10 mA/cm^2 it needed 20 minutes and finally at 5 mA/cm^2, the removal was achieved in 30 minutes. (Please refer Fig.5.3) below. For further details refer Appendix Table A13.

The reason for high efficiency removal by diamond electrode is attributed to its important characteristics such as, an inert surface with low adsorption properties, remarkable corrosion stability even in strong acidic media, an extremely wide potential window in aqueous and non-aqueous electrolytes, andthe efficient production of hydroxyl radicals at the diamond electrodes' surface. That is why oxidation of organic contaminations in water can be removed to a well defined level.

From the study it is realized that the increase in current density had increased the percent of p-cresol removal and decreased the time of treatment; optimum removal is observed at $20mA/cm^2$.

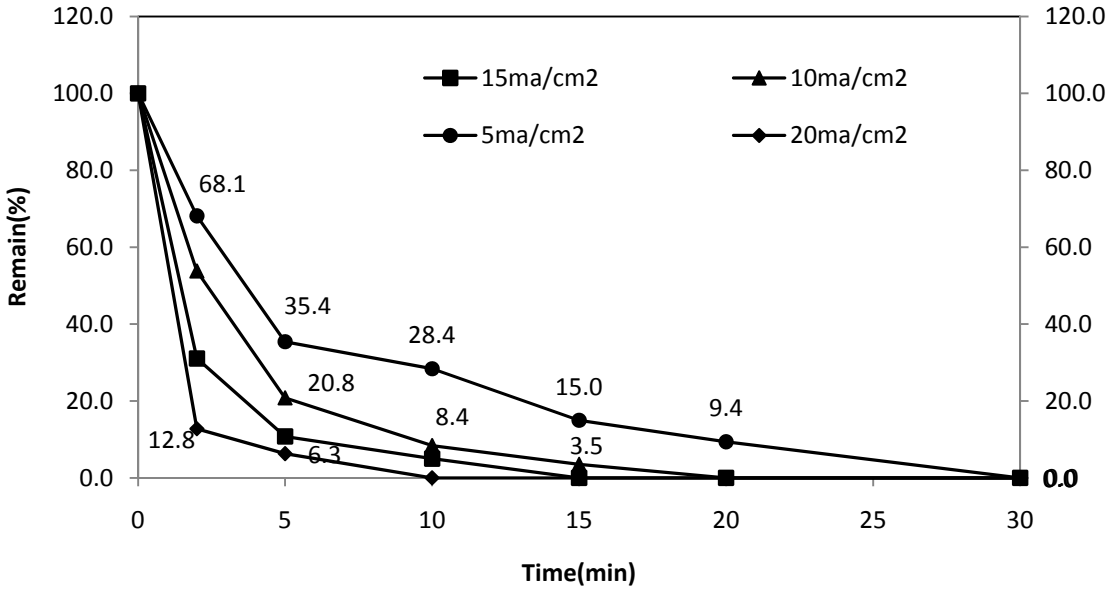

Figure (5.3): Effect of current density on the degradation of p-Cresol by using diamond electrodes at 75 ppm initial concentration and a current density of 20, 15, 10, and 5 mA/cm^2

5.2.3. CURRENT INVESTIGATION OF STAINLESS STEEL ELECTRODE

Four experiments were conducted by using Stainless Steel anode and Cathode. Current densities were 20, 15, 10, and 5 mA/cm^2. The residual of p-cresol decreased sharply at 20 mA/cm^2 current density and 4.2% residual of p-cresol achieved at 60 minutes, while at 15 mA/cm^2 it took 60 minutes to have residual of 58.3% of p-cresol. At 10 mA/cm^2 it needed 60 minutes to have residual of 63.9% of p-cresol and finally at 5 mA/cm^2, 72% of residual was achieved in 60 minutes. Please refer Figure (5.4) below. For further details refer Appendix Table A14. As noticed in figure (5.4) for the current density 20ma/cm2, the residual of p-cresol at 20 minutes interval time is 0.5%, then there is slow incremental reduction in percentage of residual p-cresol, this could be attributed to a metal transition phenomenon since the active stainless steel electrodes are considered precipitating electrodes and in this case metals such as chromium and nickel will migrate from the electrode surface to the water matrix, and this might lead to reduction in oxidation and formation of reversible reactions in the water matrix. From the study it is realized that the increase in current density had increased the percent of p-cresol removal, optimum of which in observed to be at $20mA/cm^2$.

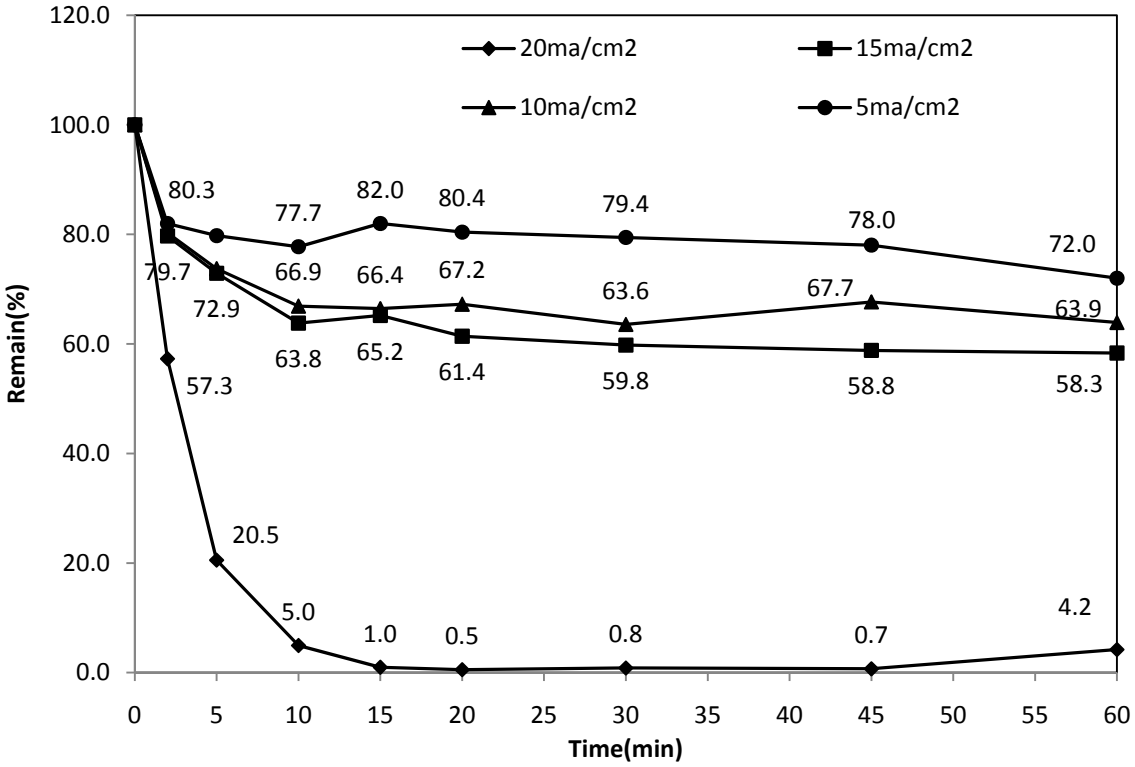

Figure (5.4): Effect of current densities on the degradation of p-Cresol by using stain less steel electrode at initial concentration 75mg/l and a current densities of 20, 15, 10 and 5 mA/cm^2

5.2.3.1. Effect of Stainless Steel Material on P-Cresol Degradation.

As it was noticed in section (5.2.3) there were no much removal for p-Cresol by using stainless steel (SS-316L) specially current dencities (15,10,and 5 mA/cm2) ,so its decided to use another type of stainless steel (SS-304L) and make comparison between the two type of stainless steel. It's known that stainless steel is considered as precipitating electrodes, they take a part in the reaction within the water matrix. So, it was important to study removal efficiency of the two types of the stainless steel electrodes. Table (5.1) below presents chemical composition of two types of stainless steel used in the study. The result of experiments shows that at current density of 15 mA/cm2 and p-Cresol Concentration of 75 ppm, the residual after treatment by SS-304L is lower than SS-316L. As shown below figure (5-5) the remaining of p-Cresol after 60 minutes of treatment with (SS-316L) is 58.3%, while for SS-304L the remaining was 32.7%. Such results are attributed to the difference in composition of these two materials, From the composition of the two materials it is noticed that SS-316L, is more resistant to corrosion than SS-304L, since it has higher percentage in, nickel, chromum and molybdenum., That's why using material which has properties of less resistant to corrosion may give high percentage removal of p-Cresol, the reason for that could attributed to the fact of formation of passivation film, this film is thicker in material

resistant to corrosion and due to this film the reaction on the electrode surfaces (oxidation and reduction) could be prevented or slow down. For further details refer Appendix Table A15.

TABLE (5.1): COMPOSITION STAINLESS STEEL SS-304LAND SS-316L

SS-Type	Cr%	Ni%	C%	Mn%	Si%	P%	S%	N%	Others
SS-3o4L	18-20	8-12	0.03	2	0.75	0.05	0.03	0.1	0
SS-316L	16-18	10-14	0.03	2	0.75	0.05	0.03	0.1	MO (2-3%)

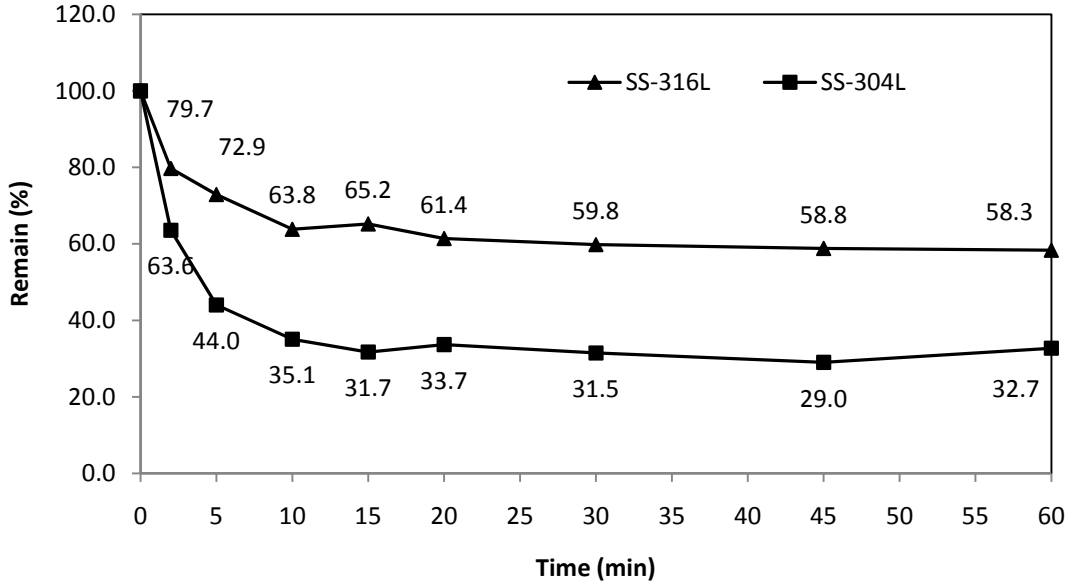

Figure (5.5): Effect of stainless steel material type on the degradation of p-Cresol with initial concentration of 75 ppm and current density of 15 mA/cm²

5.2.3.2. Stainless Steel Electrode Degradation.

Five experiments were conducted on one stainless steel anode (SS-304- L) to investigate the deterioration of the anode by continues usage of same electrode .After each experiment, the anode is completely cleaned by sand paper and water mixed with detergents, then rinsed by deionized water. It was founded that after 5 hours running in treatment of p-Cresol, the anode loses completely its efficiency and the removal of p-Cresol becomes negligible. As shown below in figure (5-6) , in the first experiment the remaining of p-Cresol after one hour of treatment was 64.5 % , in the third experiment, the remaining of p-Cresol was 88.3% ,while in the fifth experiment the remaining p-Cresol was 99.3 % which means no removal happened at the end of the fifth hour from usage of the same electrode. For further information refer to table (A16) in the appendix. This may be attributed to the metal transition phenomenon since active stainless steel electrodes (precipitating electrodes) were used. In this case, metals such as nickel and chromium will migrate from the stainless steel electrodes to the water matrix.

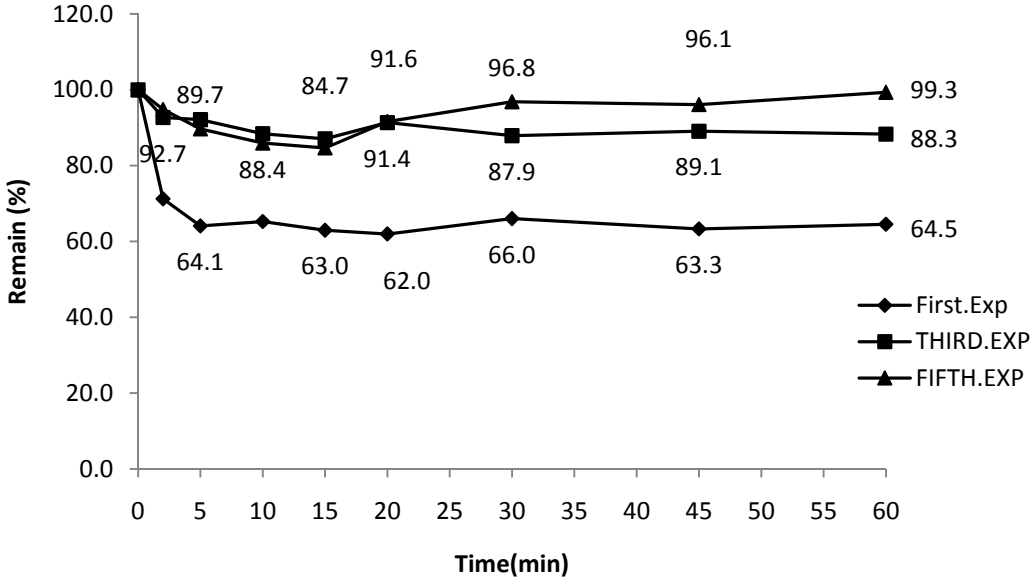

ff

Figure (5.6): Remaining percentage of p-Cresol vs. time after treatment of p-Cresol with same anode of stainless steel SS-304-L initial concentration 75 ppm at current density of 15mA/cm2

5.2.4. CURRENT INVESTIGATION OF ALUMINUM ELECTRODE

Four experiments were conducted at 20, 15, 10, and 5 mA/cm^2 using an aluminum electrode (commercial grade) were used to remove p-Cresol from deionized water. Concentration of p-Cresol was 75 ppm and sodium chloride used was 4 g/L.

In all these experiments as shown below in Figure (5.7), zero removal was achieved for the p-Cresol after 60 minutes of treatment. For further information please refer to table A17 in the appendix.

The reason behind that could be the formation of thick oxidation film during treatment process. The result of scanning electron microscope in section (5.2.6.1) shows such formation of oxide film.

Based on aforementioned results it was decided to exclude the aluminum electrode from the further investigation in this study.

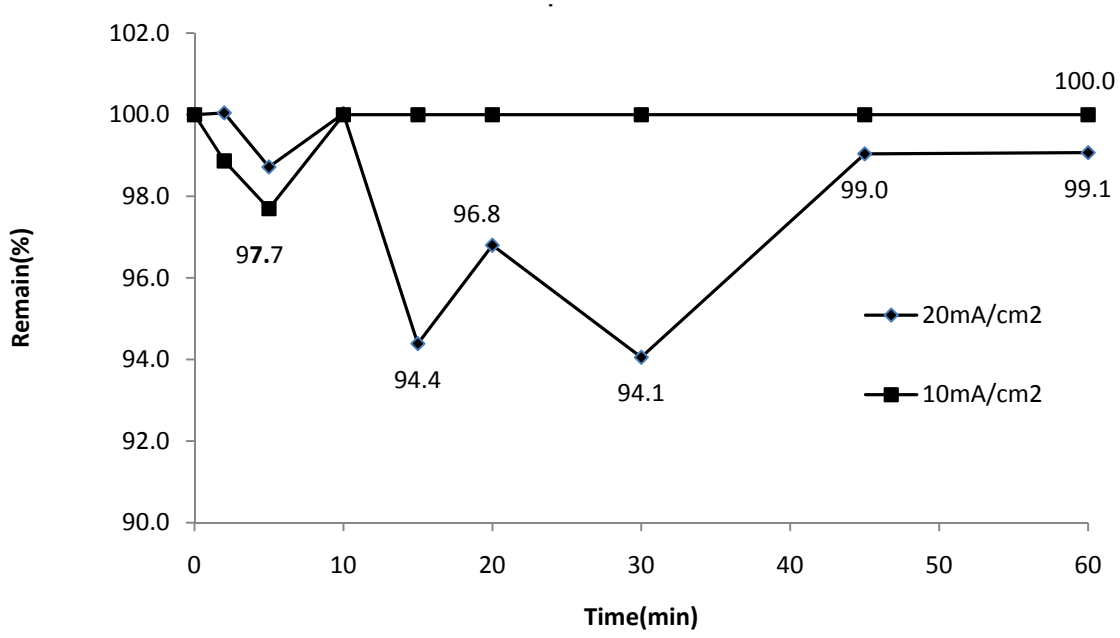

Figure (5.7): Effect of aluminum electrode on the degradation of p-Cresol with initial concentration of 75 ppm and current densities 20, and 10 ma/cm2

5.2.5. COMPARISON BETWEEN OPTIMUM CURRENT OF ELECTRODES

From results obtained, it is noticed that the best performing electrode in removing the p-Cresol is the diamond and then the graphite, followed by the stainless steel. The most important properties of diamond electrode are a large potential window, lower adsorption, corrosion stability in very aggressive media, high efficiency in oxidation processes, very low double-layer capacitance and background current. All of these characteristics make this material ideal in the elimination of organics from water and give high removal comparing to others electrodes. The graphite electrode is carbon electrode it yielded better results than stainless steel electrode.

The stainless steel shows moderate removal of p-Cresol, but the deterioration of electrode and the enormous quantity of sludge formed during the treatment keep the stainless steel application limited to certain types of electrochemical application especially in electro coagulation process.

On the other hand, the aluminum electrode shows no removal. Figure (5.8) below clarify the comparison between, graphite, diamond, stainless steel, and aluminum electrodes. For further information refer to appendix figure (A 22, A30, A38, and A46).

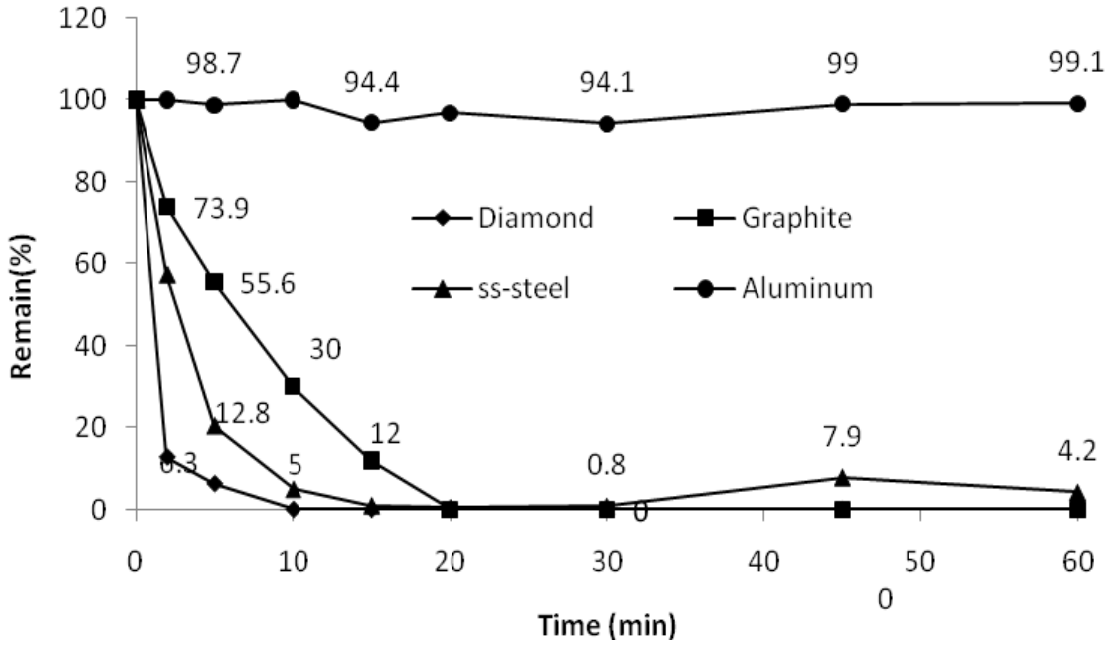

Figure (5.8): Comparisons between different electrodes at optimum current 20 ma/cm2 in degradation of p-Cresol with initial concentration of 75 ppm

5.2.5.1. COD Test for Optimum Current Density 20 mA/cm^{2}for Three Electrodes.

Figure (5.8) illustrates comparisons between four types of electrodes diamond, graphite, stainless steel and aluminum at optimum current density of 20 mA/cm^2. The HPLC analysis shows that p-cresol disappears from the solution after 10 minutes of treatment by diamond electrodes while in the case of graphite electrodes it disappears after 20 minutes, 0.5% of p-cresol remains till 60 minutes of treatment with the stainless steel electrodes, and the aluminum electrode has negligible removal of p-cresol.

For further confirmation to previous results obtained by HPLC, two experiments were repeated with the same operational parameters and a COD test was performed. This test assisted in providing further information on the complete mineralization of p-cresol, at the end of 30 minutes of contact time the COD values for the diamond electrodes was (0 mg/l) while at end of 60 minutes of contact time the graphite electrodes achieved (0 mg/l). In addition, the average of the COD results for stainless steel electrodes is 78 mg/l at 60 minutes of contact time. See figures (5-9, 5-10, and 5-11 below).

From these results it was concluded that to obtain a complete mineralization for p-cresol in the case of diamond electrodes and graphite electrodes the experiment should be extended for an extra 20 minutes and 40 minutes respectively.

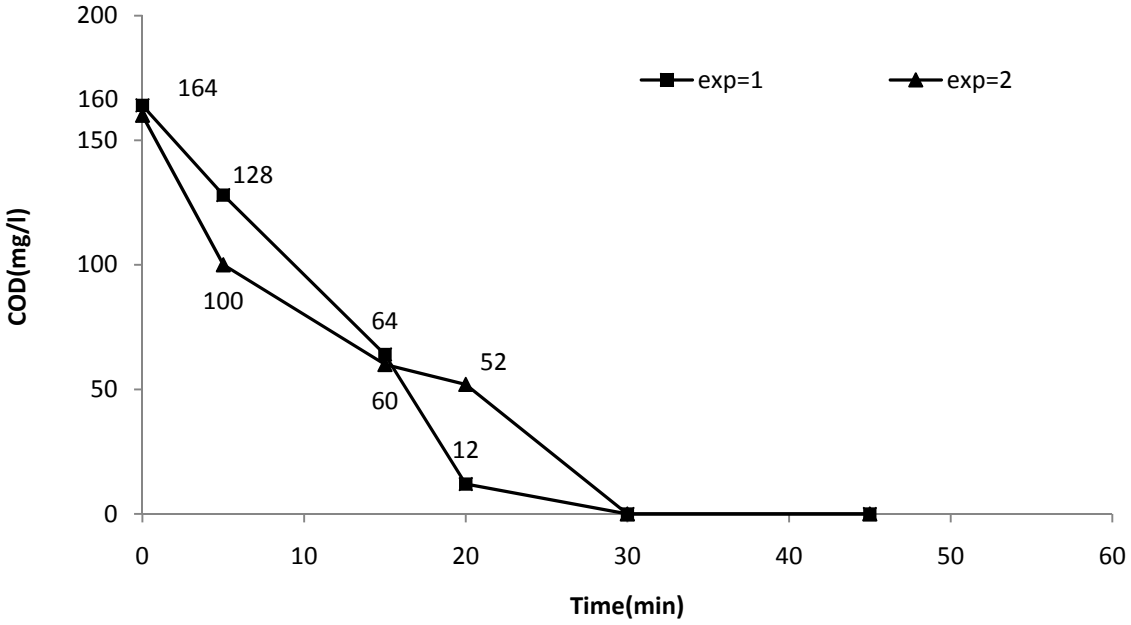

Figure (5.9): COD (mg/l) versus contact time for 2 experiments of deionized water treated by diamond electrode at optimum current 20 mA/cm^2 and initial concentration for p-Cresol 75 ppm

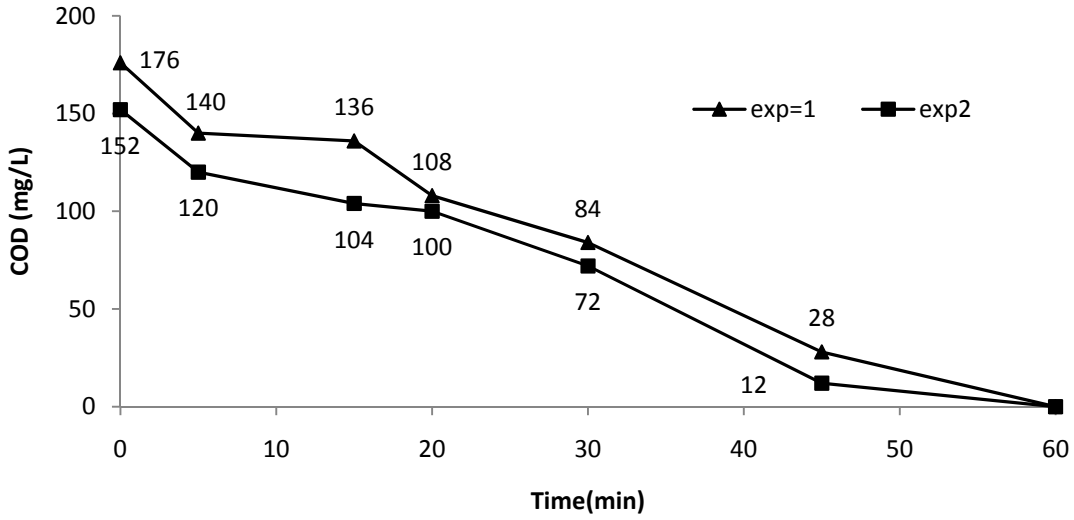

Figure (5.10): COD (mg/l) versus contact time for 2experiments of deionized water treated by graphite electrode at optimum current 20 mA/cm^2 and initial concentration for p-Cresol 75 ppm

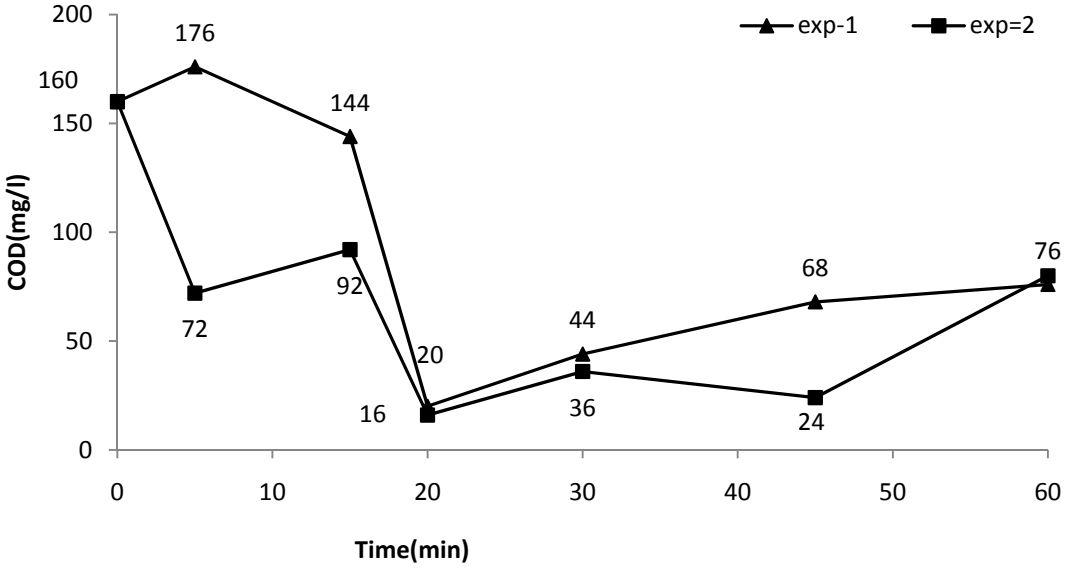

Figure (5.11): COD (mg/l) versus contact time for 2experiments of deionized water treated by stainless steel electrode at optimum current 20 mA/cm^2 and initial concentration for p-Cresol 75 ppm

5.2.5.2. TOC Test for Optimum Current Density 20 mA/cm^2 for Stainless Steel Electrode.

For more confirmation one experiment was conducted for the stainless steel electrodes. A TOC test was performed for the collected samples and figure (5.12) below shows the results.

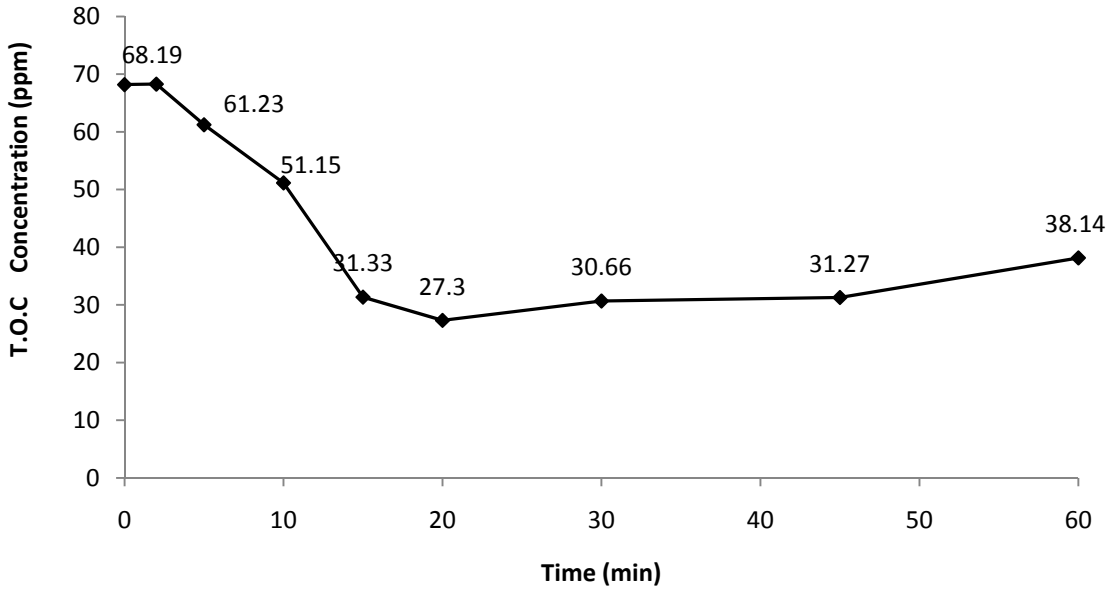

Figure (5.12): TOC concentration (ppm) versus contact time for 1experiment of deionized water treated by stainless steel electrode at optimum current 20 mA/cm^2 and initial concentration for p-Cresol 75 ppm

5.2.6. SCANNING ELECTRON MICROSCOPE FOR DISSOLVED ELECTRODES

The results previously mentioned in the current investigation showed that the aluminum electrode did not remove p-Cresol from water matrix. In addition, the stainless steel electrode deteriorated after a certain time of its usage, so to understand better the reason why, aluminum didn't remove the p-Cresol, why stainless steel lost its efficiency, and why stainless steel (SS-304L) removed p-Cresol better than stainless steel electrode (SS-316L), it was decided to use the scanning electron microscope to see what happened for the surface of electrode, since the surface of electrode play important role in the oxidation of p-Cresol

As result of scanning it was found that high percentage of contamination film was formed on the surface of Aluminum electrode and moderate percentage on the stainless steel electrode was detected. This contamination varied from electrode to electrode, but in common, all electrodes have oxide films which act as barrier and prevent the treatment. It was observed that huge number of cavities formed on the anode surface, with probable inclusions of deposits of contamination. In addition it was found that stainless (SS-316L) formed thicker film than (SS-304L).

The reduction in surface area of electrodes due to formation of small cavities and formation of oxidation could be the reasons of deterioration of stainless steel electrodes, and therefore the polarization instrument was used to clean the surface and break the passivation film formed on the surface of electrodes during the treatment process.

5.2.6.1. Result of Scanning of Aluminum Electrode.

Two samples were randomly taken from used electrodes, one each from the used and unused portions respectively. The result of scanning shows that 29.39% of total weight of material is contaminated material on the surface. After treatments of p- cresol, 28.85% out of contaminant is oxidized film. The reason for that oxidation is attributed to the passivation pHenomena of the aluminum electrode and this oxidation film prevents the degradation of p-Cresol.

Table (5.2) below shows the comparison between Scand surface for used and unused electrodes oxygen element is in form of oxide with metal itself or with other contaminated elements on the surface , also below the spectrum for unused and used electrode figure (5.13 and figure 5-14) respectively.

TABLE (5.2): SCANNED ALUMINUM ELECTRODE SURFACE

Scand Element	Weight% Unused Electrode	Weight %Used Electrode
O2	0	28.85
Mg	2.14	1.14
AL	97.86	69.47
Si	0	0.54
TOTAL %	100%	100%

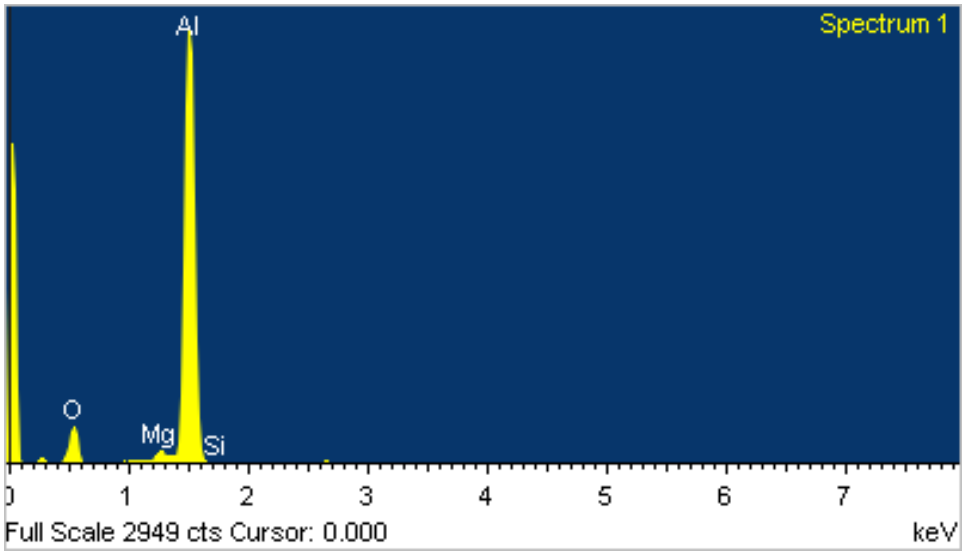

(a)

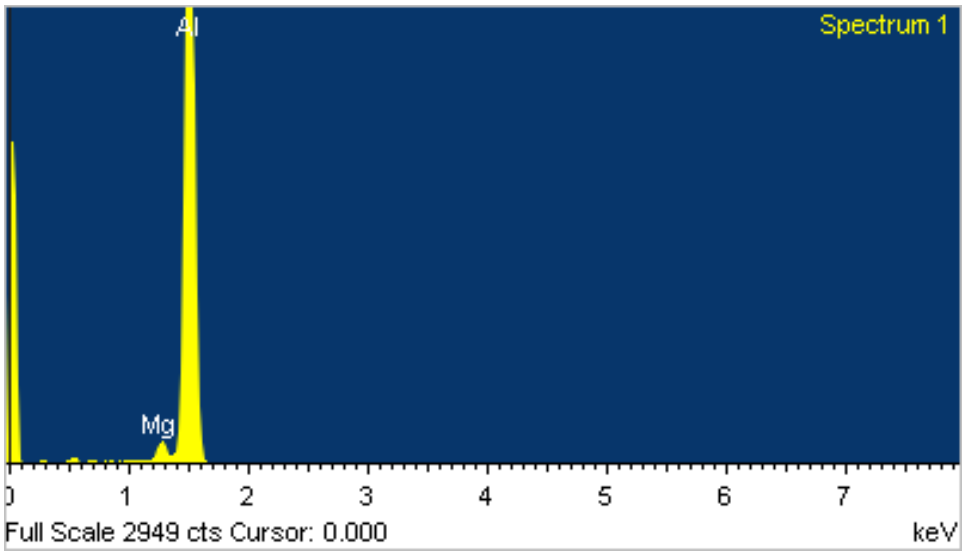

(b)

Figure (5.13): Spectrum for Aluminum Surface Area of Electrode and Electron Image for (a) Used, (b) Unused Electrode

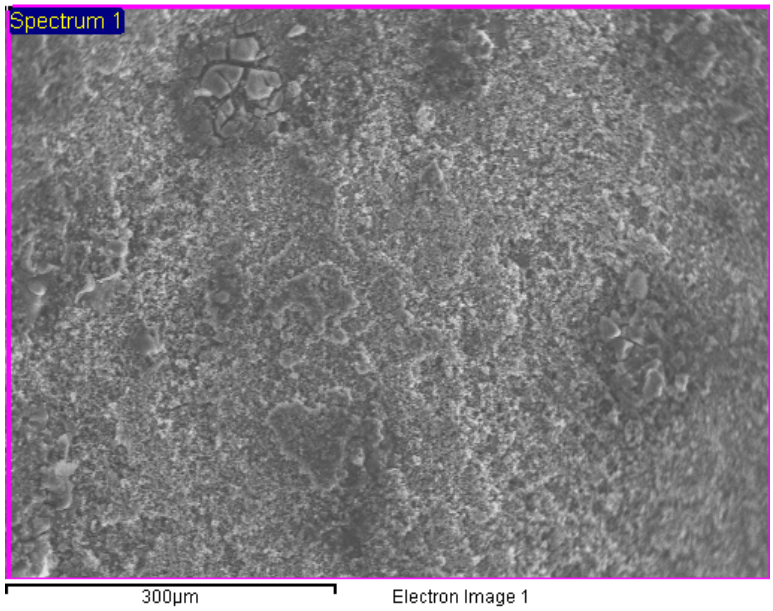

(a)

(b)

(b)Figure (5.14): Surface Scanning View for Aluminum Electrode Image for (a) Used, (b) Unused Surface Electrode

5.2.6.2. Result Scanning of Stainless Steel (SS-316L) Electrode.

Two samples were randomly taken from used electrodes, one each from the used and unused portions. The result of scanning shows that 8.9% of total weight of material is contaminated material on the surface. After treatments of p- cresol, 8.03% out of contaminant is oxidized film.

The reason for that oxidation is attributed to the passivation phenomena of the stainless steel electrode; this oxidation film prevents the degradation of p-Cresol.

Table (5.3) below shows the comparison between the used and unused electrode, also the results of scanned surface for unused and used electrode figure (5.15) and figure (5-16) shows the spectrum for electrodes.

TABLE (5.3): SCANNED SURFACE FOR STAINLESS STEEL ELECTRODE

Scand Element	Weight % Unused Electrode	Weight %Used Electrode
O2	0	8.03
AL	0	0.87
Si	0	0.56
Cr	19.16	18.22
Fe	72.29	65.43
Ni	8.31	6.89
TOTAL%	**100%**	**100%**

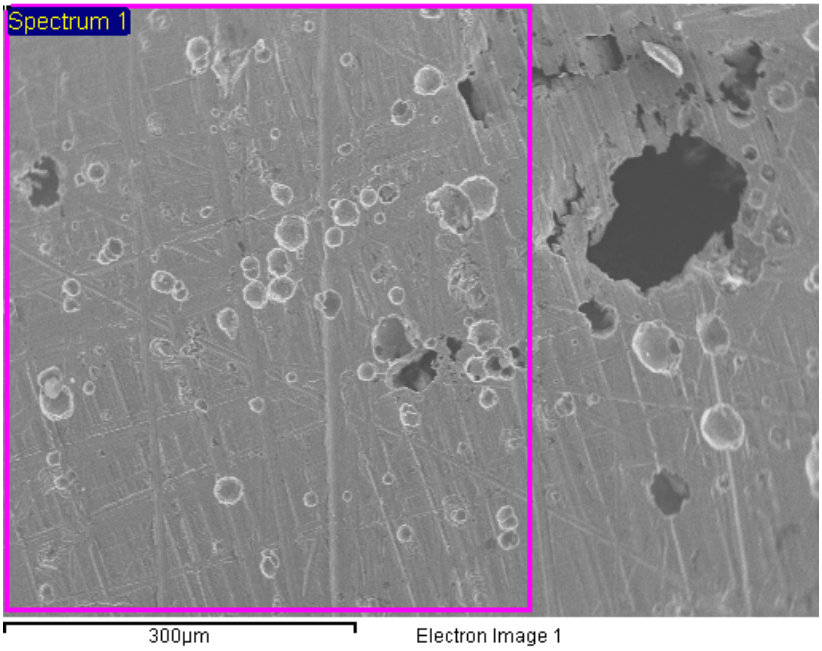

(a)

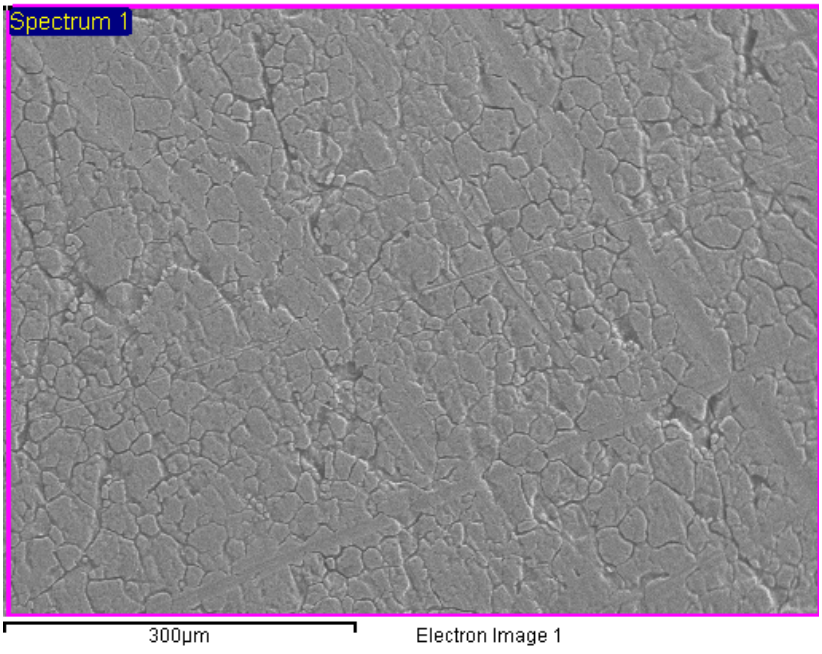

(b)

Figure (5.15): Scanned Surface of Stainless Steel (SS-316 L) (a) Used and (b) Unused

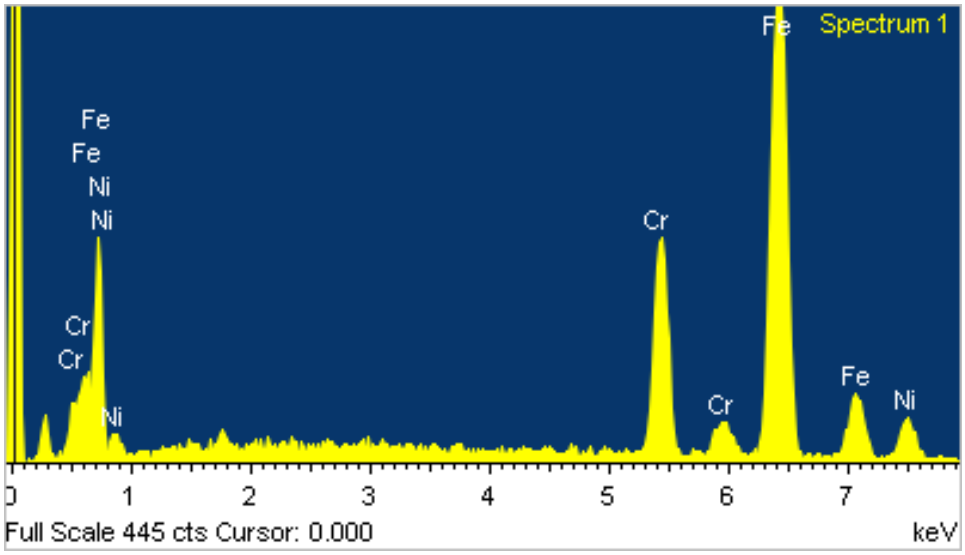

(a)

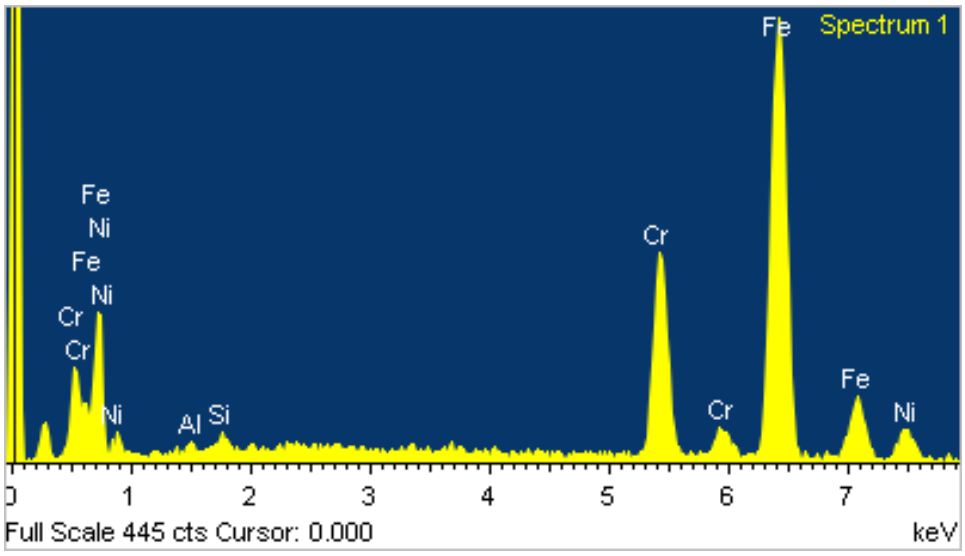

(b)

Figure (5.16): Spectrum for (SS-316 L) Surface of Stainless Steel

(a) Used and (b) Unused

5.2.6.3. Result Scanning of Stainless Steel (SS-304L) Electrode.

Two were samples randomly taken from electrodes, one each from the used and unused portions. The result of scanning shows that 3.04% of total weight of material is contaminated material on the surface. After treatments of p- cresol, 2.58% out of contaminant is oxidized film.

The reason for that oxidation is attributed to the passivation pHenomena of stainless steel electrode and this oxidation film prevents the degradation of p-Cresol.

Comparing the two types of stainless steel (SS-304L) and (SS-316L) electrodes, the results show that (SS-304L) is less resistant to corrosion, because the contaminants percent is 3.04 while for (SS-316L) it was 8.03%.

Table (5.4) below shows the comparison between the used and unused electrode, also the result of scanned surface for unused and used electrode figure (5.17). Figure (5-18) shows result for the spectrum for electrodes.

.

TABLE (5. 4): SCANNED FOR (SS-304L) ELECTRODE SURFACE

Scanned Element	Weight % Unused Electrode	Weight% Used Electrode
O2	0	2.58
AL	0	0.46
Si	0.79	0.73
Cr	19.16	18.87
Fe	72.21	69.48
Ni	7.84	7.89
TOTAL%	**100%**	**100%**

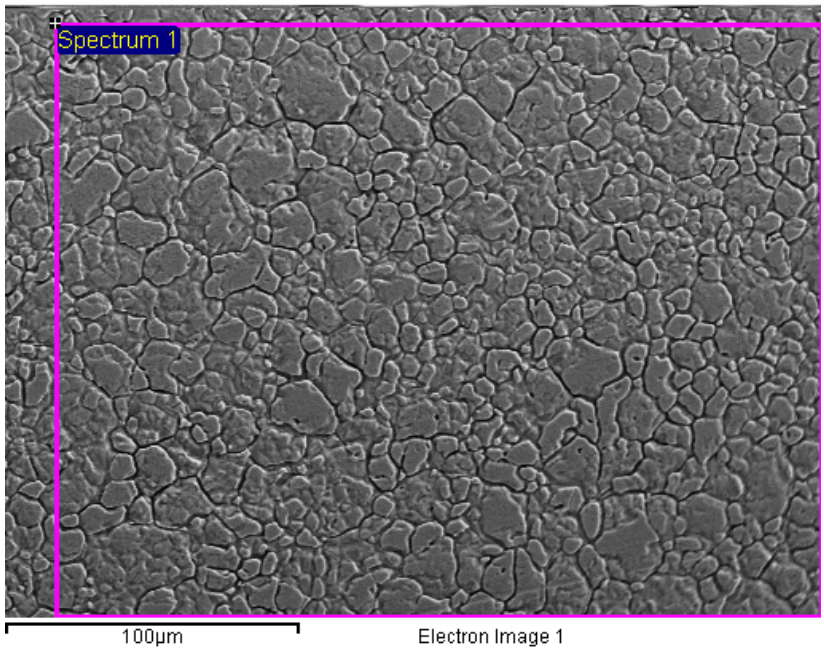

(a)

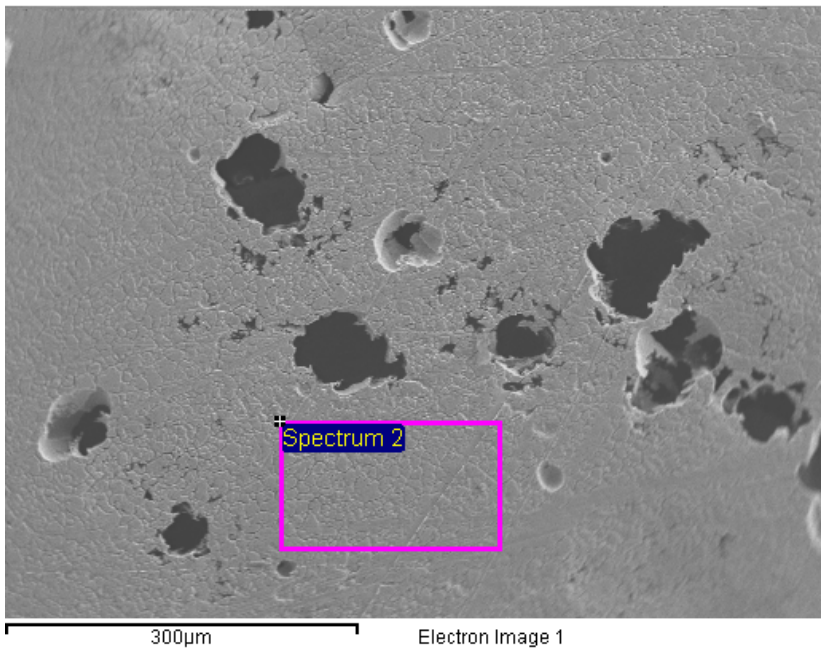

(b)

Figure (5.17): Scanned for (SS-304 L) Surface of Stainless Steel (a) Used and (b) Unused

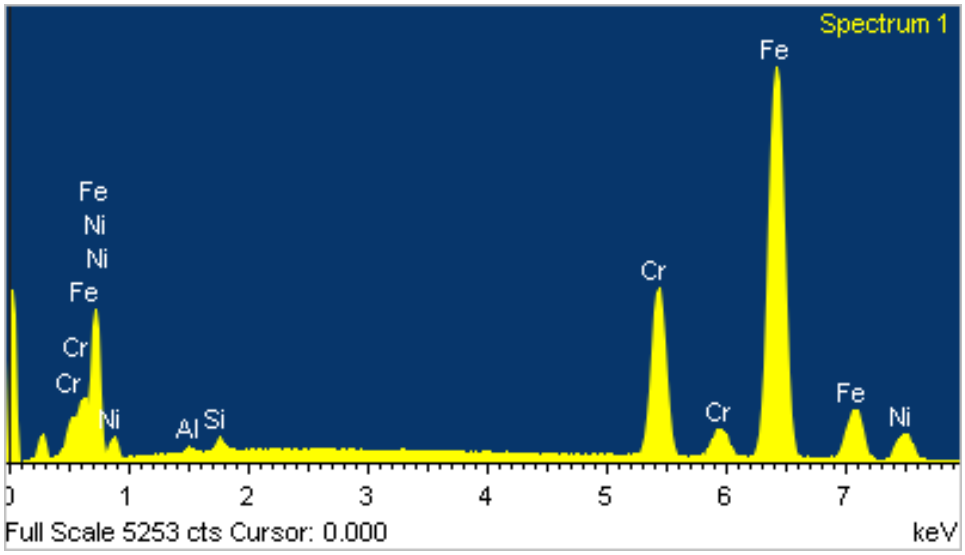

(a)

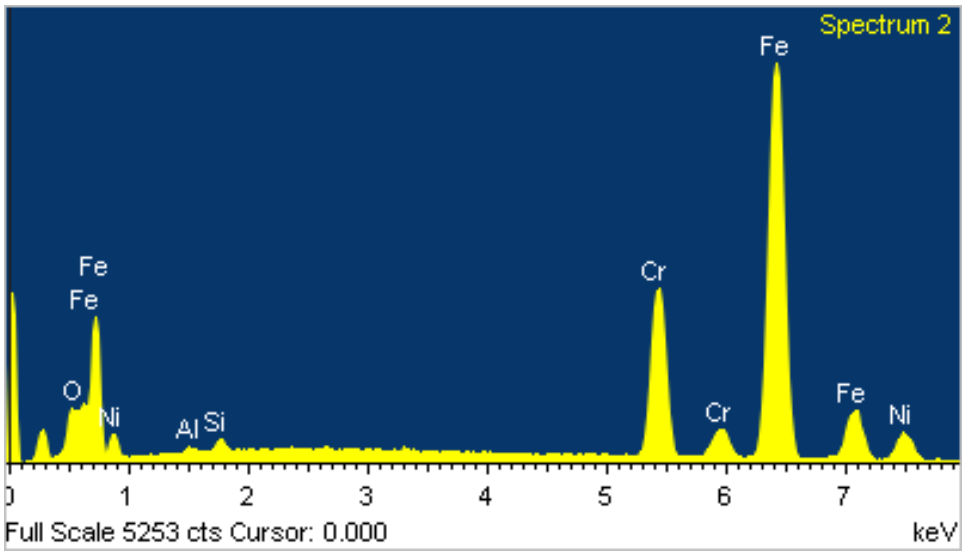

(b)

Figure (5.18): Spectrum for (S-304 L) Surface of Stainless Steel (a) Used and (b)Unused

5.3. POLARITY INVESTIGATION

Electrochemical polarization can improve the surface cleanliness, alter the surface microstructure, and/or change the surface chemistry. Numerous methods have been reported in the literature. Generally, anodic and cathodic polarization can provide the highest degree of activation. The study results show that the polarization time which gives highest removal is 30 seconds, and the current densities were variable from electrode to electrode. Our aim is to see if the polarity can improve the degradation of p-Cresol. As we mentioned previously, we excluded the aluminum electrode from the study because it did not show any effect on the removal of P-Cresol, the polarity investigations were therefore conducted for graphite, diamond, and stainless steel.

5.3.1 POLARITY OF GRAPHITE ELECTRODE

Four experiments were done by using a graphite electrode at current density of 15mA/cm2 to investigate the effect of polarity by reversing the electric current, the polarity time conducted was (0,30,45, and 60 seconds), in all experiments the initial concentration of p-Cresol was 75 ppm , as shown in Figure (5-19). After 15 minutes of treatments, and polarity time of 30 seconds, the remaining of p-Cresol was 0%, while at the same interval time and polarity of 45 seconds the remaining percentage was 7%,on other hand at polarity 60 seconds the remaining of p-Cresol was 0%. The remaining of p-Cresol at zero polarity times 26.4 %. At 15 minutes interval time ,nearly in 30.45, 60 seconds polarity time the p-Cresol

removed completely while at zero polarity time the p-Cresol was removed at 30 minutes interval which means that if polarity time used 30 seconds we can save 15 minutes in time of treatments therefore we have saving in cost. For further detail refer appendix table (A18).

5.3.2. POLARITY OF DIAMOND E ELECTRODE

Four experiments were done by using diamond electrode at current density of 10 mA/cm2 to investigate the effect of Polarity by reversing the electric current. The polarity time conducted as (0, 30, 45, and 60 Seconds), in all experiments. The initial concentration of p-Cresol was 75 ppm, as shown in Figure (5-20) below. After 15 minutes of treatment and polarity time of 30 seconds, the remaining of p-Cresol was 0%, while at the same interval time and polarity of 45 seconds the remaining percentage is 3.1%. In addition at polarity 60 seconds the removal of p-Cresol is 0.6%. The remaining of p-Cresol at zero polarity times for the same interval of time is 15.8% and complete removal of p-Cresol achieved at time interval of 30 minutes, which means that if use polarity time of 30 seconds, we are saving 15 minutes in treatment of p-Cresol and therefore we have a saving by using the polarity of 30 seconds. For further detail refer appendix table (A19).

5.3.3 POLARITY OF STAINLESS STEEL E ELECTRODE

Four experiments were done by using stainless steel electrode at current density of 15mA/cm2to investigate the effect of Polarity by reversing the electric current. The polarity time conducted at (0, 30, 45, and 60 seconds). In all experiments, the initial concentration of p-Cresol was 75 ppm, as shown in figure (5-21) below. After 60 minutes of treatments and polarity of 30 seconds, the remaining p-Cresol was 33.2 %, while for 60 seconds it is 46.4%, and 63% for 45 seconds. However the remaining of p-Cresol at zero second of polarization is 64.9%. It was found that polarization time of 45 seconds did not yield improvement in removing the p-Cresol, for further detail refer appendix table (A20).

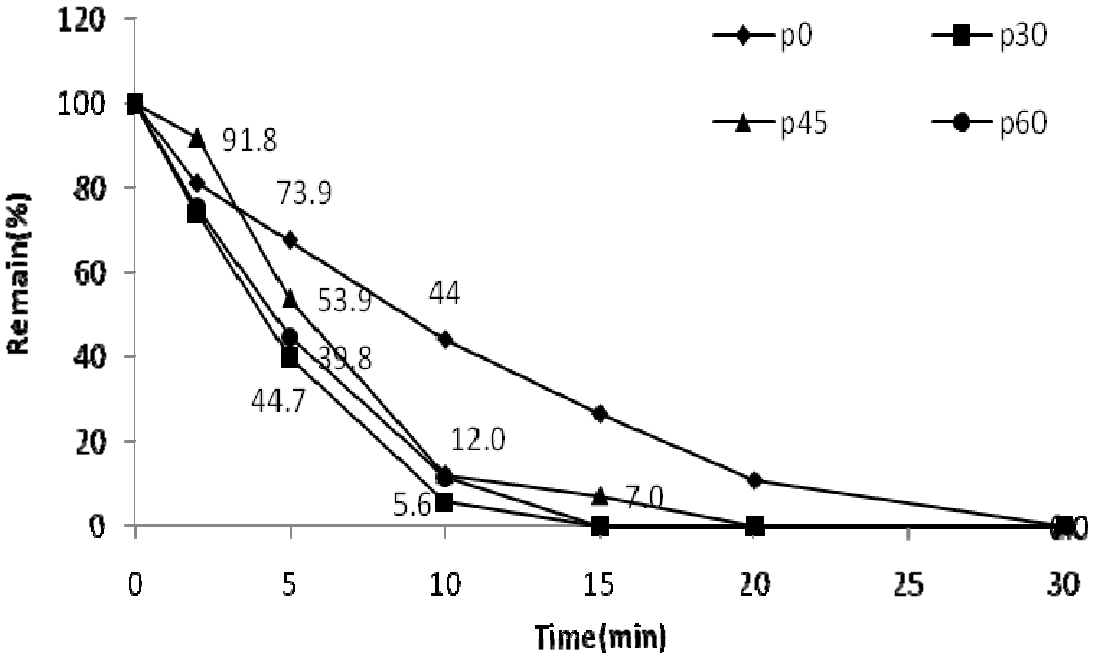

Figure (5.19): Effect of polarity investigation by using graphite electrode and polarity time (0, 30, 45, and 60 seconds) and 15 mA/cm^2 current density

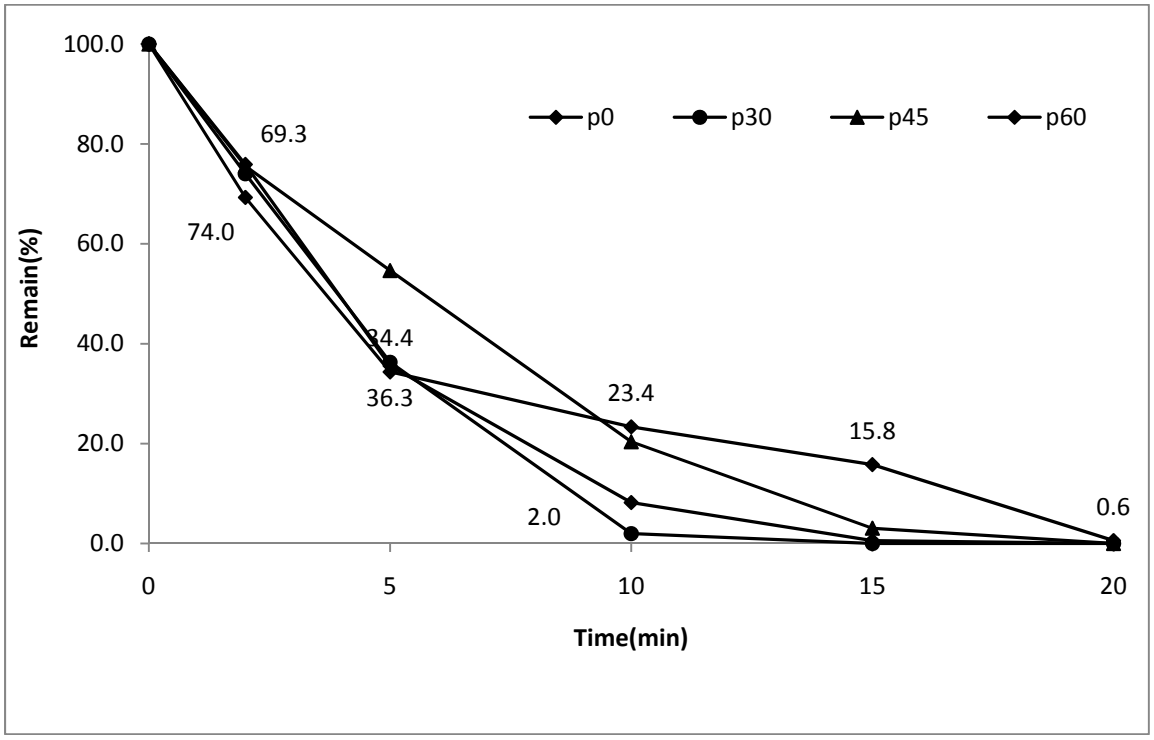

Figure (5.20): Effect of polarity investigation by using diamond electrode and polarity time (0, 30, 45, and 60 seconds) and 5 mA/cm^2 current density

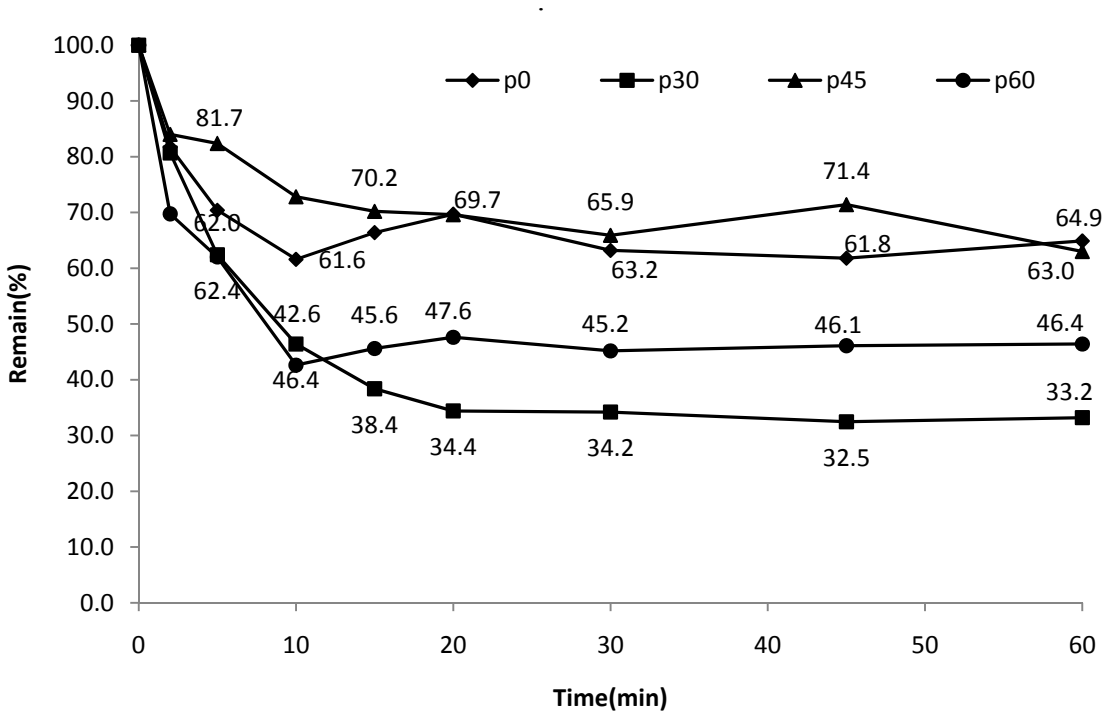

Figure (5.21): Effect of polarity investigation by using stainless steel electrode and polarity time (0, 30, 45, and 60 seconds) and 15 mA/cm^2 current density

5.4. EFFECT OF ELECTRODES ON REMOVING P-CRESOL FROM RAW WATER

Final experiments were conducted using raw water as a base solvent for p-Cresol. The concentration of p-Cresol was detected throughout the experiment at time intervals of 0, 2, 5, 10, 15, 20, 30, 45, and 60 minutes. Three experiments were done by using diamond, graphite, and stainless steel electrode (SS-316L) to compare the removal of p-Cresol from raw water. The initial concentration of p-Cresol was 75 ppm and current density was 20 mA/cm^2. After 10 minutes of treatment, the diamond electrode removed the p-Cresol completely, while the graphite electrode took 20 minutes. The residual of p-Cresol achieved by a stainless steel electrode at 20 minutes of treatment was 84.6%. This indicates that lower removal percentage of the electrode in tap water is happened for different reasons one of them could be chemical composition of raw water in matrix.

Comparing the removal of p-Cresol from deionized water and from raw water, it was realized that graphite and diamond electrodes took same time to remove the p-Cresol in both water matrix, while the stainless steel electrode has fluctuating results, and was affected by the type of water used. Figure (5-22) below shows the p-Cresol remaining after treatment with 3 types of electrodes by using raw water. For further information please refer to appendix table (A21).

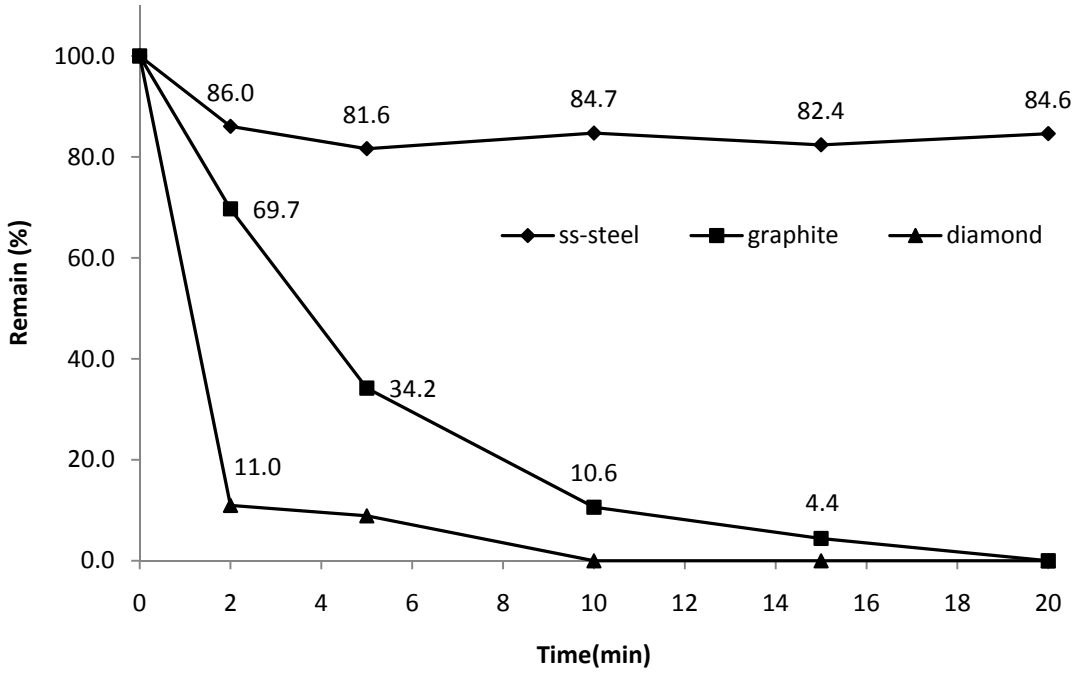

Figure (5.22): Comparison between stainless steel electrode, graphite and diamond by using raw water and p-Cresol at 75 ppm with 20 ma/cm2 current density

5.5. PH VARIATION FOR OPTIMUM CURRENT OF GRAPHITE, DIAMOND, STAINLESS STEEL AND ALUMINUM

Several experiments were conducted on each electrode; the same type of electrode was used as both anode and cathode with different current densities. The readings of pH - cresol r was taken. The high alkalinity of the medium was achieved after 30 minutes of treatments as shown in figure (5-23), the stainless steel pH, after a 20 minute interval, sharply increased until it reached a value of 12.5.

On the other hand, the pH values for diamond and graphite after a 20 minutes interval were almost constant. For additional information please review figures A22, A30, A38 and A46, in the appendix.

It was observed that the p-Cresol removal has no relation with pH variation for diamond, graphite and aluminum electrode. In contrast, for a stainless steel electrode, there is a relation between p-Cresol removal and the increment of pH. It was observed that p-Cresol removal increased with the increment of pH.

For more details about other pH comparisons at different current density level, refer to table A98, A99 and A100, in the appendix.

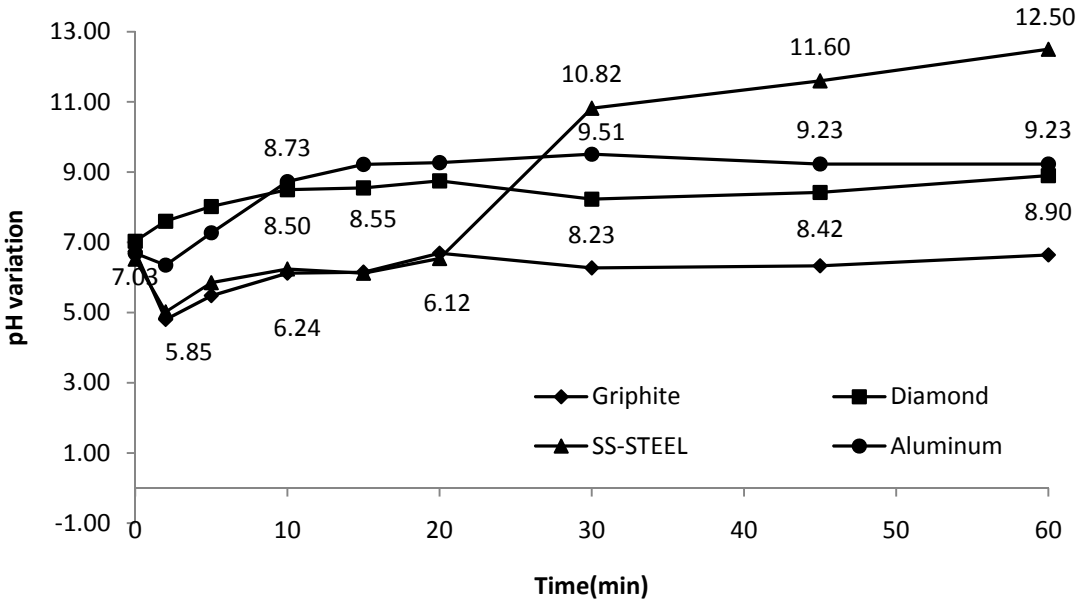

Figure 5.23: PH variation versus time for different electrodes at optimum current density of 20 mA/cm^2

CONCLUSIONS & RECOMMENDATIONS

The disposal of p-Cresol has always been a major environmental issue and its degradation is a serious challenge to degrade. The attempts of previous studies, which were based on the standard parameters available in the literature, indicate that p-Cresol removal was affected in most of the cases by the electrode material which has high impact on the removal of the p-Cresol. Therefore, the first goal of this study was to optimize the current density. As a result, 20 mA/cm^2 was found to be the optimum current density for all electrodes to degrade the p-Cresol. The results of experimental analyses confirmed that only two electrodes among the investigated ones, namely, diamond and graphite yielded the highest removal, while stainless steel has moderate removal and lost its efficiency very fast. This was proved by conducting 5 experiments with same anode after cleaning it thoroughly on completion of each experiment.

Aluminum electrode (commercial type) can't be used in removing the p-Cresol since it gave negligible percentage removal. For stainless steel electrode the analysis indicate that, in high (pH) alkalinity medium, more p-Cresol degradation can be achieved. While for other electrodes there is no relation between p-Cresol removal and pH.

In addition, when the commonly used stainless steel electrodes were used as both cathode and anode, in the electrochemical oxidation process, it was found that the stainless steel electrodes undergo a metal transition process in which Ni, Cr, and Fe are released into the

water matrix giving colors interfering with the spectrophotometer reading of the p-Cresol. This suggests that the UV spectrophotometer, which has been used in most recent p-Cresol removal studies, could give false readings and therefore proper background measurements and precise data analysis such as digital subtraction are required. Therefore, further analysis were carried out using HPLC.

To further enhance the p-Cresol removal, 12 experiments were conducted with different polarity levels (current reversal) for each type of electrode and it was found that the polarity time which enhances the degradation of p-Cresol is 30 seconds. This enhancement is due to the possible affect of the surface cleaning and breaking the passivation layer which formed on electrode surface.

It was found from scanning the surface of aluminum, stainless steel (SS-304) and stainless steel (SS-316L) that material which has less resistance to corrosion can remove p-Cresol faster than material with high resistance to corrosion.

From previous result it was found that polarization increases the removal of p-Cresol since it can clean the surface of electrode and break the passivation layer formed on the surface of electrodes. It will not be costly to have the polarization device in practical application.

This study may establish a good basis for further investigations on the microstructural properties of electrodes to enhance the electrodes efficiency. Also the use of different electrodes such as chrome silicon or other types of electrodes instead of stainless steel electrodes can be investigated. This could help to extend the efforts toward the practical application of removal of p-Cresol from live refinery and petrochemical waste.

APPENDIX

TABLE A1: DATA OF STANDARD CALIBRATION CURVE FOR p-Cresol AT 270 NM:

Concentration (mg/l)	Absorbance (nm)
0	0.0421
3.125	0.0657
6.25	0.1355
12.5	0.2178
25	0.3676
50	0.7915
75	1.1343

TABLE A2: DATA OF CHEMICAL OXYGEN DEMAND (COD) TEST FOR p-Cresol:

No. of sample in replicates	p-Cresol concentration (mg/l)	COD (mg/l)
1	0	0
2	6.25	18
3	12.5	42
4	25	82
5	50	140
6	75	245

TABLE A3: DATA OF HPLC CALIBRATION CURVE FOR p-Cresol:

No. of sample in replicates	p-Cresol concentration (mg/l)	Area of p-Cresol (microvolt/cm2)
1	0	0
2	6.25	29316
3	12.5	60270
4	25	118848
5	50	242780
6	75	344739
7	100	475414

TABLE A4: PH AND CONCENTRATION DATA FOR 75PPM OF p-Cresol AFTER TREATMENT BY USING STAINLESS STEEL ELECTRODE AT CURRENT DENSITY OF 20 MA/CM2

No. of sample	Time (min)	Absorption (nm)	Concentration (ppm)	PH
1	0	1.1404	75.0	6.2
2	2	1.0692	70.2	6.42
3	5	0.9309	60.8	7.73
4	10	1.1624	76.5	8.13
5	15	1.3851	91.5	8.79
6	20	1.3313	87.9	9.02
7	30	2.0714	137.9	9.82
8	45	1.244	82.0	10.83
9	60	1.2935	85.3	11.09

TABLE A5: PH AND CONCENTRATION DATA FOR 75PPM OF p-Cresol AFTER TREATMENT BY USING STAINLESS STEEL ELECTRODE AT CURRENT DENSITY OF 15 MA/CM2

No. of sample	Time (min)	Absorption (nm)	Concentration (ppm)	pH
1	0	1.132	74.4	6.75
2	2	0.8698	56.7	8.77
3	5	0.8782	57.3	8.11
4	10	0.8458	55.1	9.53
5	15	0.6929	44.8	11.01
6	20	0.6478	41.7	11.39
7	30	0.7455	48.3	11.68
8	45	0.7704	50.0	11.97
9	60	0.7067	45.7	12.1

TABLE A6: PH AND CONCENTRATION DATA FOR 75PPM OF p-Cresol AFTER TREATMENT BY USING STAINLESS STEEL ELECTRODE AT CURRENT DENSITY OF 10 MA/CM2

No. of sample	Time (min)	Absorption (nm)	Concentration (ppm)	pH
1	0	1.134	74.6	6.42
2	2	0.9052	59.1	6.8
3	5	0.9252	60.4	5.97
4	10	0.9327	61.0	9.25
5	15	0.8479	55.2	10.22
6	20	0.8341	54.3	10.64
7	30	0.7933	51.5	11.15
8	45	0.7717	50.1	11.61
9	60	0.7172	46.4	12.18

TABLE A7: PH AND CONCENTRATION DATA FOR 75PPM OF p-Cresol AFTER TREATMENT BY USING STAINLESS STEEL ELECTRODE AT CURRENT DENSITY OF 5MA/CM2

No. of sample	Time (min)	Absorption (nm)	Concentration (ppm)	pH
1	0	1.155	76.0	7.51
2	2	0.9885	64.7	5.59
3	5	0.952	62.3	5.67
4	10	0.8514	55.5	6.88
5	15	1.0184	66.7	7.86
6	20	0.8801	57.4	8.68
7	30	0.8453	55.0	10.26
8	45	0.8323	54.2	10.51
9	60	0.8046	52.3	10.69

TABLE A8: PH AND CONCENTRATION DATA FOR 75PPM OF p-Cresol AFTER TREATMENT BY USING ALUMINUM ELECTRODE AT CURRENT DENSITY OF 20MA/CM2

No. of sample	Time (min)	Absorption (nm)	Concentration (ppm)	pH
1	0	1.185	78.0	7.63
2	2	1.0015	65.6	5.05
3	5	1.0369	68.0	5.79
4	10	1.0901	71.6	8.48
5	15	1.0117	66.3	8.85
6	20	1.1107	73.0	8.97
7	30	1.1437	75.2	9.06
8	45	1.0237	67.1	8.97
9	60	1.0354	67.9	9.05

TABLE A9: PH AND CONCENTRATION DATA FOR 75PPM OF p-Cresol AFTER TREATMENT BY USING ALUMINUM ELECTRODE AT CURRENT DENSITY OF 15MA/CM2

No. of sample	Time (min)	Absorption (nm)	Concentration (ppm)	pH
1	0	1.12	73.6	6.63
2	2	0.9856	64.5	8.4
3	5	0.9653	63.2	8.45
4	10	0.8511	55.4	8.38
5	15	0.8531	55.6	8.73
6	20	0.9576	62.6	8.77
7	30	0.9285	60.7	8.9
8	45	0.9449	61.8	9.4
9	60	0.7845	50.9	9.01

TABLE A10: PH AND CONCENTRATION DATA FOR 75PPM OF p-Cresol AFTER TREATMENT BY USING ALUMINUM ELECTRODE AT CURRENT DENSITY OF 10MA/CM2

No. of sample	Time (min)	Absorption (nm)	Concentration (ppm)	pH
1	0	1.1343	74.6	5.87
2	2	1.1138	73.2	6.09
3	5	1.26	83.1	6
4	10	1.2681	83.6	6.37
5	15	0.9725	63.6	7.75
6	20	1.165	76.6	9
7	30	1.1946	78.6	9.01
8	45	1.072	70.4	9.13
9	60	1.0697	70.2	9.19

TABLE A11: PH AND CONCENTRATION DATA FOR 75PPM OF p-Cresol AFTER TREATMENT BY USING ALUMINUM ELECTRODE AT CURRENT DENSITY OF 5MA/CM2

No. of sample	Time (min)	Absorption (nm)	Concentration (ppm)	pH
1	0	1.173	77.2	5.87
2	2	1.0626	69.7	6.09
3	5	1.0269	67.3	6
4	10	1.1031	72.5	6.37
5	15	1.0188	66.8	7.75
6	20	0.9926	65.0	9
7	30	0.9491	62.1	9.01
8	45	1.0338	67.8	9.13
9	60	0.9043	59.0	9.19

TABLE A12: REMAINING PERCENTAGE OF p-Cresol VS. TIME AFTER TREATMENT OF p-Cresol BY USING GRAPHITE ELECTRODE AT CURRENT DENSITY OF 20, 15, 10, AND 5MA/CM2

Time (min)	20mA/cm2	15mA/cm2	10mA/cm2	5mA/cm2
0	100	100	100	100
2	73.9	81.1	88.1	97.2
5	55.6	67.6	79.4	90.7
10	30.0	44.0	56.3	84.2
15	12.0	26.4	50.8	77.4
20	0.0	10.6	40.7	66.5
30	0.0	0.0	19.9	56.1
45	0.0	0.0	5.2	43.8
60	0.0	0.0	0.0	30.7

TABLE A13: REMAINING PERCENTAGE OF p-Cresol VS. TIME AFTER TREATMENT OF p-Cresol BY USING DIAMOND ELECTRODE AT CURRENT DENSITY OF 20, 15, 10, ND5MA/CM2

Time (min)	20mA/cm2	15mA/cm2	10mA/cm2	5mA/cm2
0	100.0	100.0	100.0	100.0
2	12.8	31.1	53.8	68.1
5	6.3	10.8	20.8	35.4
10	0.0	5.0	8.4	28.4
15	0.0	0.0	3.5	15.0
20	0.0	0.0	0.0	9.4
30	0.0	0.0	0.0	0.0
45	0.0	0.0	0.0	0.0
60	0.0	0.0	0.0	0.0

TABLE A14: REMAINING PERCENTAGE OF p-Cresol VS. TIME AFTER TREATMENT OF p-Cresol BY USING STAINLESS STEEL SS-316L AT CURRENT DENSITY OF 20, 15. 10, AND5MA/CM2

Time (min)	20mA/cm2	15mA/cm2	10mA/cm2	5mA/cm2
0	100.0	100.0	100.0	100.0
2	57.3	79.7	80.3	82.0
5	20.5	72.9	73.7	79.8
10	5.0	63.8	66.9	77.7
15	1.0	65.2	66.4	82.0
20	0.5	61.4	67.2	80.4
30	0.8	59.8	63.6	79.4
45	0.7	58.8	67.7	78.0
60	4.2	58.3	63.9	72.0

TABLE A15: REMAINING PERCENTAGE OF p-Cresol VS. TIME AFTER TREATMENT OF p-Cresol BY USING TOW TYPES OF STAINLESS STEEL AT 15MA/CM2 CURRENT DENSITY

Time (min)	SS-316L	SS-304L
0	100.0	100.0
2	79.7	63.6
5	72.9	44.0
10	63.8	35.1
15	65.2	31.7
20	61.4	33.7
30	59.8	31.5
45	58.8	29.0
60	58.3	32.7

TABLE A16: REMAINING PERCENTAGE OF p-Cresol VS. TIME AFTER TREATMENT OF p-Cresol BY USING SAME STAINLESS STEEL ELECTRODE AS ANODE FOR FIVE EXPERIMENTS AT CURRENT DENSITY OF 15MA/CM2 TO TEST EFFICIENCY OF ELECTRODE

Time (min)	First.exp	Second.exp	Third.exp	fourth.exp	Fifth.exp
0	100.0	100.0	100.0	100.0	100.0
2	71.2	95.3	92.7	93.6	94.8
5	64.1	93.6	92.1	91.3	89.7
10	65.3	91.9	88.4	93.8	86.0
15	63.0	94.5	87.1	93.1	84.7
20	62.0	92.6	91.4	91.9	91.6
30	66.0	94.0	87.9	90.5	96.8
45	63.3	89.8	89.1	89.3	96.1
60	64.5	85.4	88.3	86.8	99.3

TABLE A17: REMAINING PERCENTAGE OF p-Cresol VS. TIME AFTER TREATMENT OF p-Cresol BY USING ALUMINUM ELECTRODES AT CURRENT DENSITY OF 20, 15, 10, AND5MA/CM2

Time (min)	20mA/cm2	15mA/cm2	10mA/cm2	5mA/cm2
0	100.0	100.0	100.0	100.0
2	100.0	98.0	98.9	106.1
5	98.7	99.2	97.7	107.8
10	100.0	98.9	103.5	99.8
15	94.4	98.1	102.8	105.5
20	96.8	98.0	103.0	97.9
30	94.1	96.8	102.9	100.6
45	99.0	98.0	104.6	96.4
60	99.1	99.5	104.7	105.0

TABLE A18: REMAINING PERCENTAGE OF p-Cresol VS. TIME AFTER TREATMENT OF p-Cresol BY USING GRAPHITE ELECTRODES WITH POLARITY TIME (0, 30, 45, AND 60) SECONDS AT CURRENT DENSITY OF 15MA/CM2

Time (min)	P0	P30	P45	P60
0	100	100.0	100.0	100.0
2	81.1	73.9	91.8	75.3
5	67.6	39.8	53.9	44.7
10	44	5.6	12.0	11.6
15	26.4	0.0	7.0	0.0
20	10.6	0.0	0.0	0.0
30	0	0.0	0.0	0.0
45	0	0.0	0.0	0.0
60	0.0	0.0	0.0	0.0

TABLE A19: REMAINING PERCENTAGE OF p-Cresol VS. TIME AFTER TREATMENT OF p-Cresol BY USING DIAMOND ELECTRODES WITH POLARITY TIME (0, 30, 45, AND 60) SECONDS AT CURRENT DENSITY OF 10MA/CM2

Time (min)	P0	P30	P45	P60
0	100.0	100.0	100.0	100.0
2	69.3	74.0	75.6	75.9
5	34.4	36.3	54.7	35.6
10	23.4	2.0	20.4	8.2
15	15.8	0.0	3.1	0.6
20	0.6	0.0	0.0	0.0
30	0.0	0.0	0.0	0.0
45	0.0	0.0	0.0	0.0
60	0.0	0.0	0.0	0.0

TABLE A20: REMAINING PERCENTAGE OF p-Cresol VS. TIME AFTER TREATMENT OF p-Cresol BY USING STAINLESS STEEL ELECTRODES WITH POLARITY TIME (0, 30, 45, AND 60) SECONDS AT CURRENT DENSITY OF 15MA/CM2

Time (min)	P0	P30	P45	P60
0	100.0	100.0	100.0	100.0
2	81.7	80.7	84.0	69.7
5	70.4	62.4	82.4	62.0
10	61.6	46.4	72.8	42.6
15	66.4	38.4	70.2	45.6
20	69.7	34.4	69.6	47.6
30	63.2	34.2	65.9	45.2
45	61.8	32.5	71.4	46.1
60	64.9	33.2	63.0	46.4

TABLE A21: REMAINING PERCENTAGE OF p-Cresol VS. TIME AFTER TREATMENT OF p-Cresol BY USING STAINLESS STEEL , DIAMOND , AND GRAPHITE, ELECTRODES WITH RAW WATER AT CURRENT DENSITY OF 20MA/CM2

Time (min)	St-steel electrode	Diamond electrode	GrapHite electrode
0	100.0	100.0	100.0
2	86.0	11.0	69.7
5	81.6	8.9	34.2
10	84.7	0.0	10.6
15	82.4	0.0	4.4
20	84.6	0.0	0.0
30	83.1	0.0	0.0
45	85.5	0.0	0.0
60	88.0	0.0	0.0

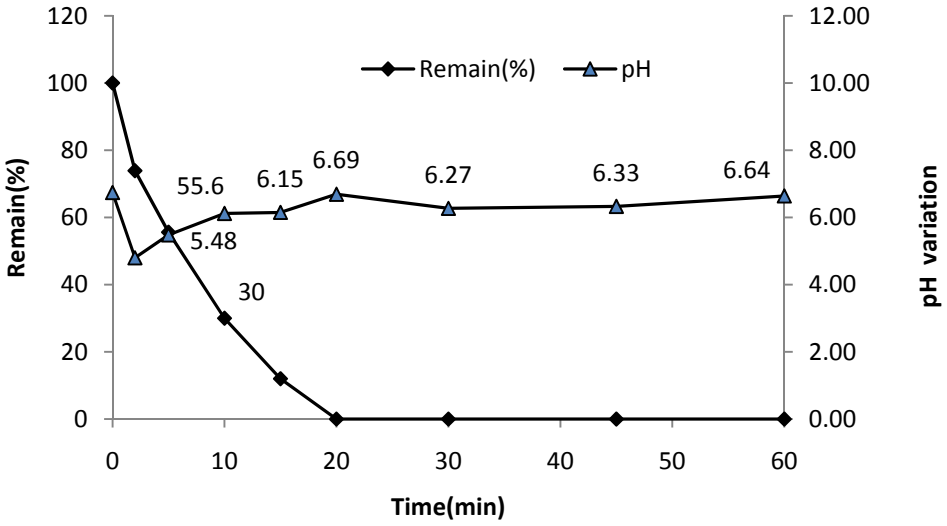

Figure (A22): Remaining percentage of p-Cresol and pH vs. time after treatment of p-Cresol by using graphite electrode at current density of 20 mA/cm2

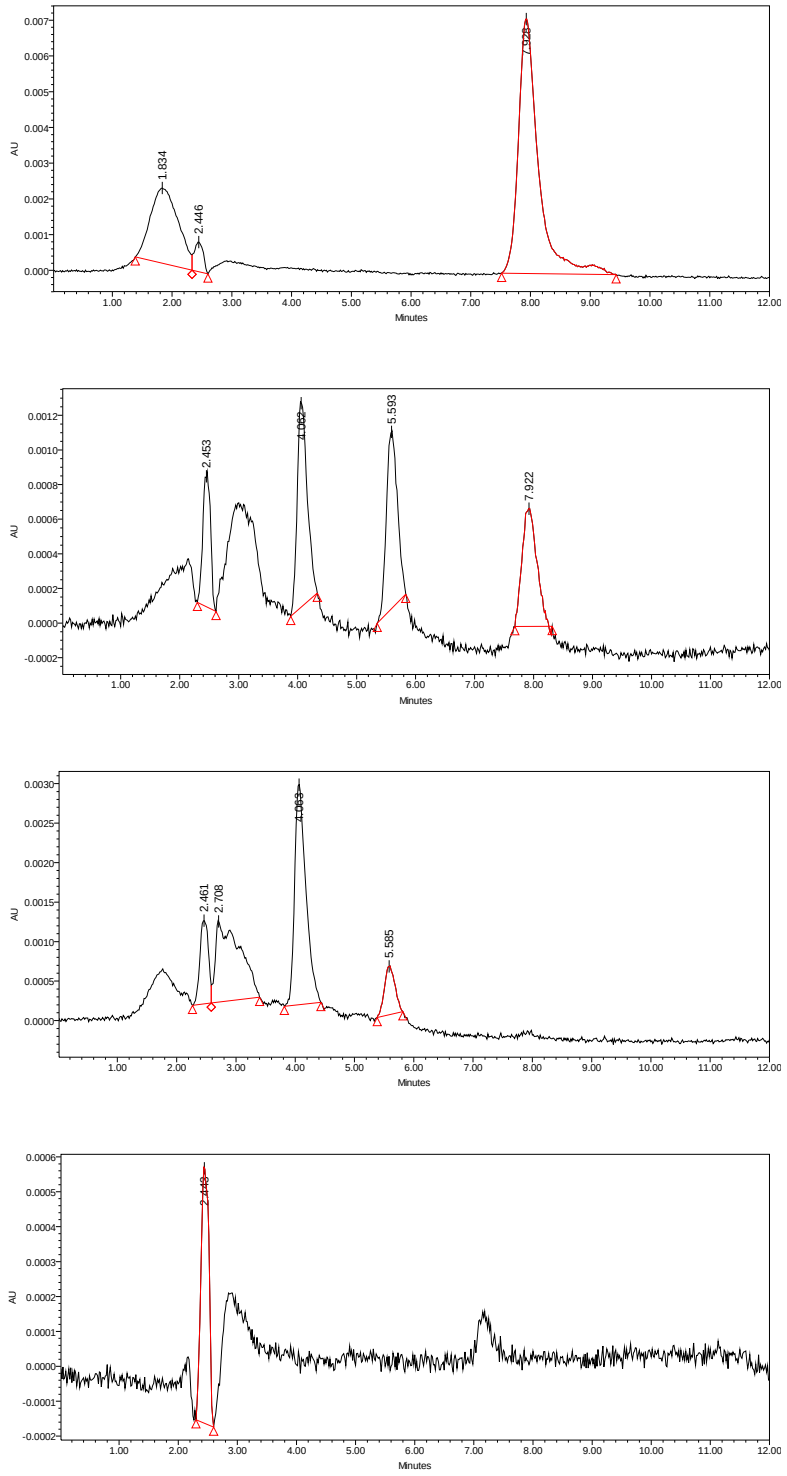

Figure (A23): HPLC chromatogram of p-Cresol for sample treated at 0, 5, 10, and 15 minute's interval time by using graphite electrode at current density of 20mA/cm^2

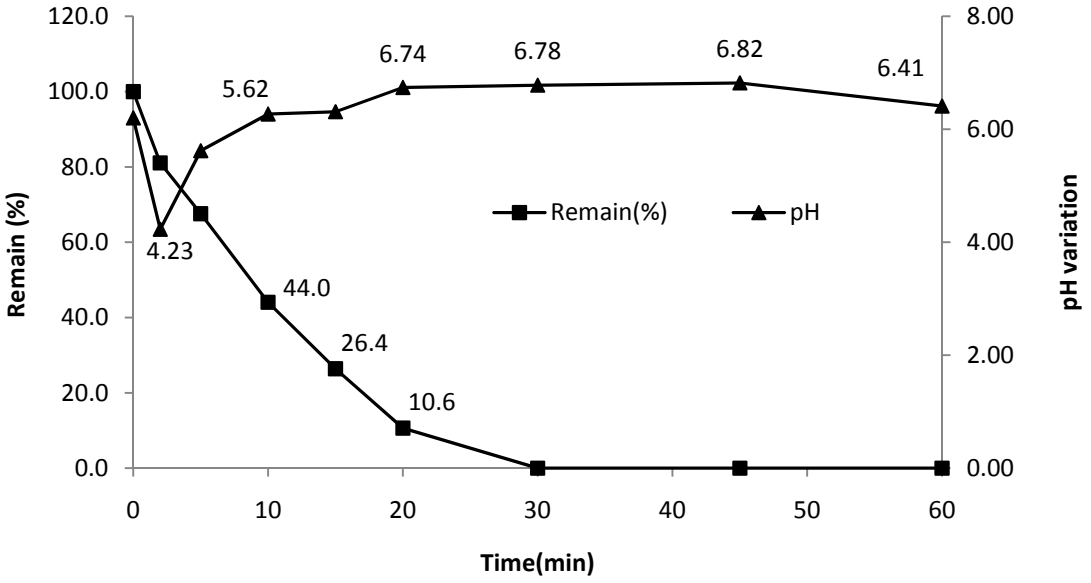

Figure (A24): Remaining percentage of p-Cresol and PH vs. time after treatment of P-Cresol by using graphite electrode at current density of 15 mA/cm^2

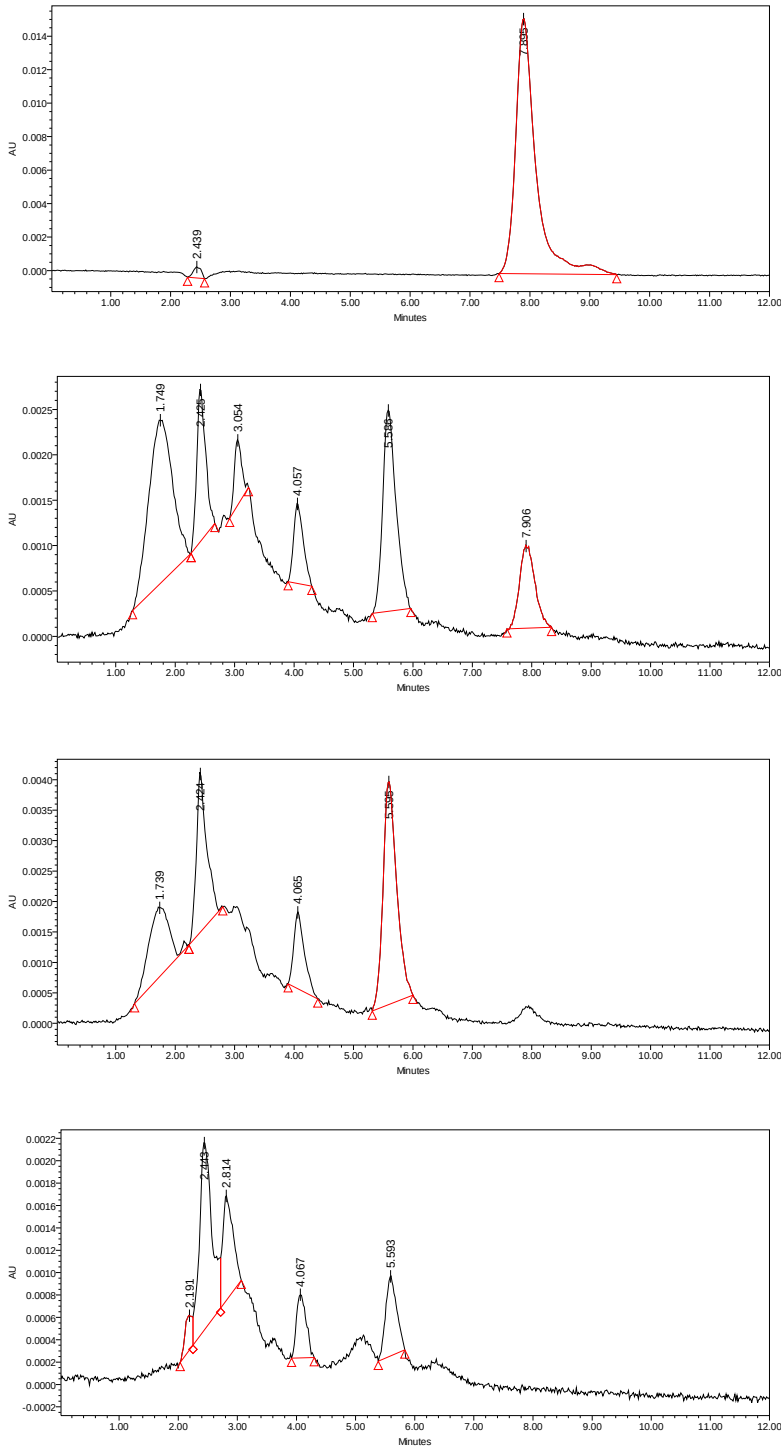

Figure (A25): HPLC chromatogram of p-Cresol for sample treated at 0, 20, 30, and 60 minutes interval time by using graphite electrode at current density of 15mA/cm2

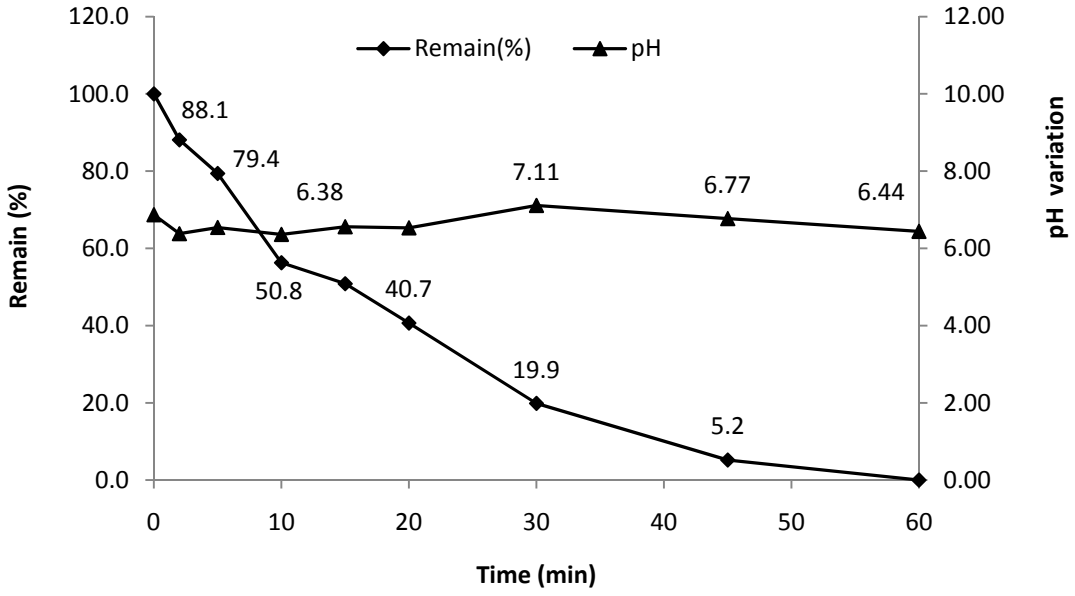

Figure (A26): Remaining percentage of p-Cresol and pH vs. time after treatment of p-Cresol by using graphite electrode at current density of 10mA/cm2

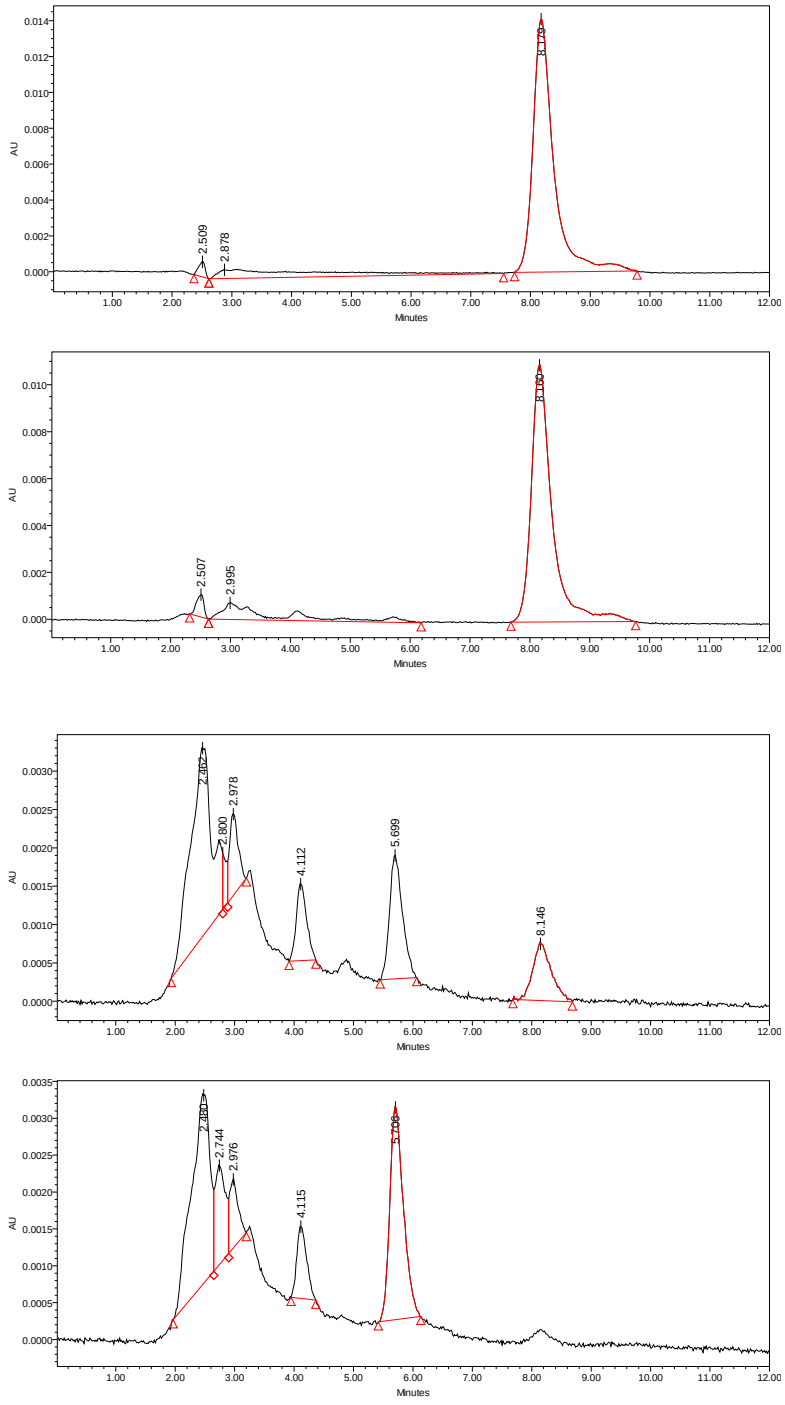

Figure (A27): HPLC chromatogram of p-Cresol for sample treated at 0, 5, 45 and 60 minutes interval time by using graphite electrode at current density of 10mA/cm2

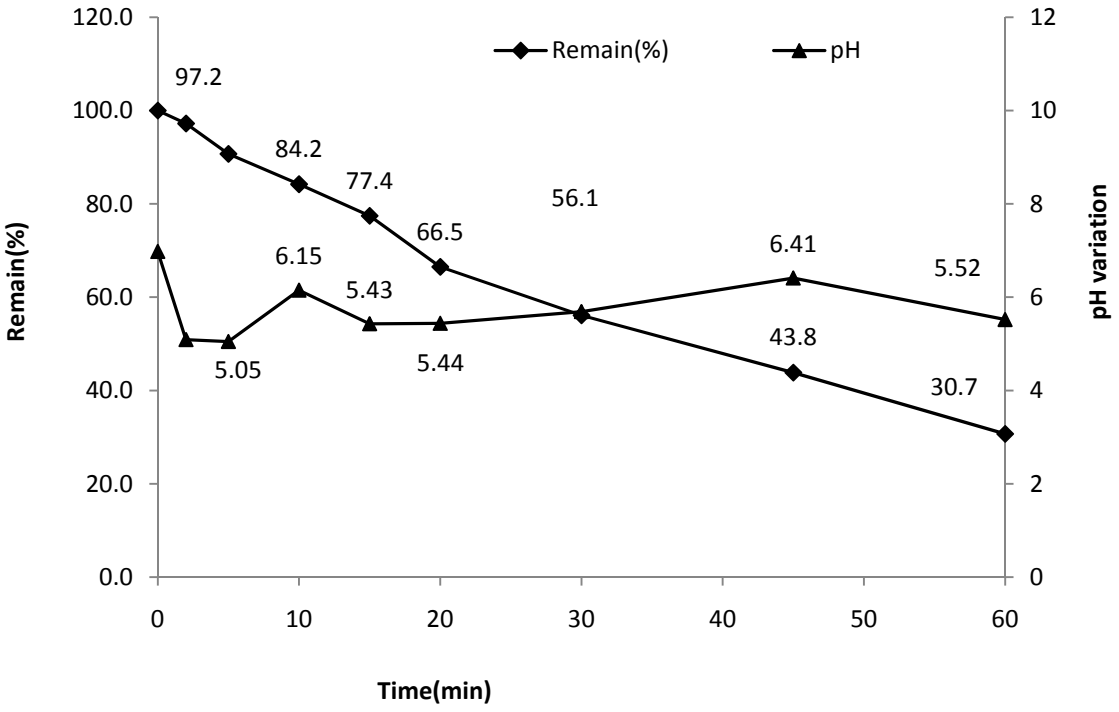

Figure (A28): Remaining percentage of p-Cresol and pH vs. time after treatment of p-Cresol by using graphite electrode at current density of 5mA/cm2

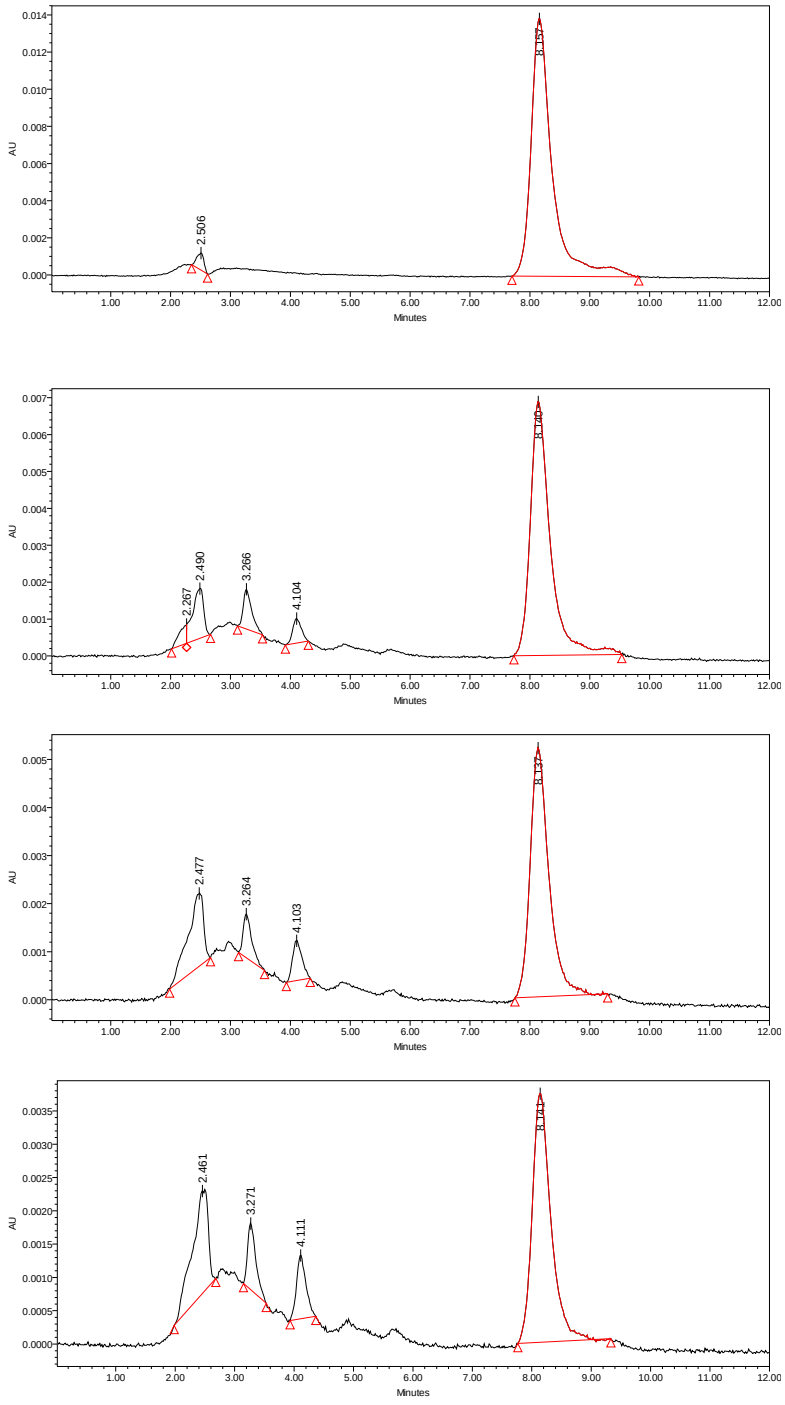

Figure (A29): HPLC chromatogram of p-Cresol for sample treated at 0, 30, 45, and 60 minute's interval time by using graphite electrode at current density of 5mA/cm2

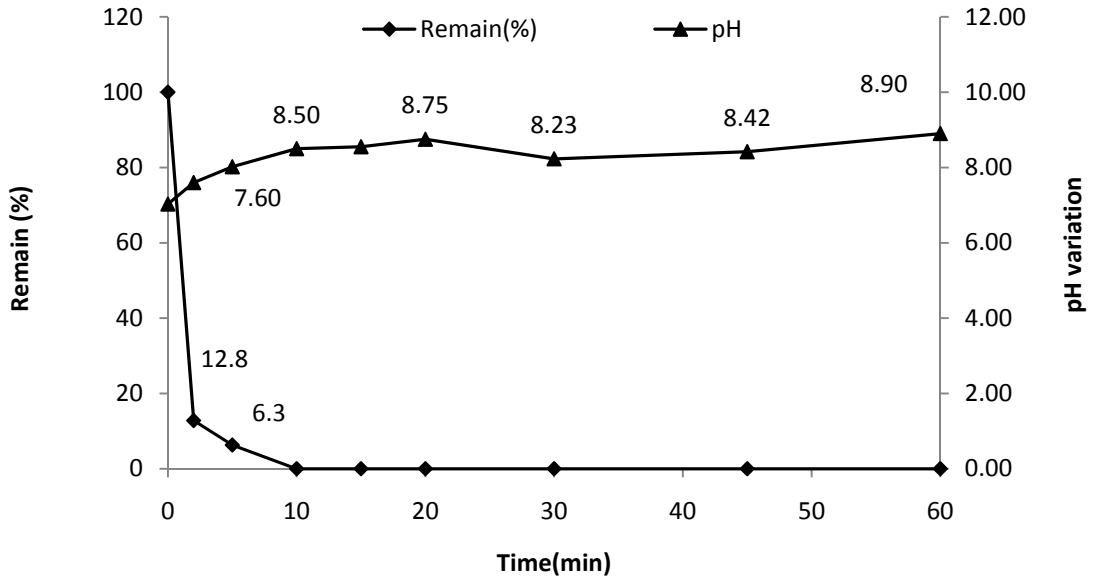

Figure (A30): Remaining percentage of p-Cresol and pH vs. time after treatment of p-Cresol by using diamond electrode at current density of 20mA/cm2

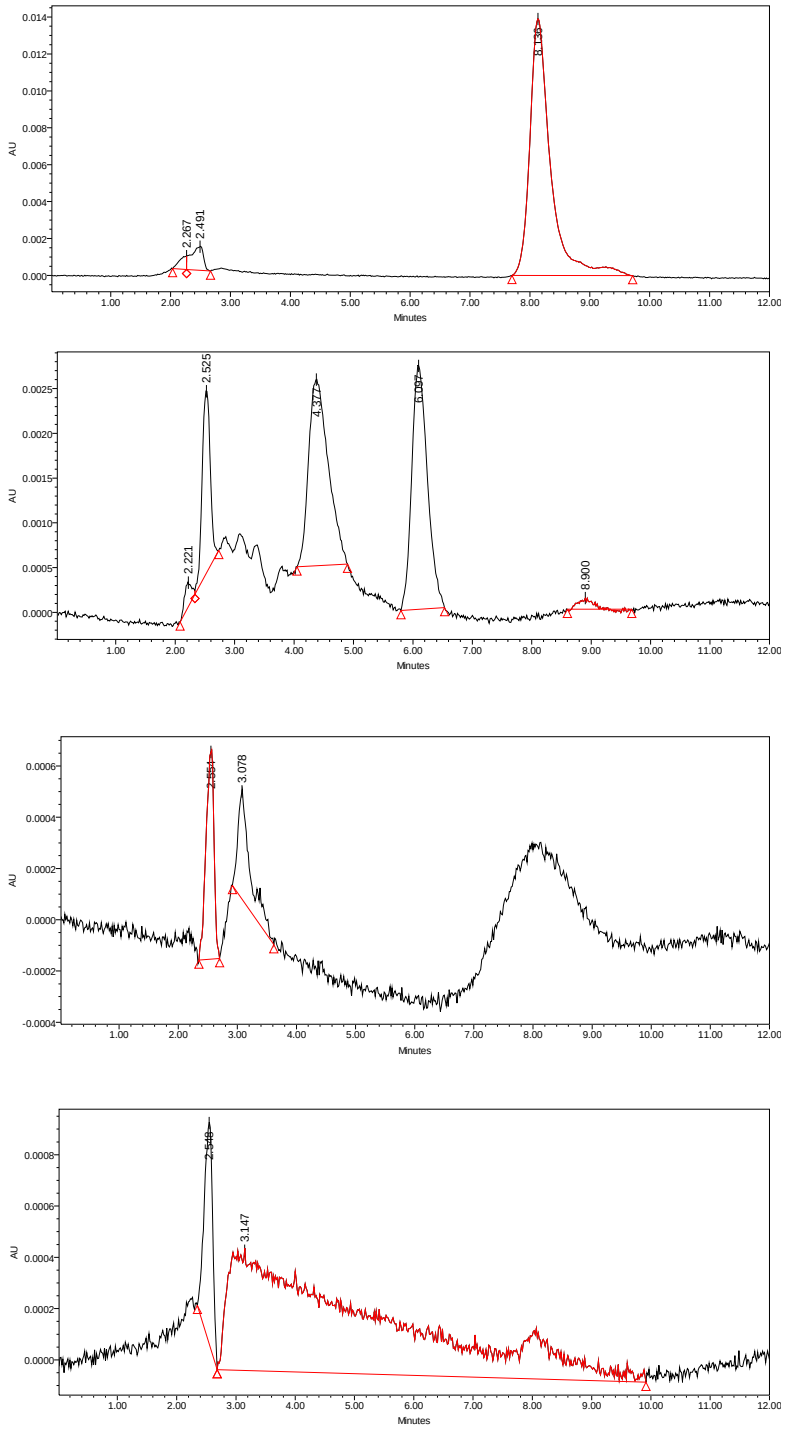

Figure (A31): HPLC chromatogram of p-Cresol for sample treated at 0, 2, 5, and 60 minutes interval time by using diamond electrode at current density of 20mA/cm2

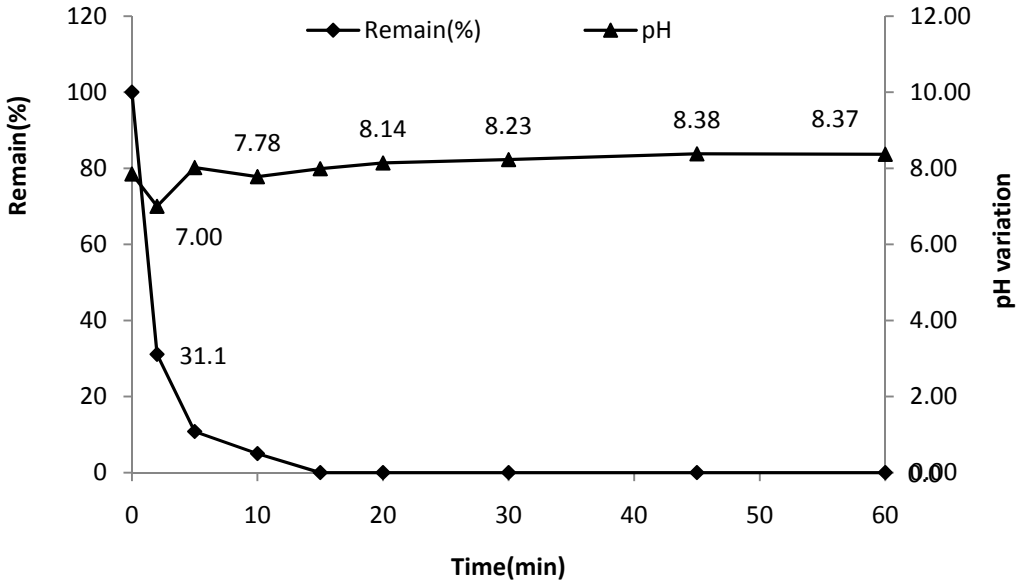

Figure (A32): Remaining percentage of p-Cresol and pH vs. time after treatment of p-Cresol by using diamond electrode at current density of 15mA/cm2

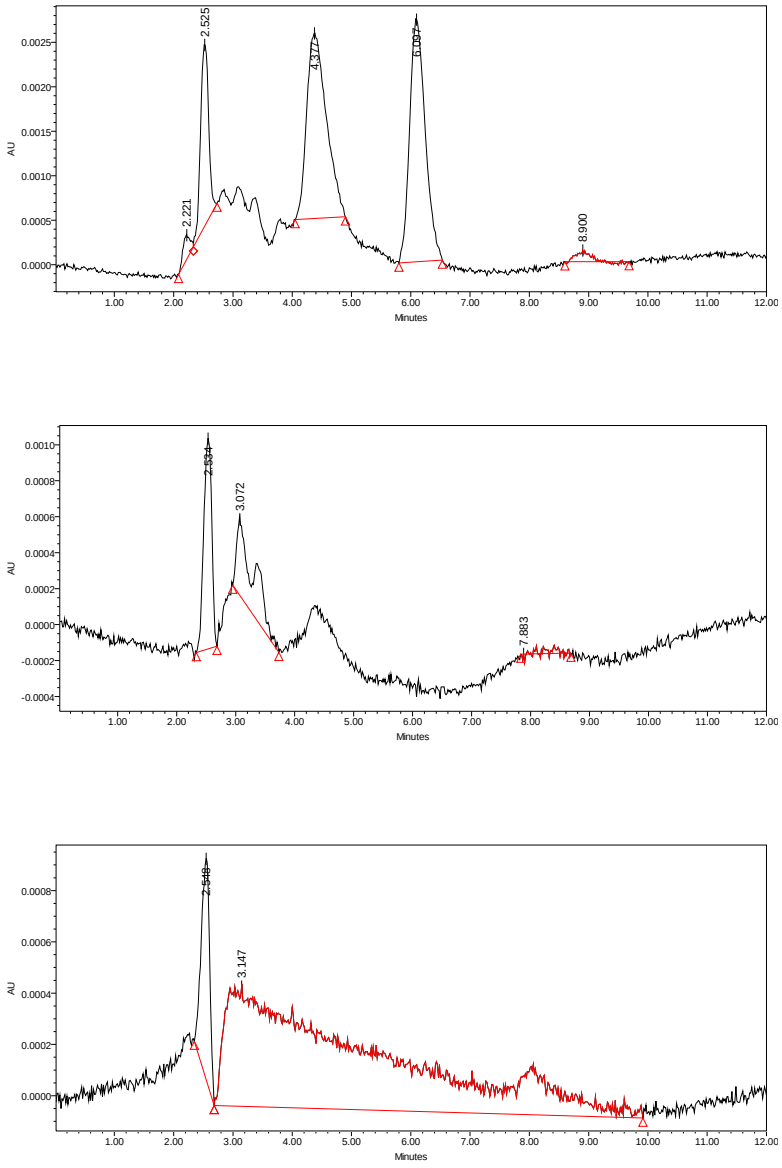

Figure (A33): HPLC chromatogram of p-Cresol for sample treated at 0, 2, 5, and 60 minutes interval time by using diamond electrode at current density of 15mA/cm2

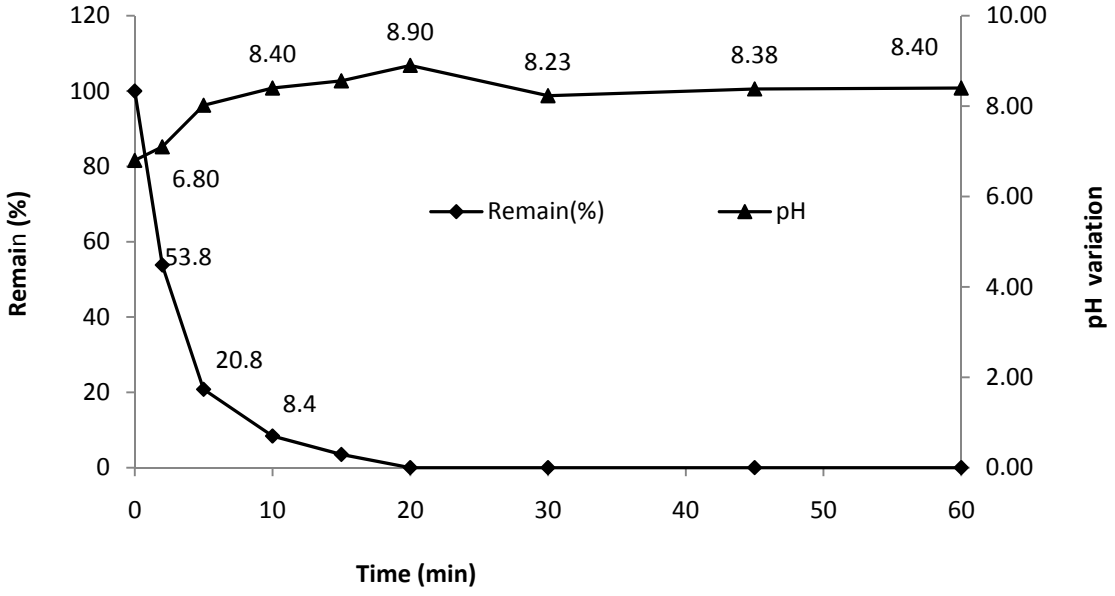

Figure (A34): Remaining percentage of p-Cresol and pH vs. time after treatment of p-Cresol by using diamond electrode at current density of 10mA/cm2

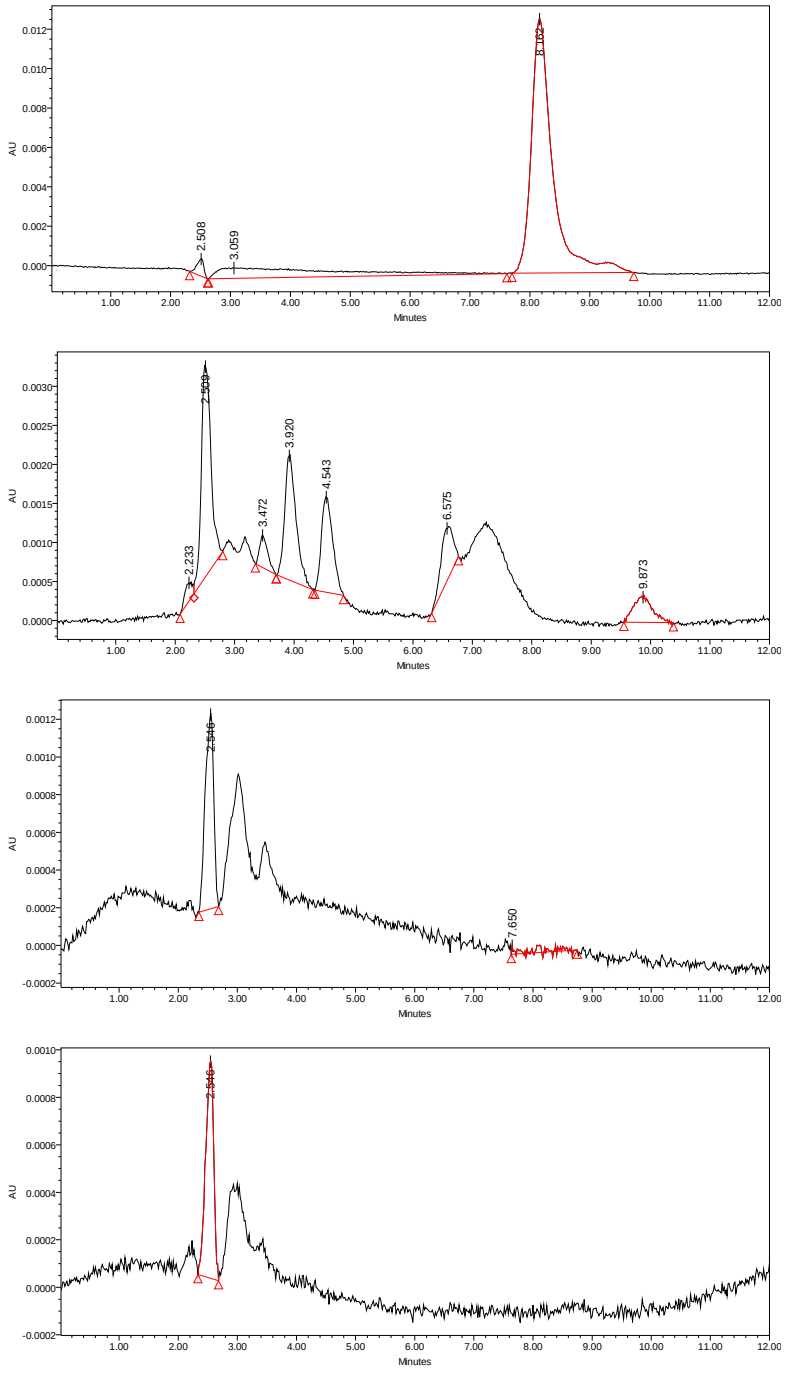

Figure (A35): HPLC chromatogram of p-Cresol for sample treated at 0, 10, 15, and 60 minutes interval time by using diamond electrode at current density of 10mA/cm2

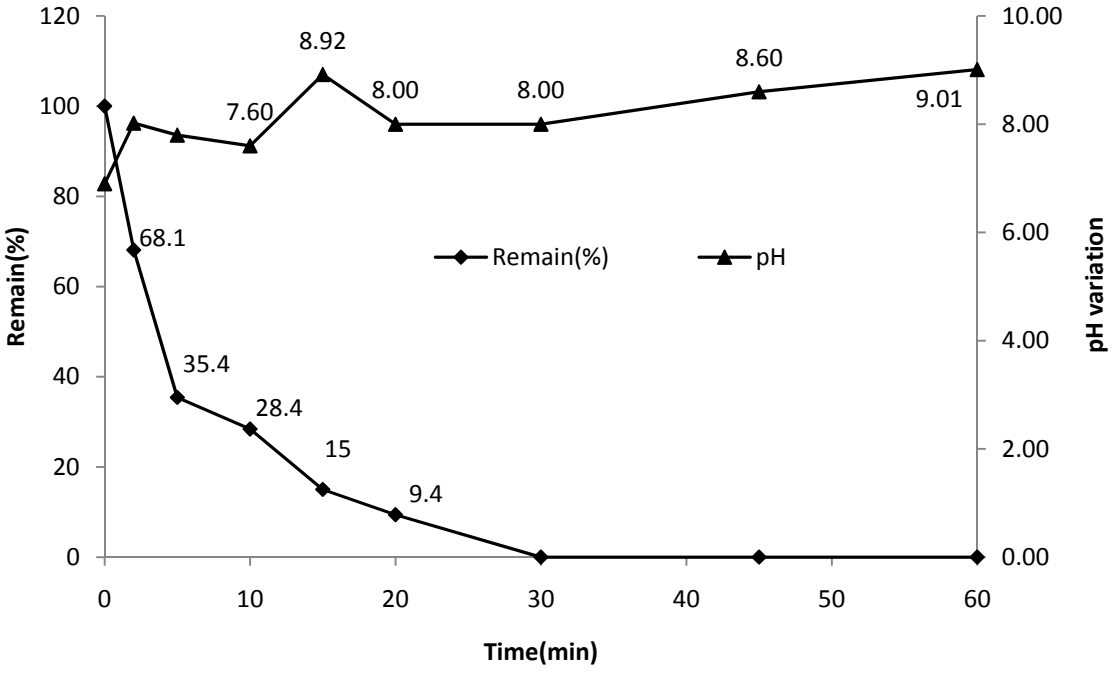

Figure (A36): Remaining percentage of p-Cresol and pH vs. time after treatment of p-Cresol by using diamond electrode at current density of 5mA/cm2

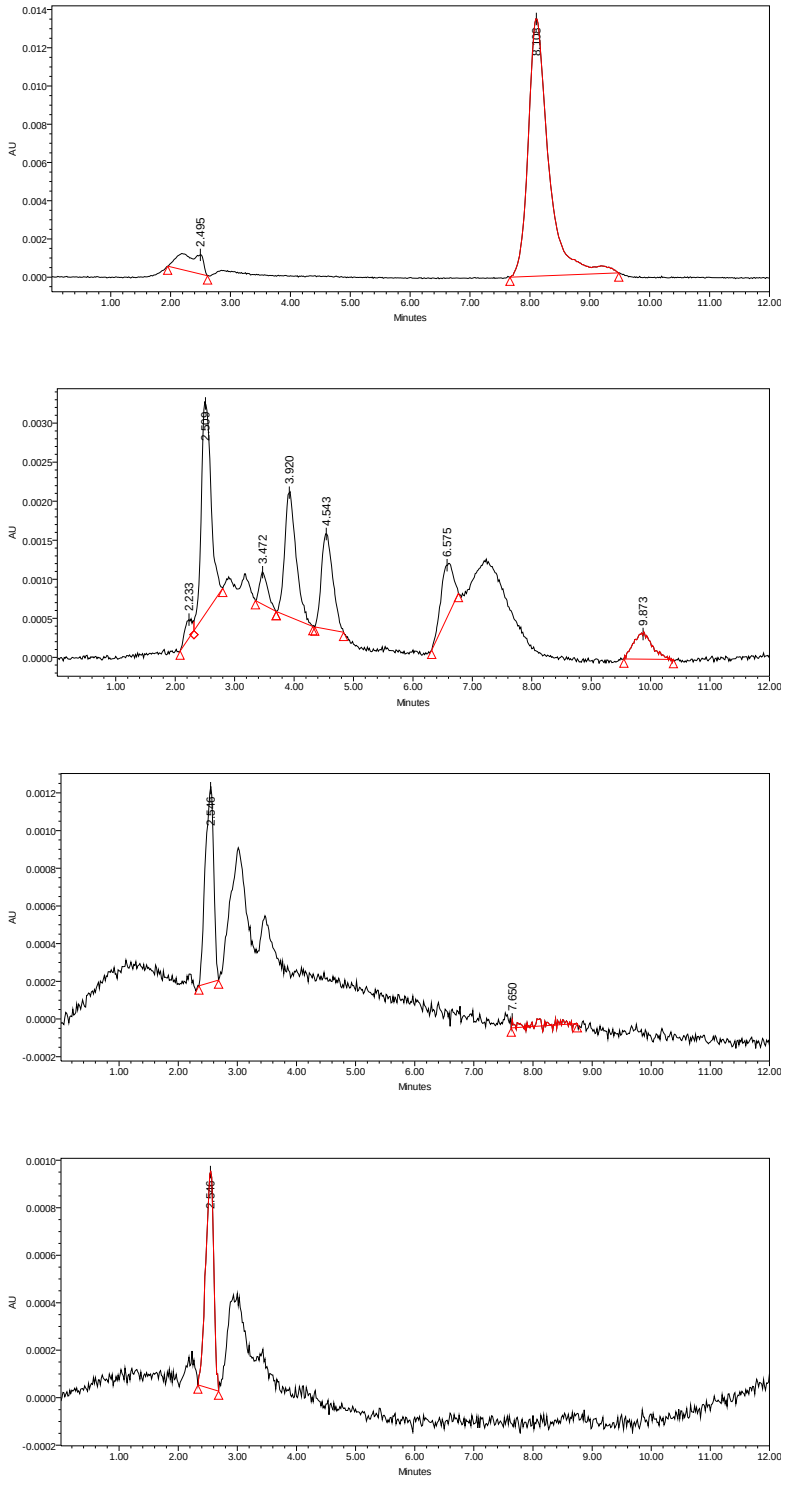

Figure (A37): HPLC chromatogram of p-Cresol for sample treated at 0, 10, 15, and 20 minutes interval time by using diamond electrode at current density of 5mA/cm2

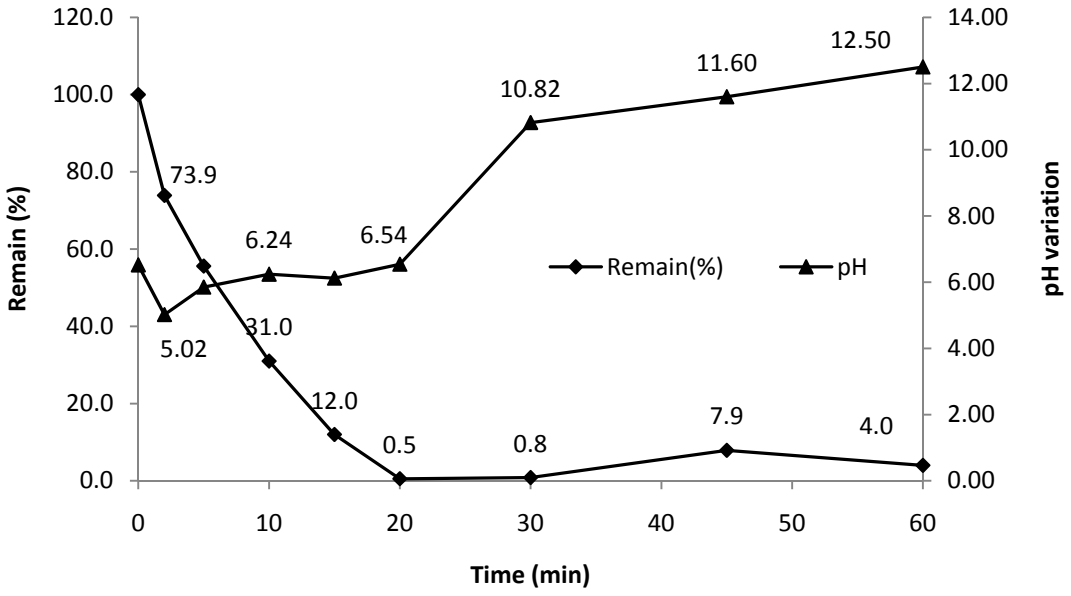

Figure (A38): Remaining percentage of p-Cresol and pH vs. time after treatment of p-Cresol by using stainless steel electrode at current density of 20mA/cm2

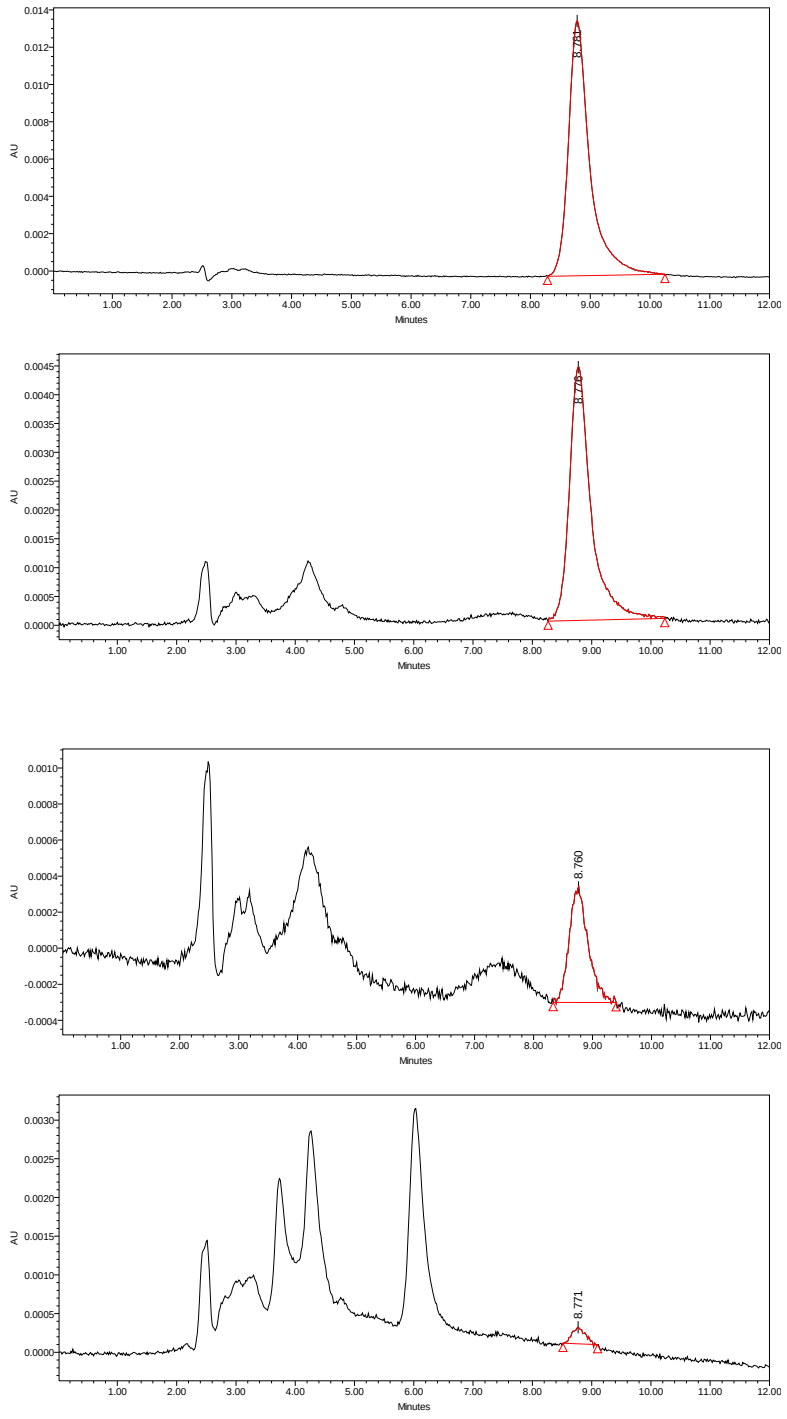

Figure (A39): HPLC chromatogram of p-Cresol for sample treated at 0, 15, 20, and 60 minutes interval time by using stainless steel electrode at current density of 20mA/cm2

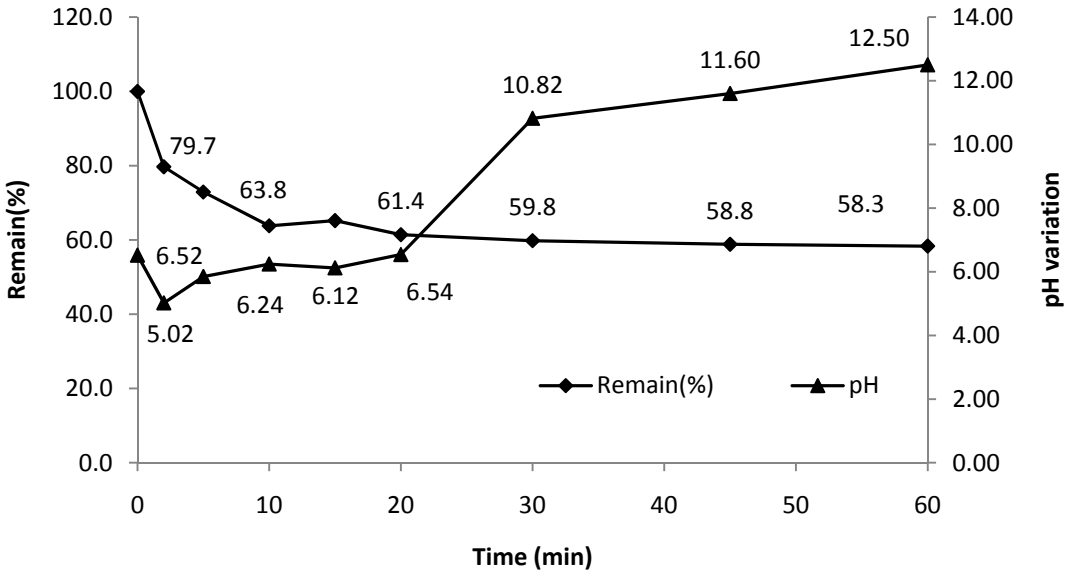

Figure (A40): Remaining percentage of p-Cresol and pH vs. time after treatment of p-Cresol by using stainless steel electrode at current density of 15mA/cm2

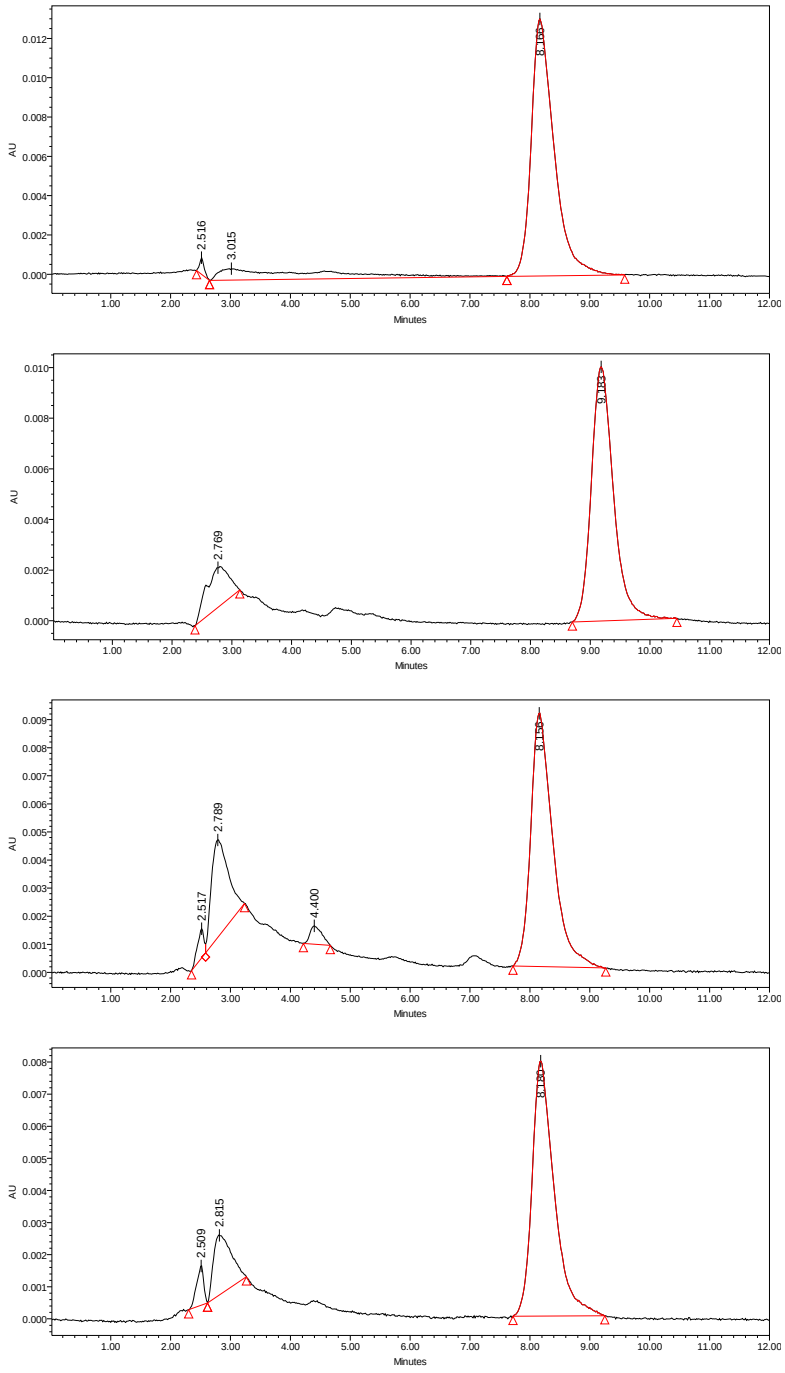

Figure (A41): HPLC chromatogram of p-Cresol for sample treated at 0, 15, 45, and 60minutes interval time by using stainless steel electrode at current density of 15mA/cm2

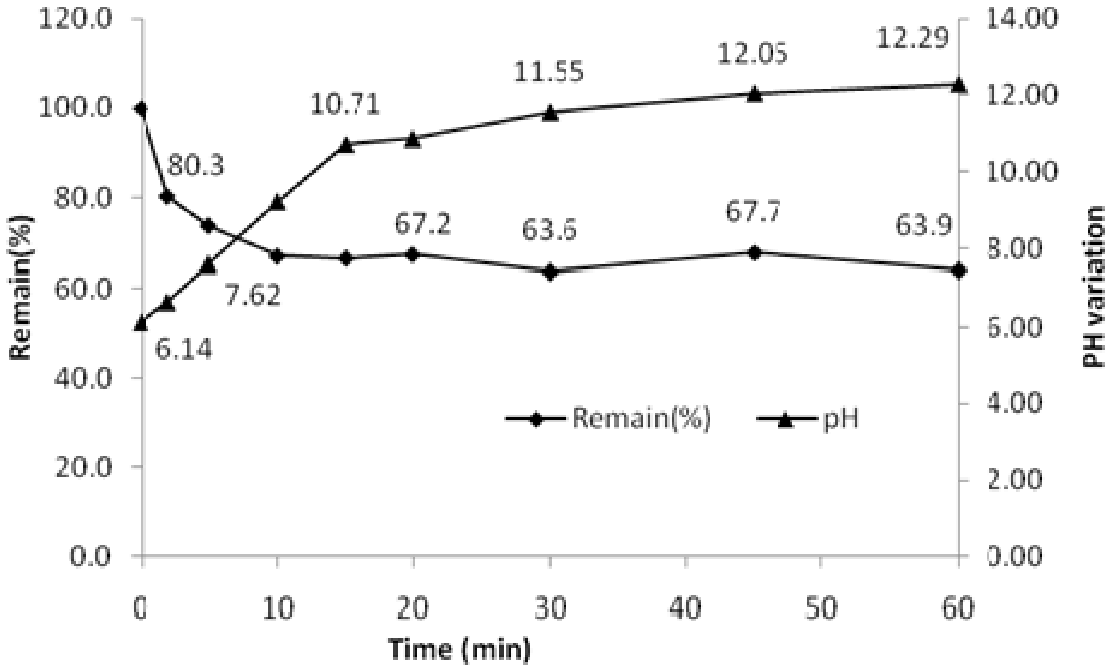

Figure (A42): Remaining percentage of p-Cresol and pH vs. time after treatment of p-Cresol by using stainless steel electrode at current density of 10mA/cm2

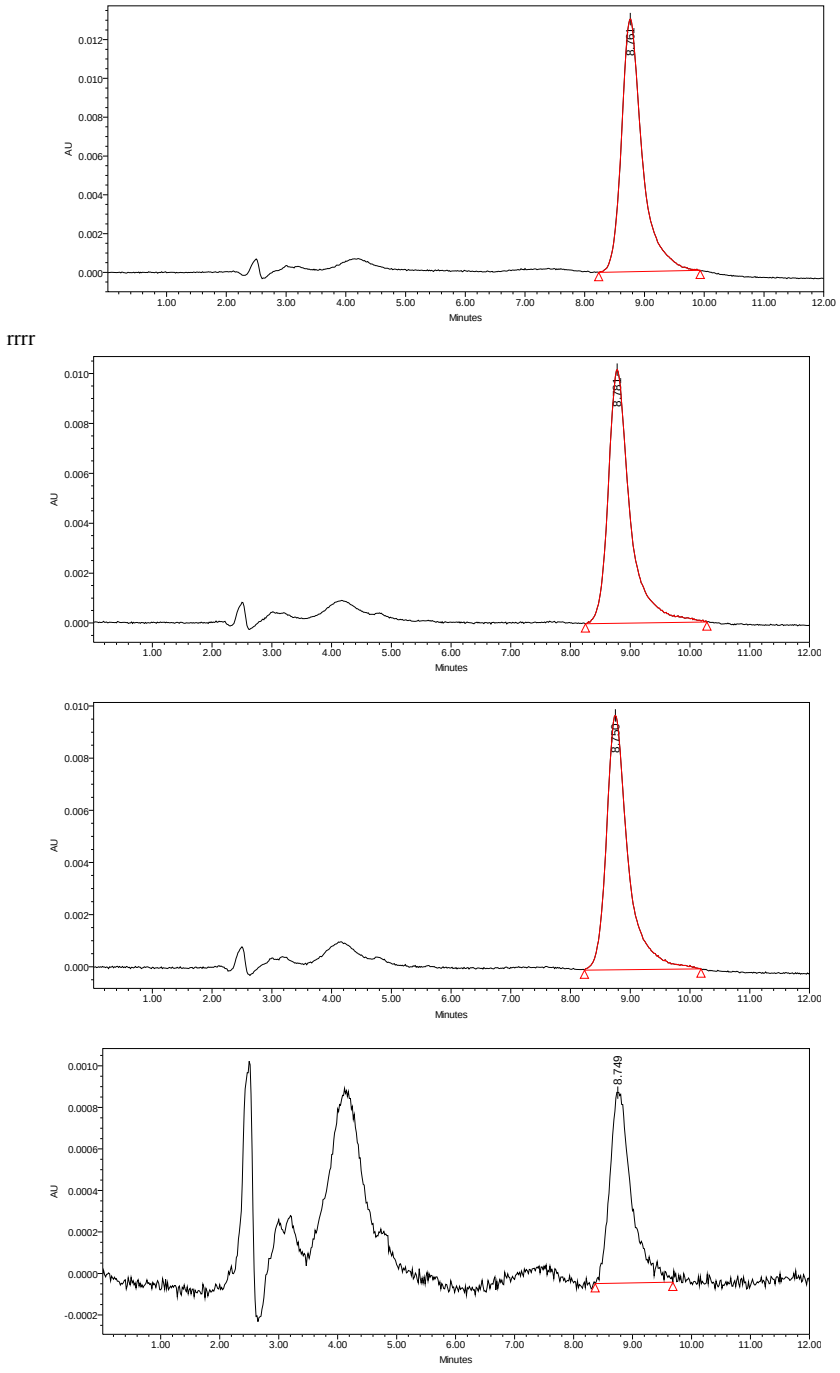

Figure (A43): HPLC chromatogram of p-Cresol for sample treated at 0, 15, 45, and 60minutes interval time by using stainless steel electrode at current density of 10mA/cm2

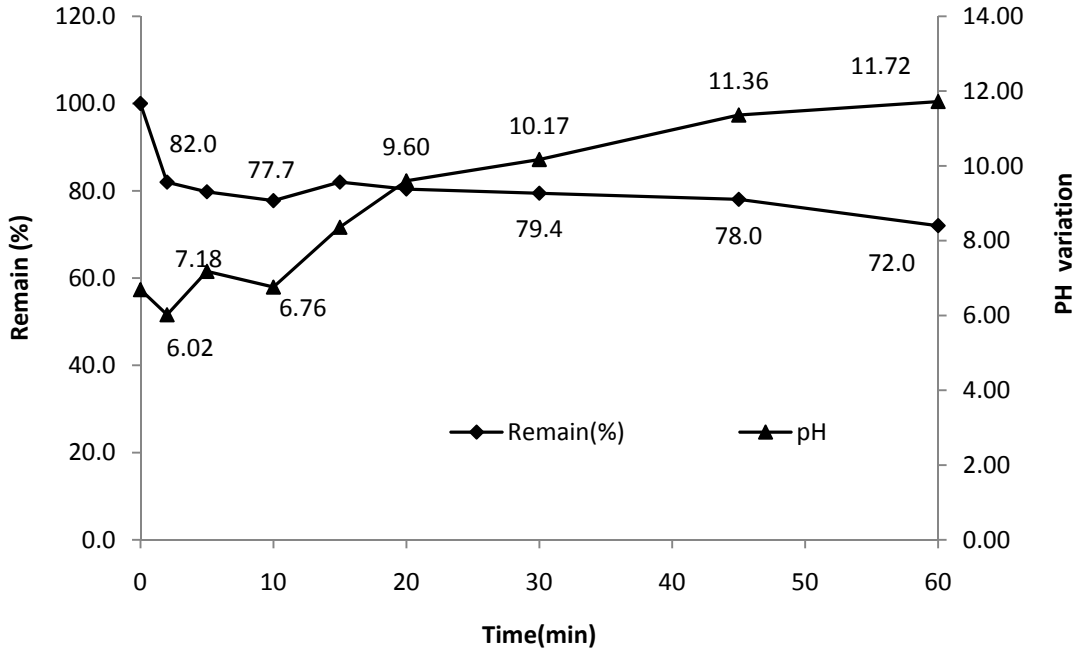

Figure (A44): Remaining percentage of p-Cresol and pH vs. time after treatment of p-Cresol by using stainless steel electrode at current density of 5mA/cm2

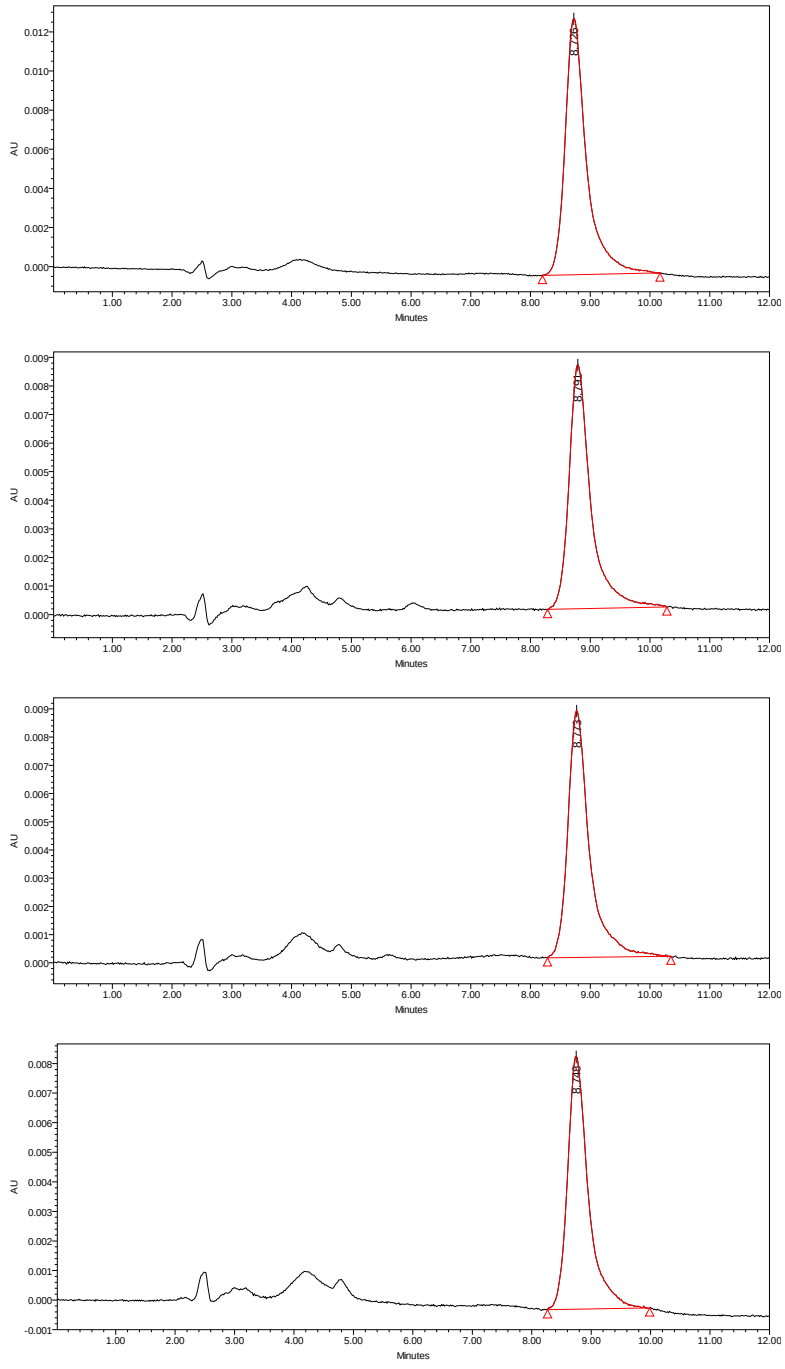

Figure (A45): HPLC chromatogram of p-Cresol for sample treated at 0, 15, 45, and 60minutes interval time by using stainless steel electrode at current density of 5mA/cm2

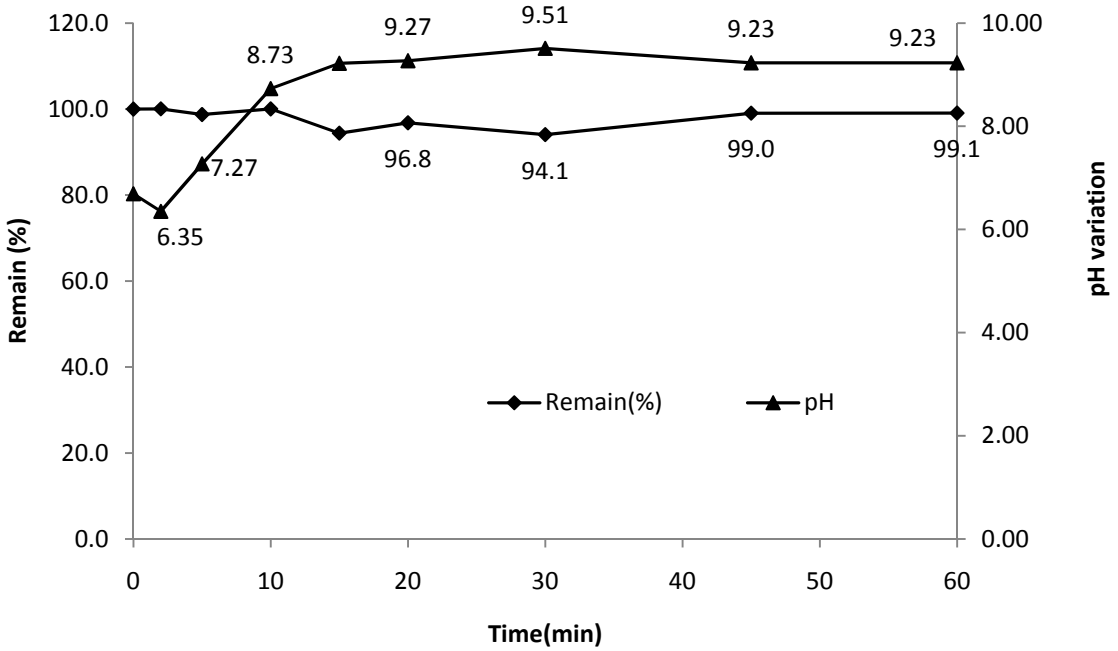

Figure (A46): Remaining percentage of p-Cresol and pH vs. time after treatment of p-Cresol by using aluminum electrode at current density of 20mA/cm2

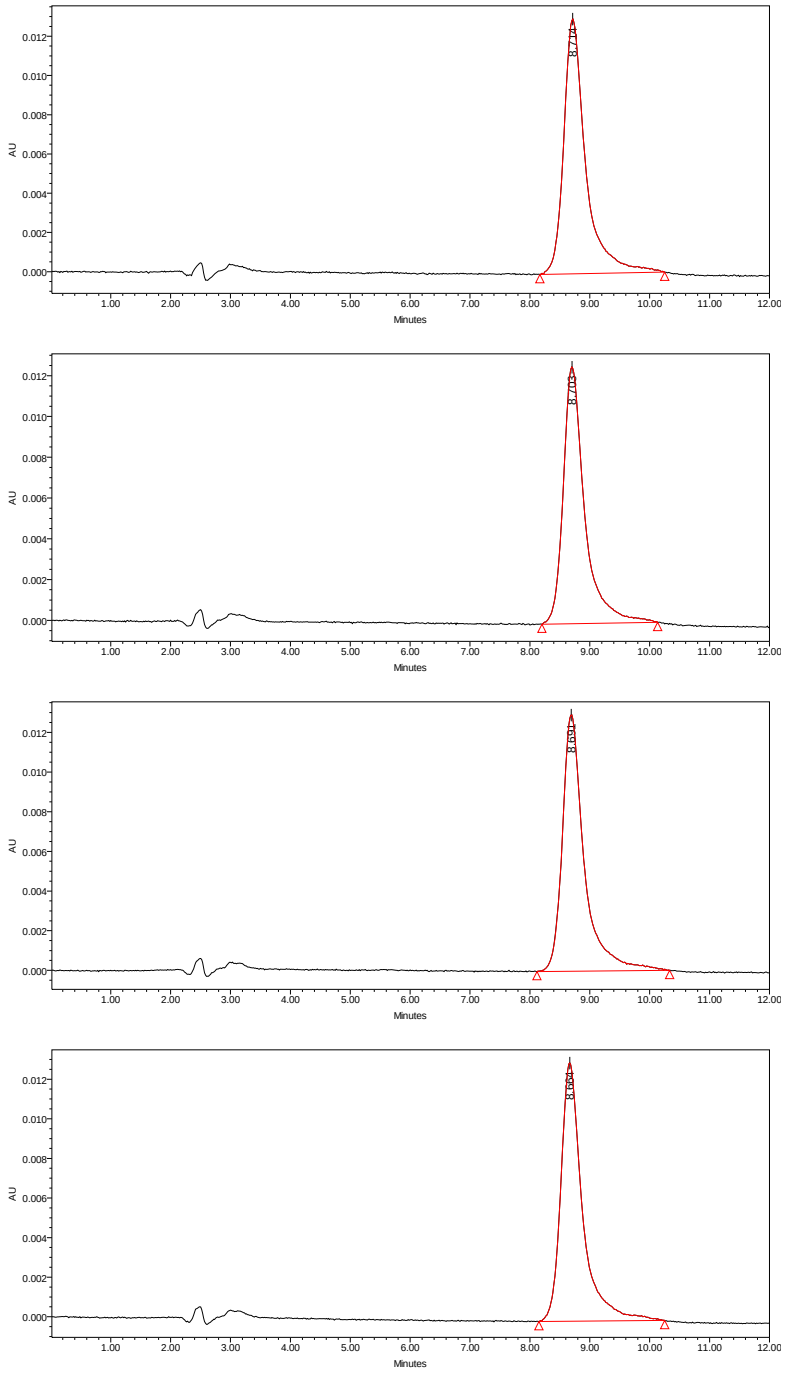

Figure (A47): HPLC chromatogram of p-Cresol for sample treated at 0, 15, 45, and 60minutes interval time by using aluminum electrode at current density of 20mA/cm2

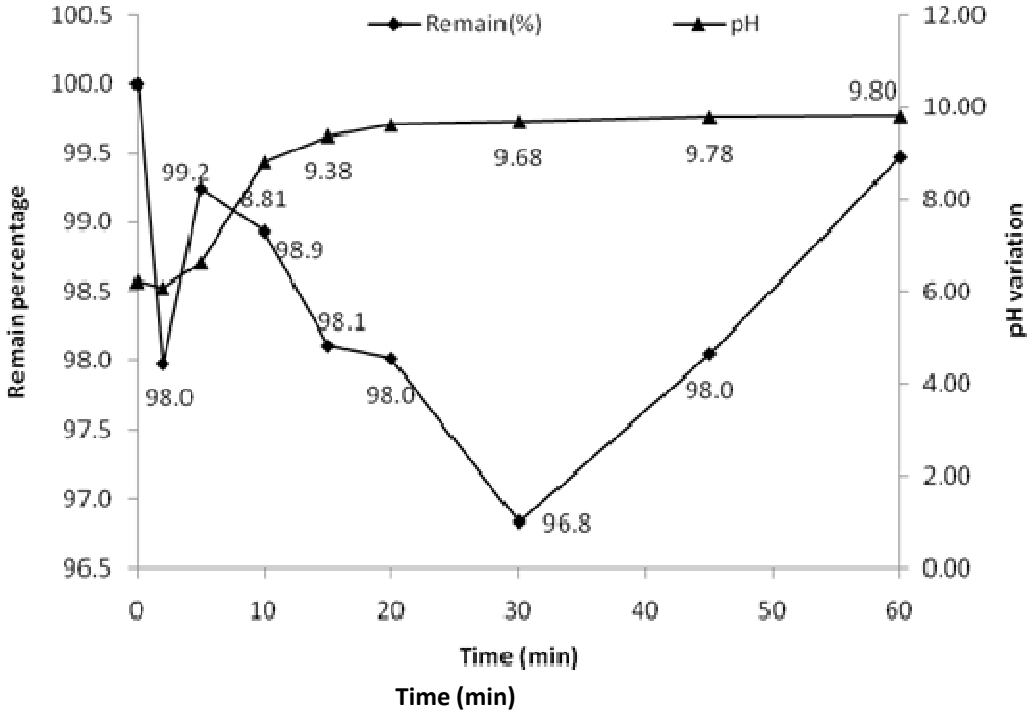

Figure (A48): Remaining percentage of p-Cresol and pH vs. time after treatment of p-Cresol by using aluminum electrode at current density of 15mA/cm2

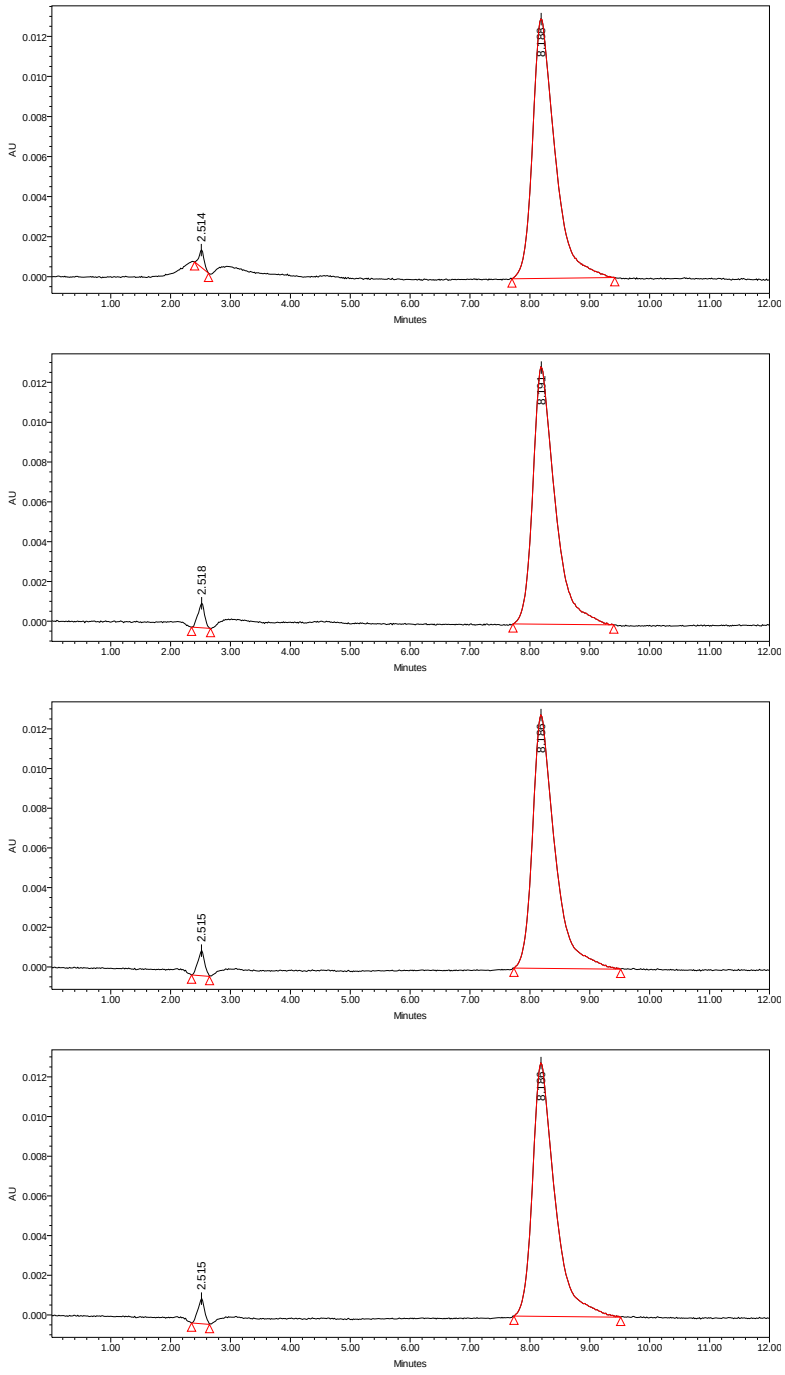

Figure (A49): HPLC chromatogram of p-Cresol for sample treated at 0, 15, 45, and 60minutes interval time by using aluminum electrode at current density of 15mA/cm2

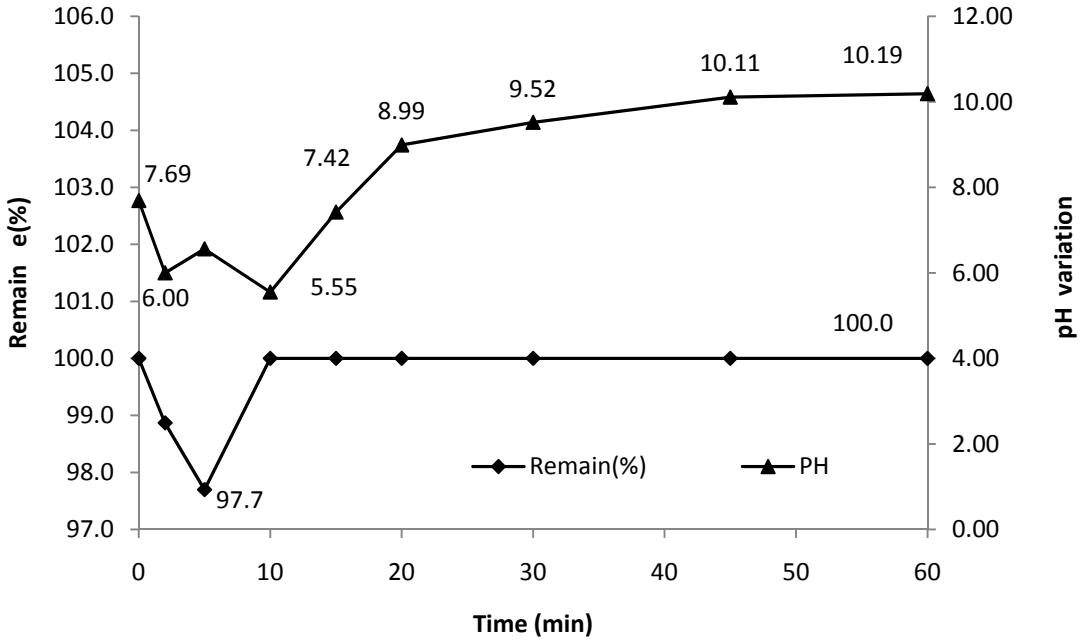

Figure (A50): Remaining percentage of p-Cresol and pH vs. time after treatment of p-Cresol by using aluminum electrode at current density of 10mA/cm2

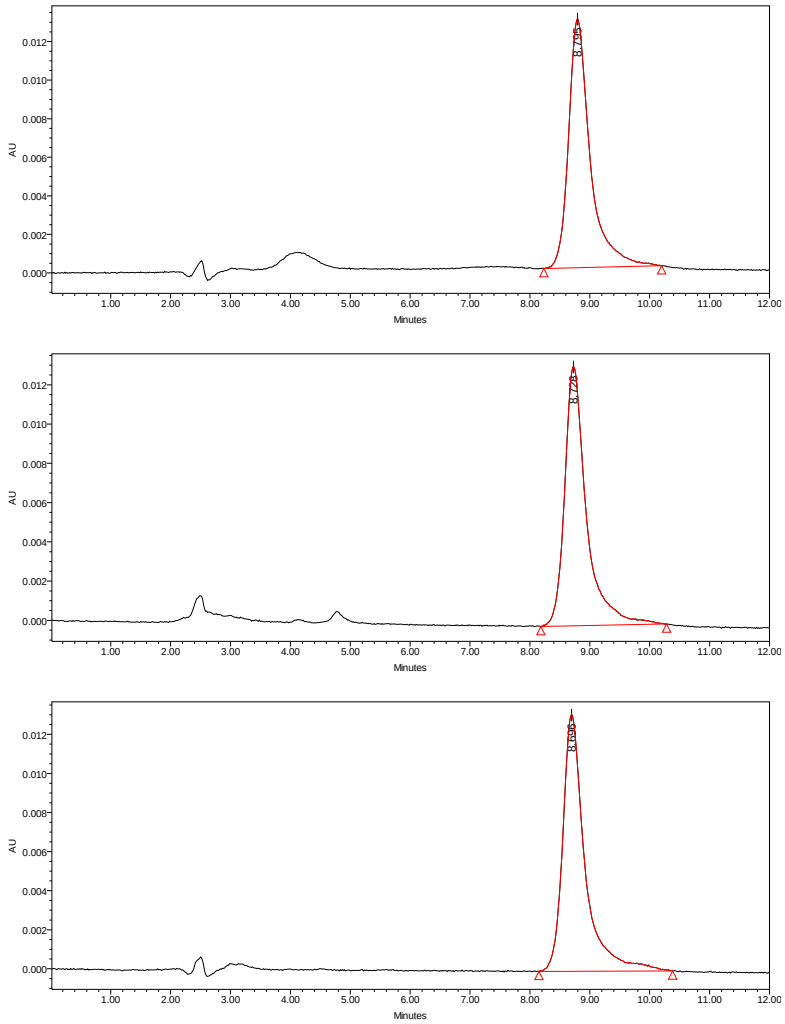

Figure (A51): HPLC chromatogram of p-Cresol for sample treated at 0, 15, 45, and 60minutes interval time by using aluminum electrode at current density of 10mA/cm2

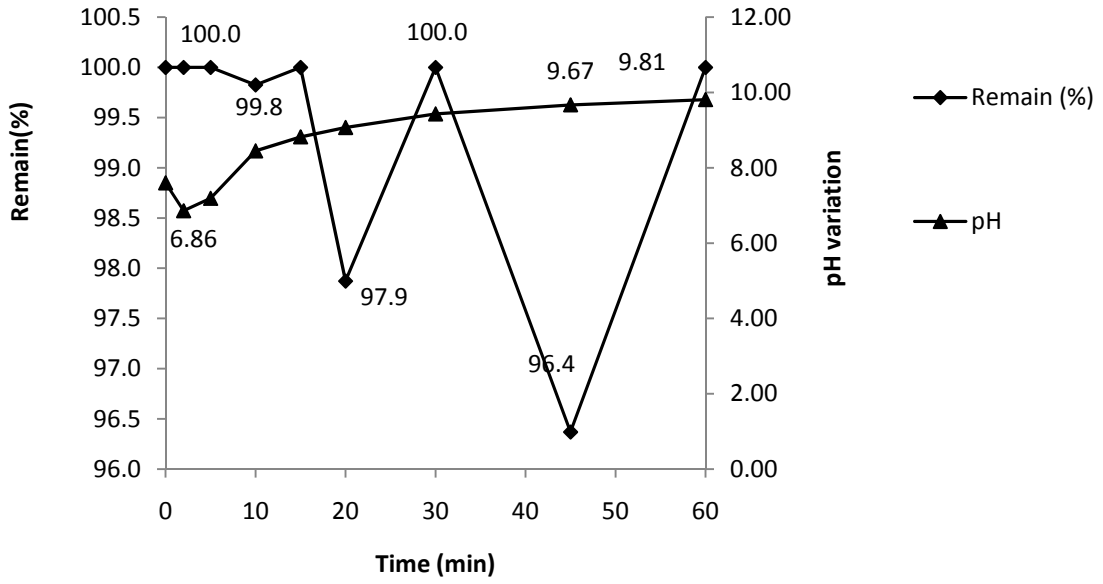

Figure (A52): Remaining percentage of p-Cresol and pH vs. time after treatment of p-Cresol by using aluminum electrode at current density of 5mA/cm2

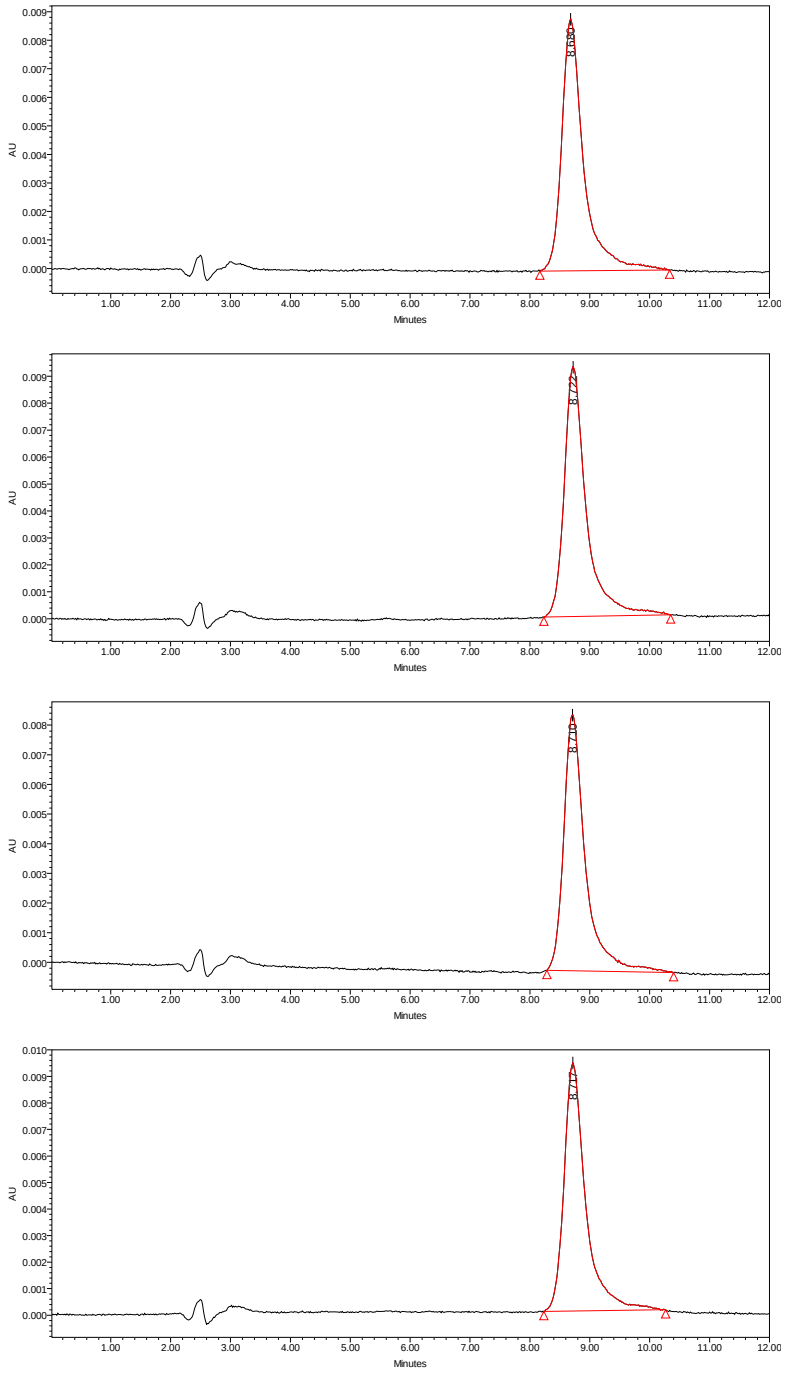

Figure (A53): HPLC chromatogram of p-Cresol for sample treated at 0, 15, 45, and 60minutes interval time by using aluminum electrode at current density of 5mA/cm2

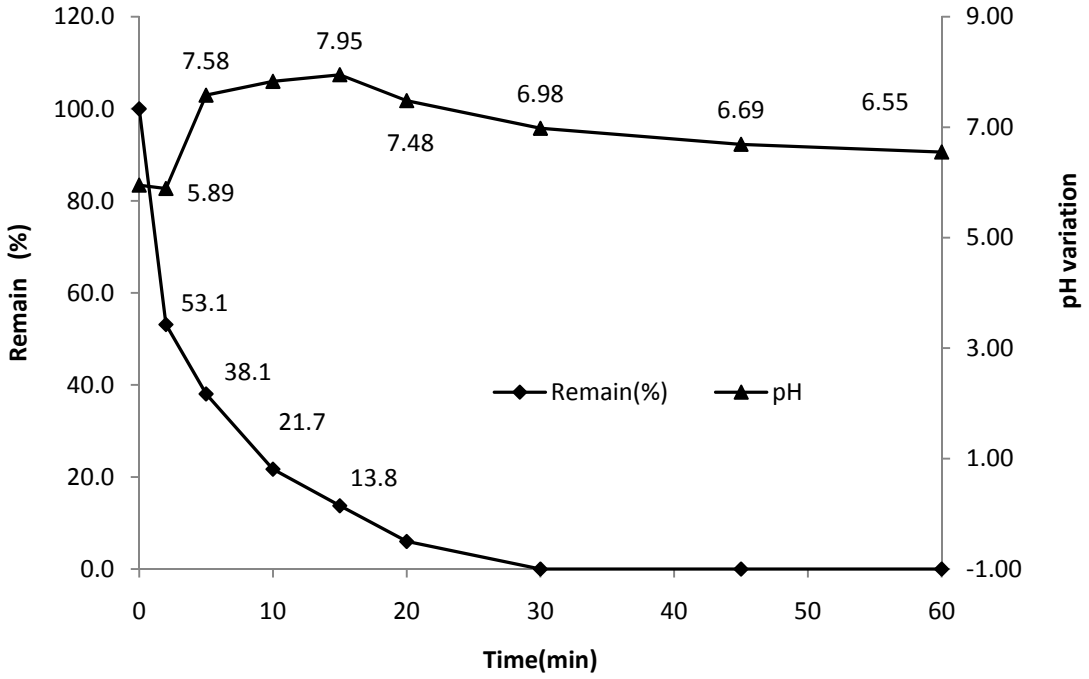

Figure (A54): Remaining percentage of p-Cresol and pH vs. time after treatment of p-Cresol by using graphite electrode with (0) second polarity time and current density of 15mA/cm2

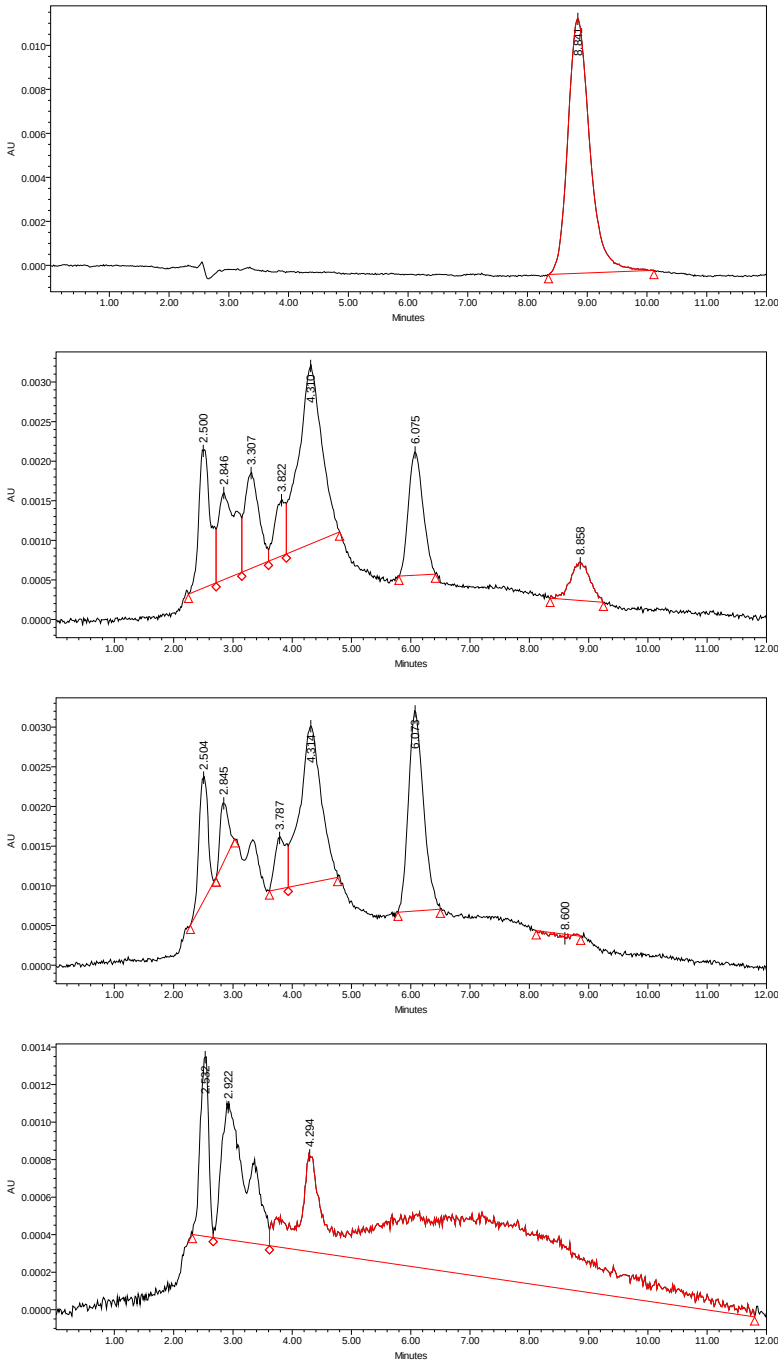

Figure (A55): HPLC chromatogram of p-Cresol for sample treated at 0, 15, 20, and 60minutes interval time by using graphite electrode at current density of 15mA/cm^2 with (0) second polarity time

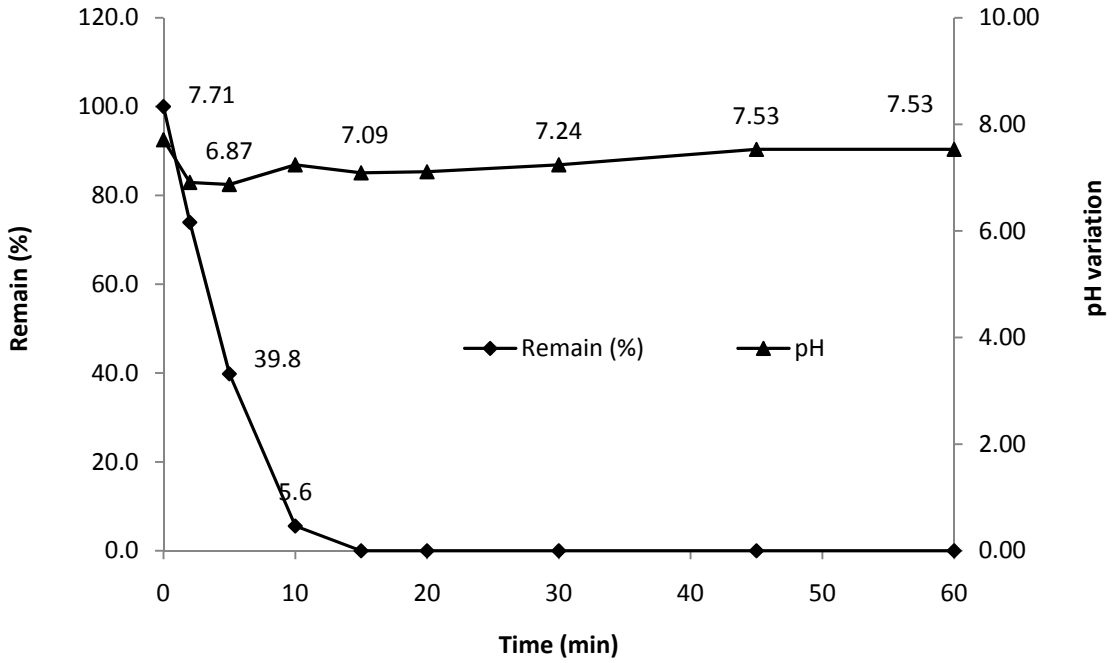

Figure (A56): Remaining percentage of p-Cresol and pH vs. time after treatment of p-Cresol by using graphite electrode with (30) second polarity time and current density of 15mA/cm2

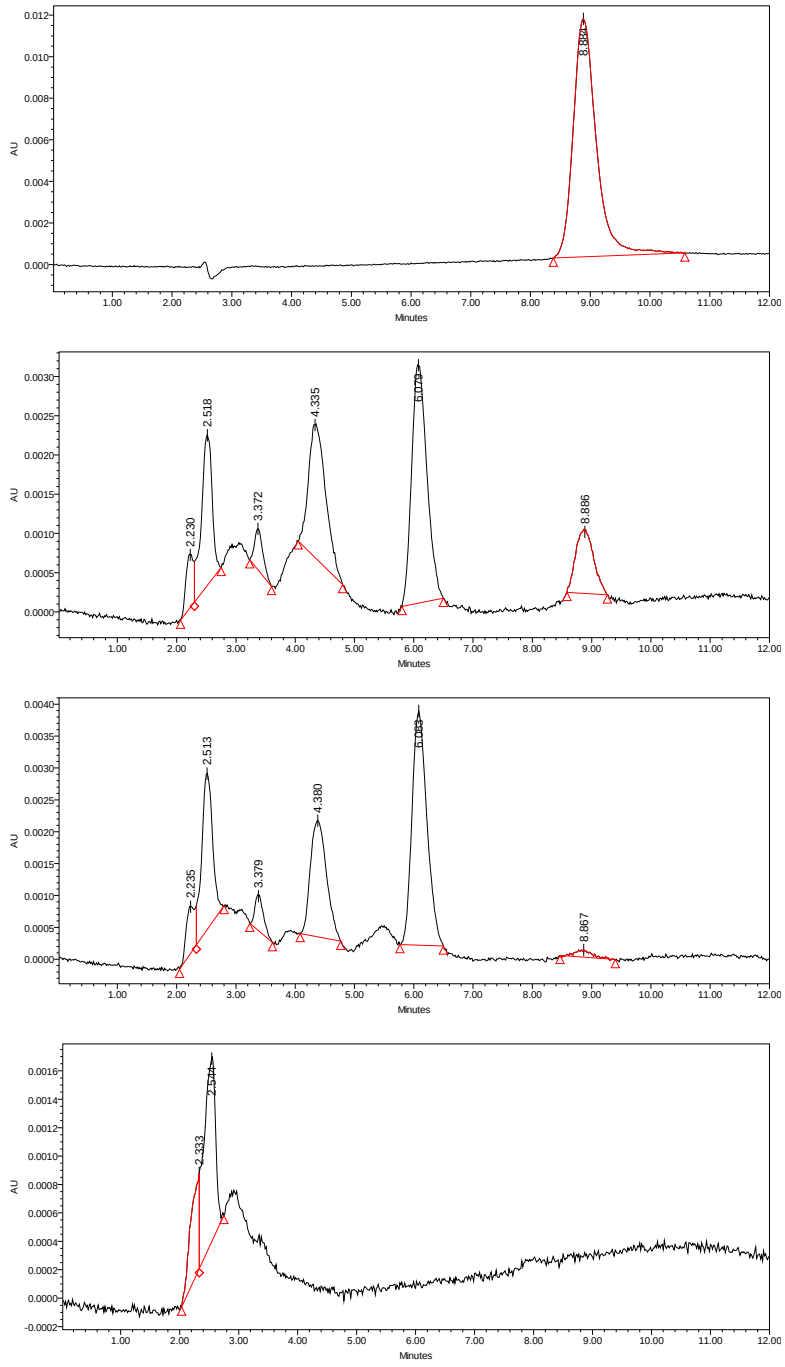

Figure (A57): HPLC chromatogram of p-Cresol for sample treated at 0, 10, 15, and 60minutes interval time by using graphite electrode at current density of 15mA/cm2 with (30) seconds polarity time

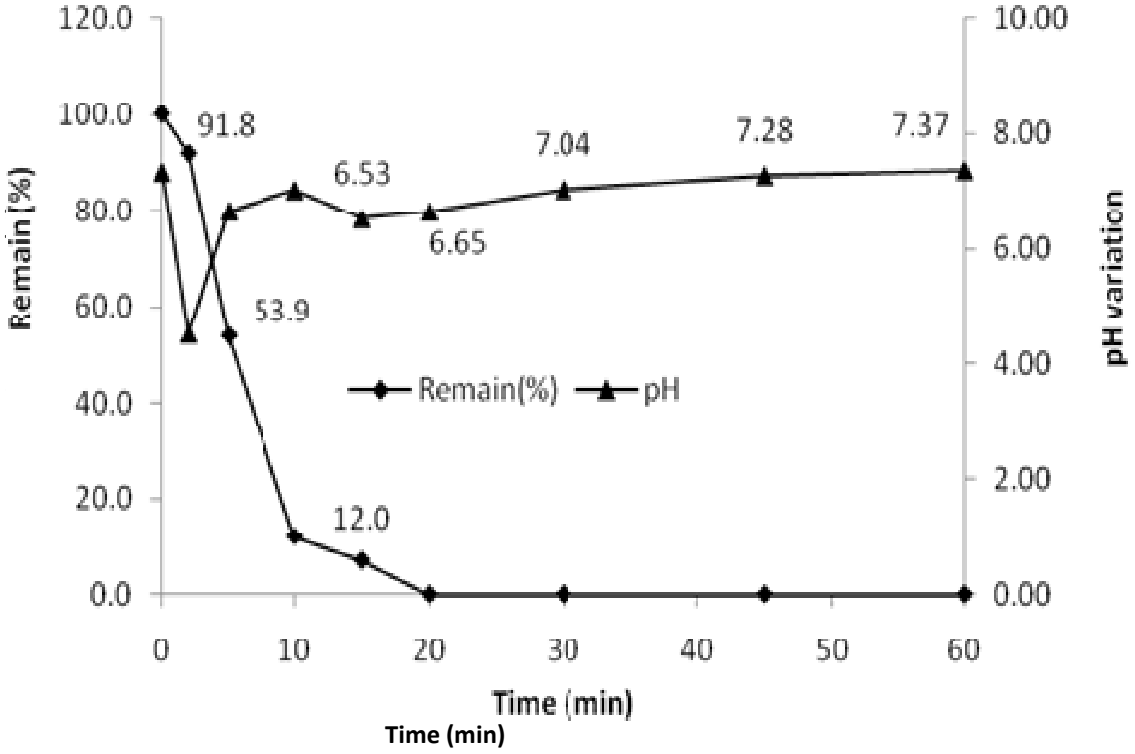

Figure (A58): Remaining percentage of p-Cresol and pH vs. time after treatment of p-Cresol by using graphite electrode with (45) second polarity time and current density of 15mA/cm2

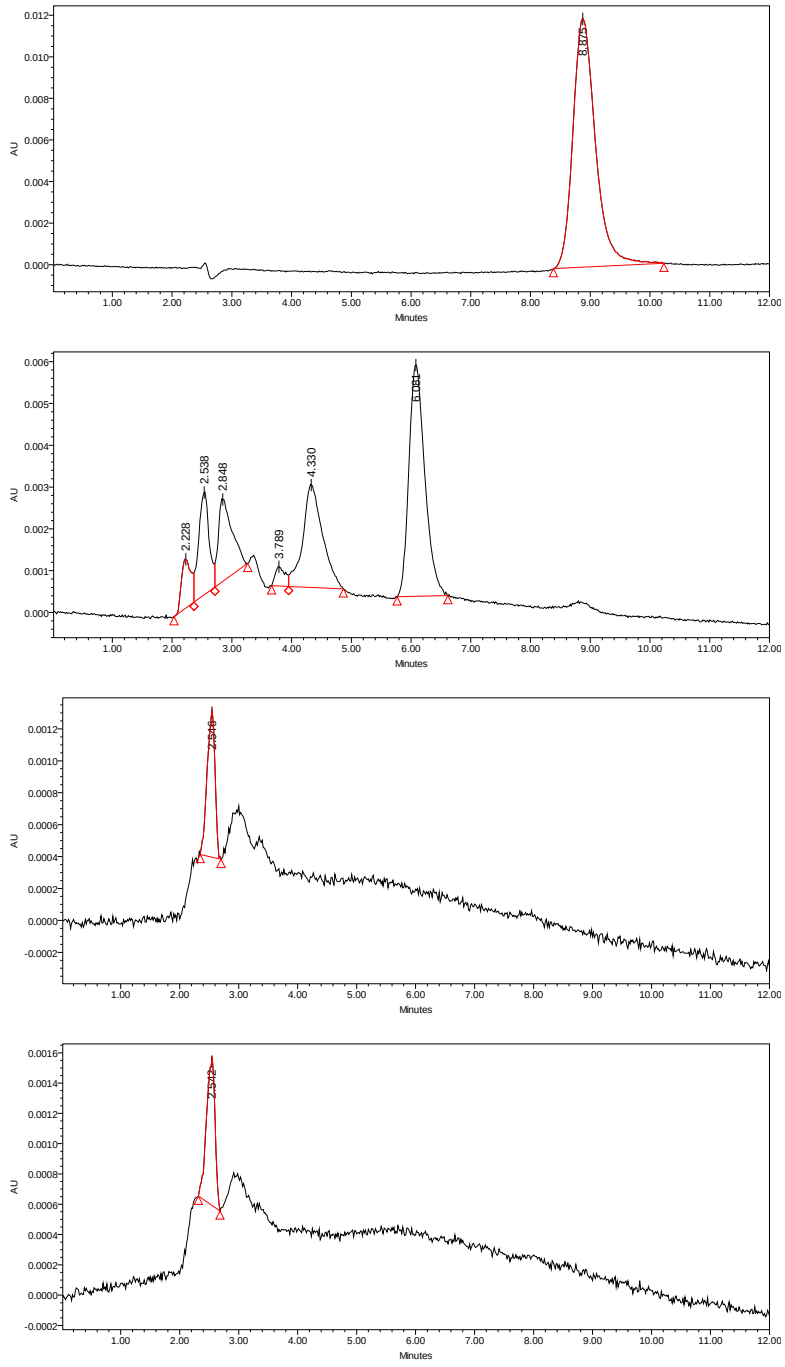

Figure (A59): HPLC chromatogram of p-Cresol for sample treated at 0, 10, 15, and 60minutes interval time by using graphite electrode at current density of 15mA/cm2 with (45) seconds polarity time

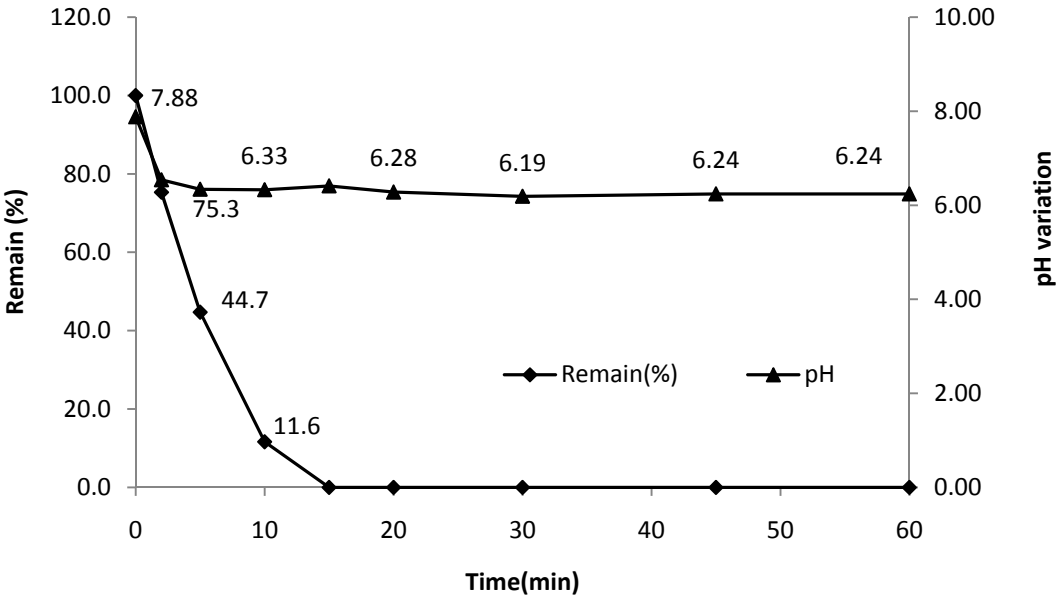

Figure (A60): Remaining percentage of p-Cresol and pH vs. time after treatment of p-Cresol by using graphite electrode with (60) second polarity time and current density of 15mA/cm2

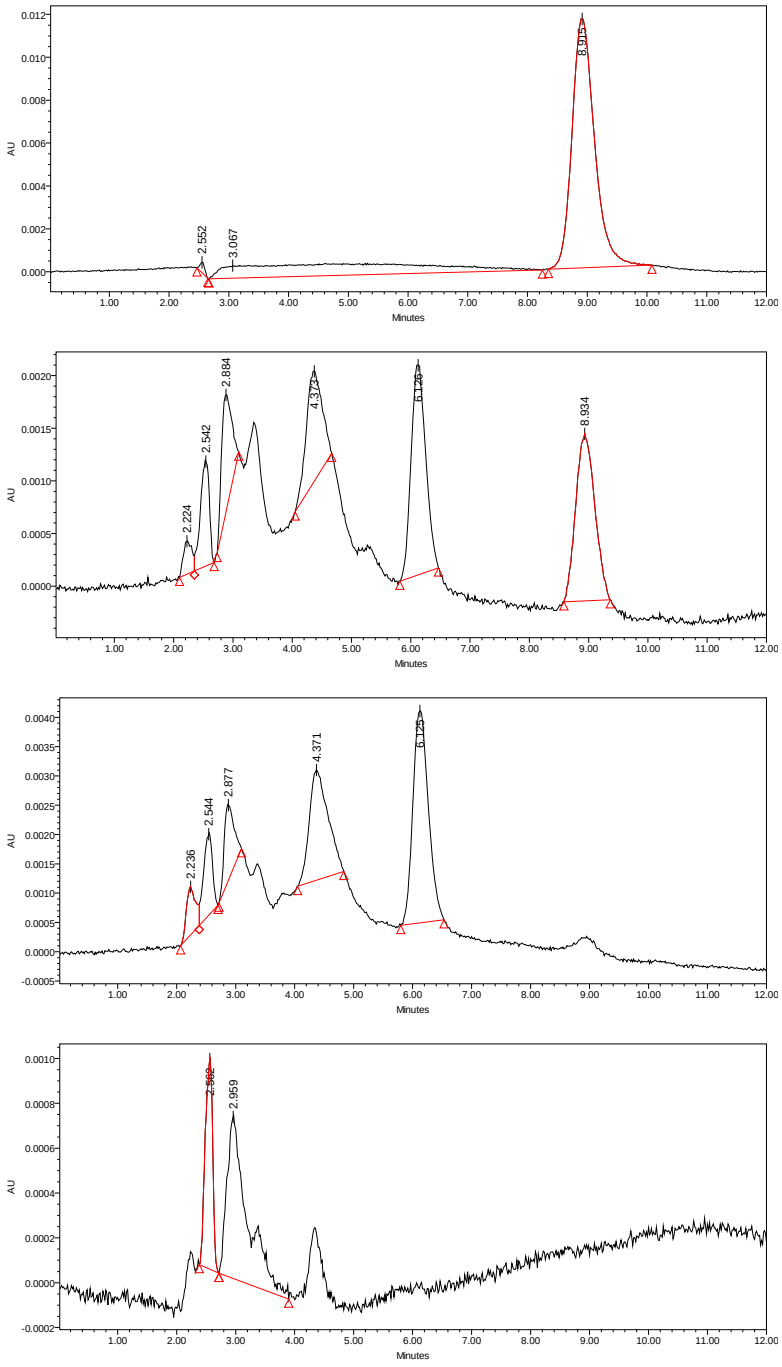

Figure (A61): HPLC chromatogram of p-Cresol for sample treated at 0, 10, 15, and 60minutes interval time by using graphite electrode at current density of 15mA/cm2 with (60) seconds polarity time

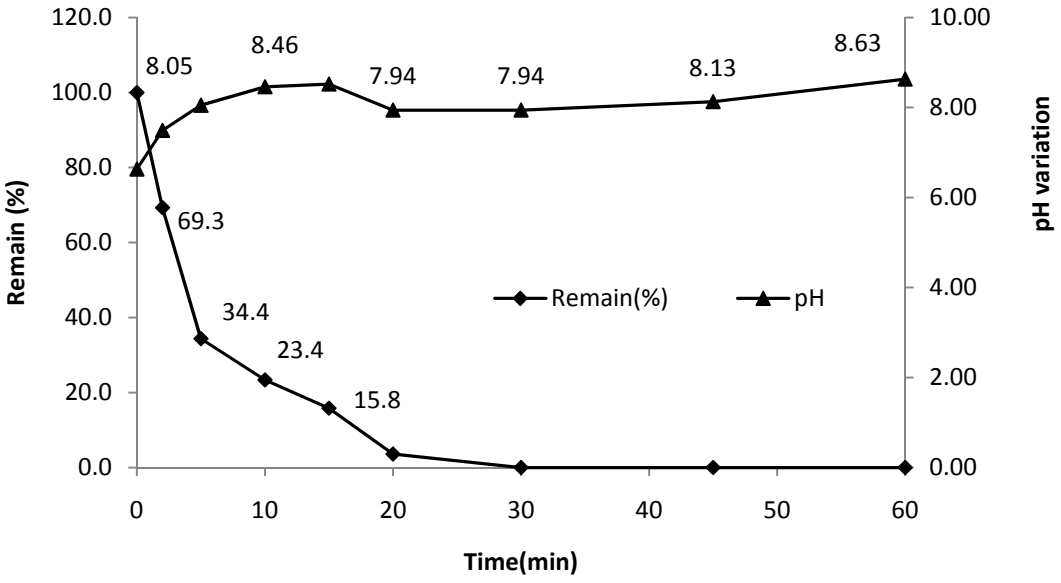

Figure (A62): Remaining percentage of p-Cresol and pH vs. time after treatment of p-Cresol by using diamond electrode with (0) second polarity time and current density of 5mA/cm2

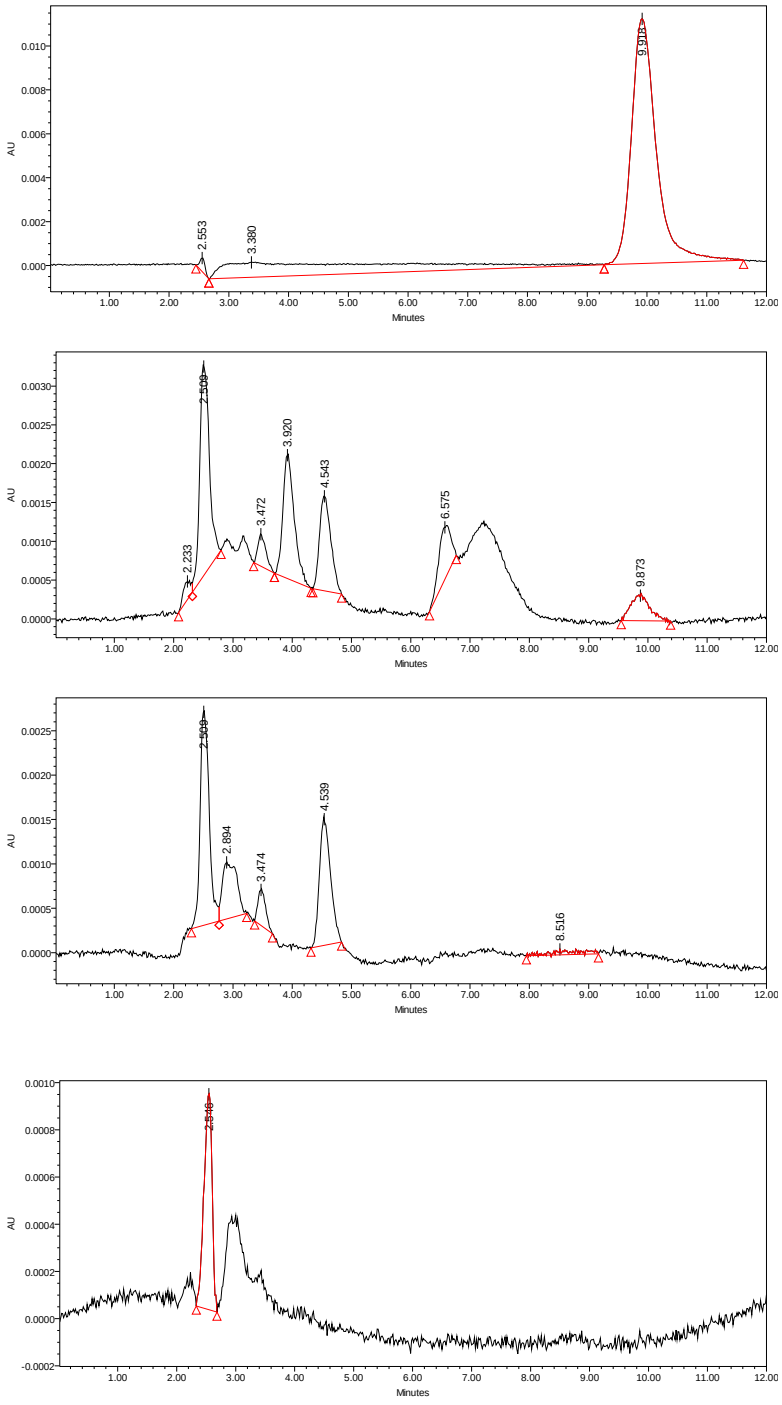

Figure (A63): HPLC chromatogram of p-Cresol for sample treated at 0, 10, 20, and 60minutes interval time by using diamond electrode at current density of 5mA/cm2 with (0) seconds polarity time

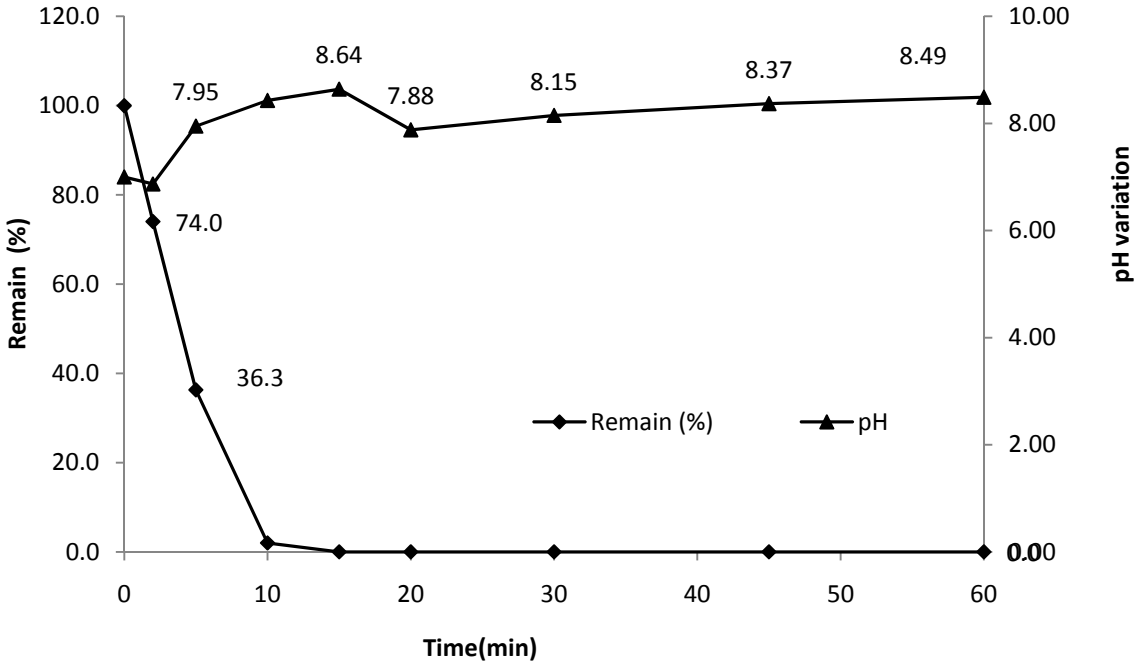

Figure (A64): Remaining percentage of p-Cresol and pH vs. time after treatment of p-Cresol by using diamond electrode with (30) seconds polarity time and current density of 5mA/cm2

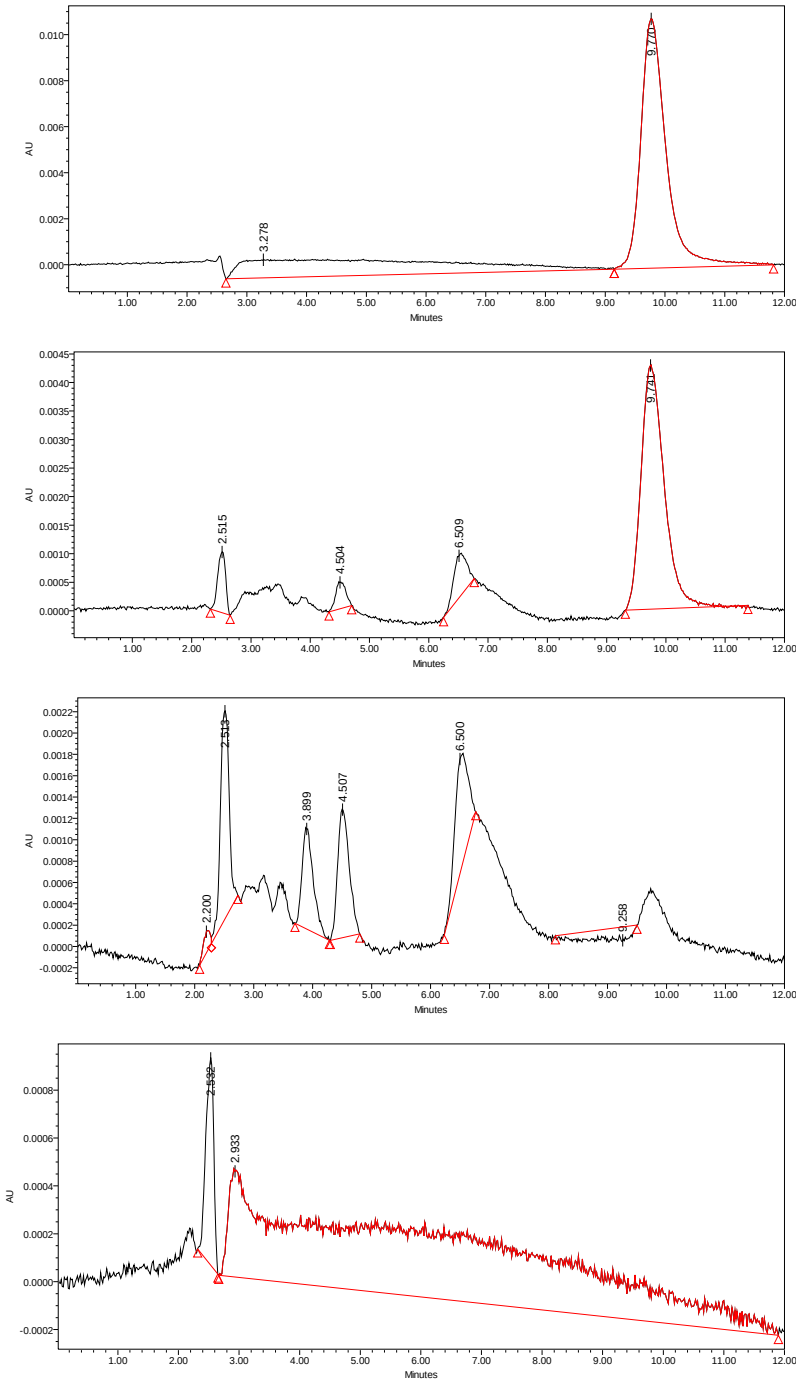

Figure (A65): HPLC chromatogram of p-Cresol for sample treated at 0, 5, 10, and 60minutes interval time by using diamond electrode at current density of 15mA/cm2 with (30) seconds polarity time

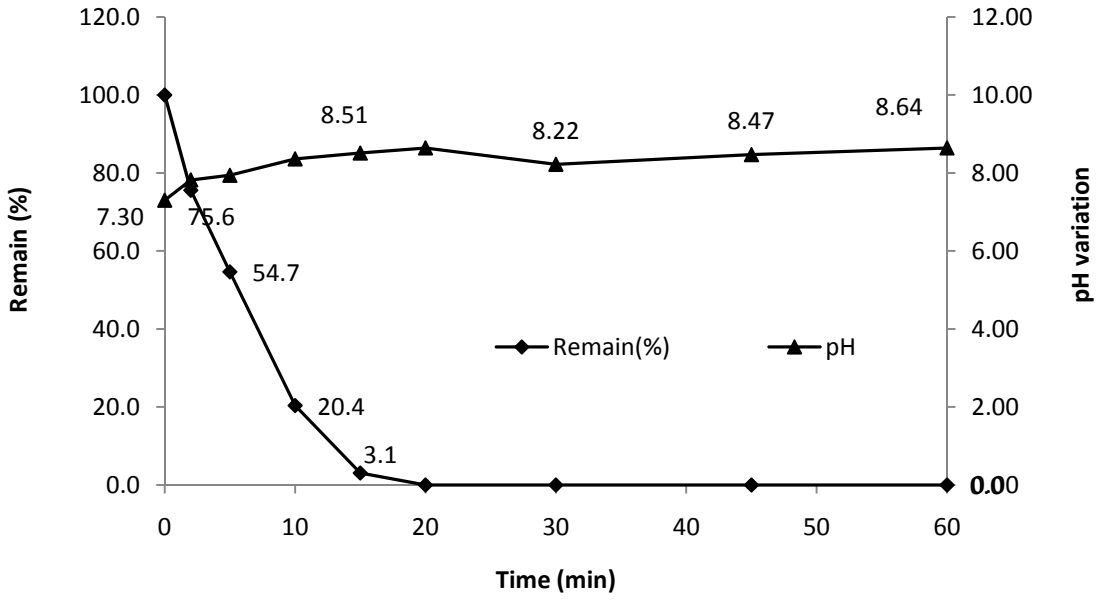

Figure (A66): Remaining percentage of p-Cresol and pH vs. time after treatment of p-Cresol by using diamond electrode with (45) seconds polarity time and current density of 5mA/cm2

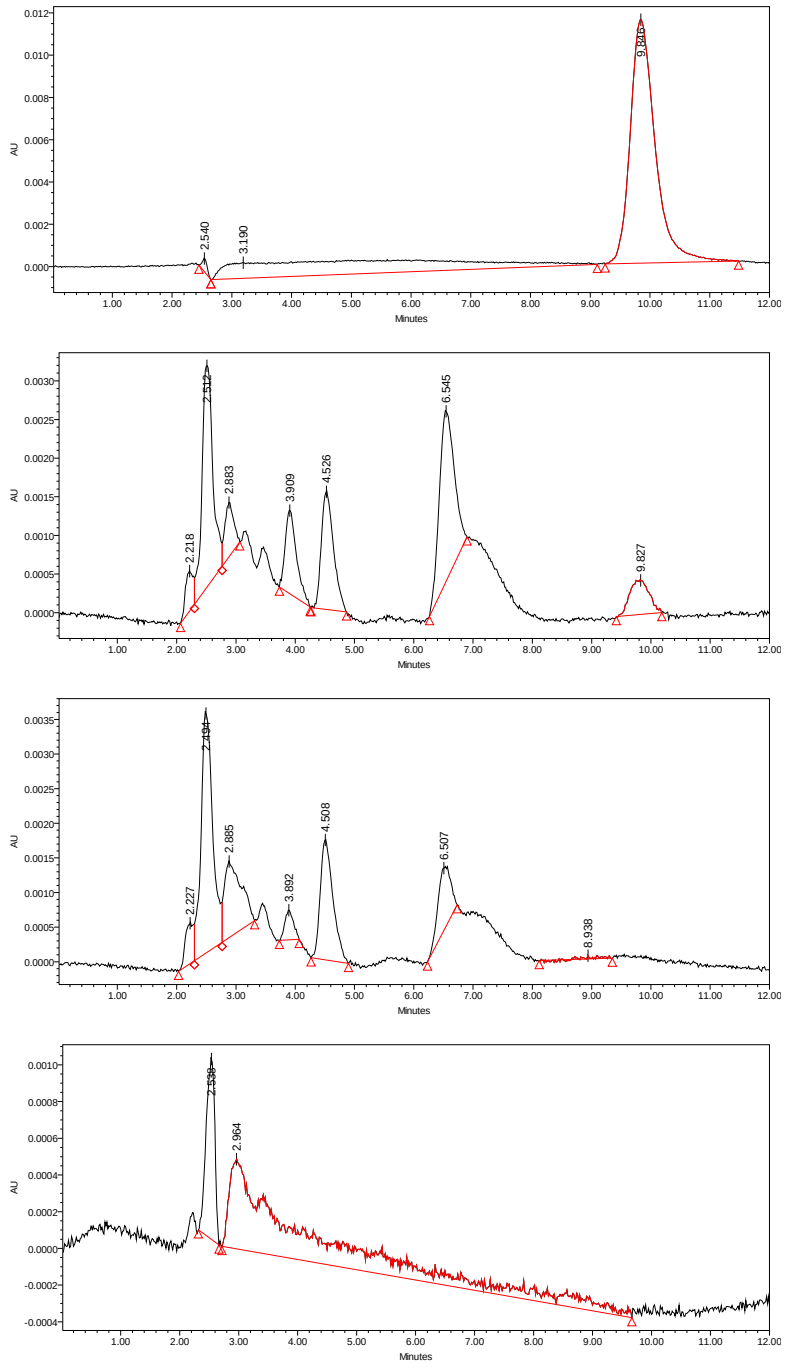

Figure (A67): HPLC chromatogram of p-Cresol for sample treated at 0, 15, 20, and 60minutes interval time by using diamond electrode at current density of 15mA/cm2 with (45) seconds polarity time with (45) seconds polarity time

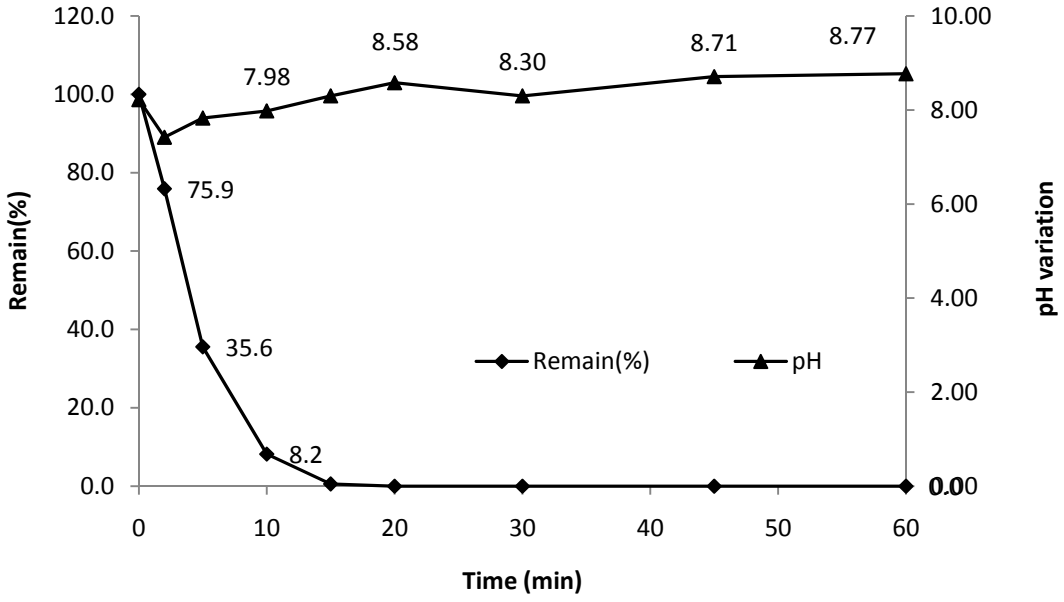

Figure (A68): Remaining percentage of p-Cresol and pH vs. time after treatment of p-Cresol by using diamond electrode with (60) seconds polarity time and current density of 5mA/cm2

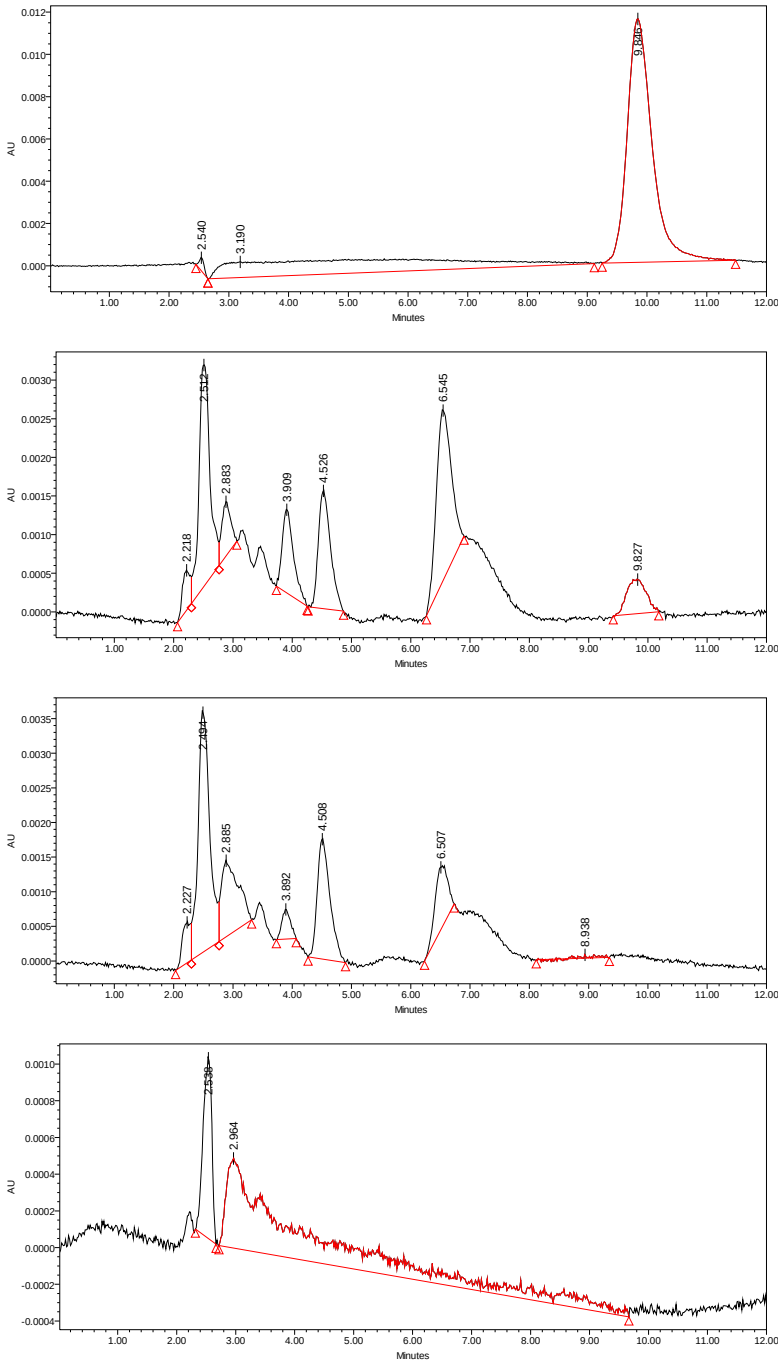

Figure (A69): HPLC chromatogram of p-Cresol for sample treated at 0, 10, 15, and 60minutes interval time by using diamond electrode at current density of 15mA/cm2 with (60) seconds polarity time

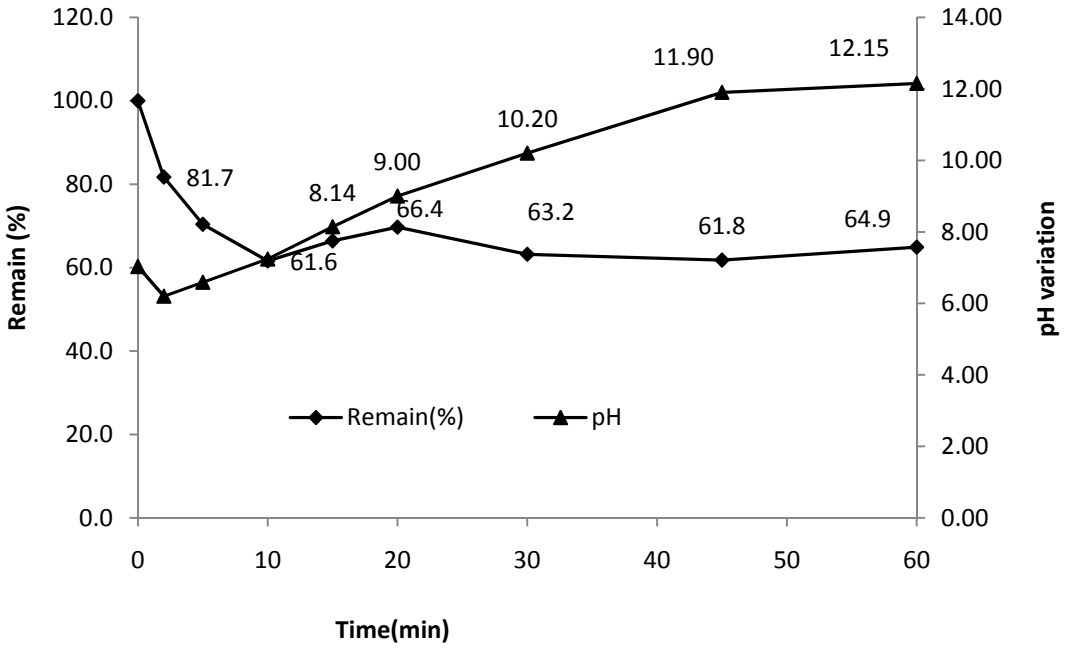

Figure (A70): Remaining percentage of p-Cresol and pH vs. time after treatment of p-Cresol by using stainless steel electrode with (0) seconds polarity time and current density of 15mA/cm2

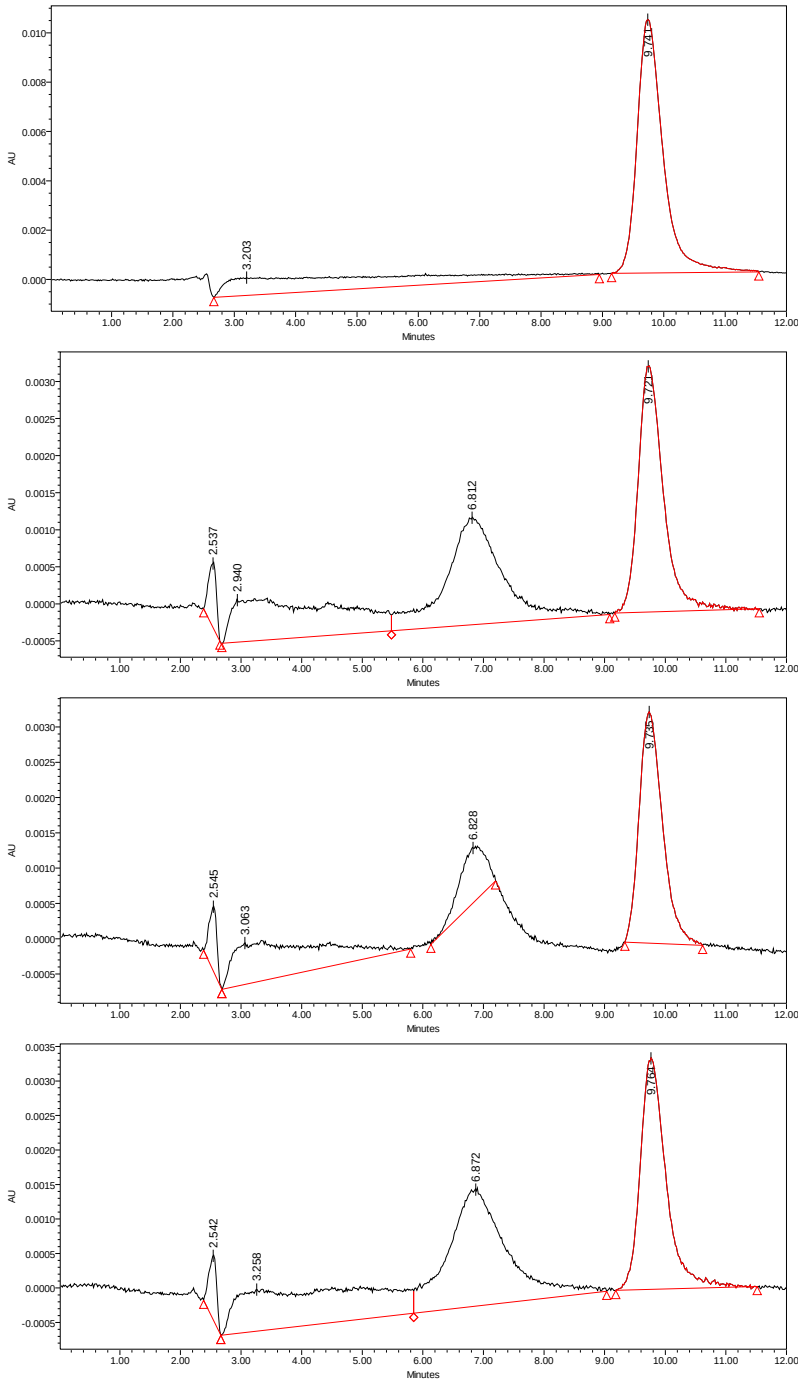

Figure (A71): HPLC chromatogram of p-Cresol for sample treated at 0, 15, 45, and 60minutes interval time by using stainless steel electrode at current density of 15mA/cm2 with (0) seconds polarity time

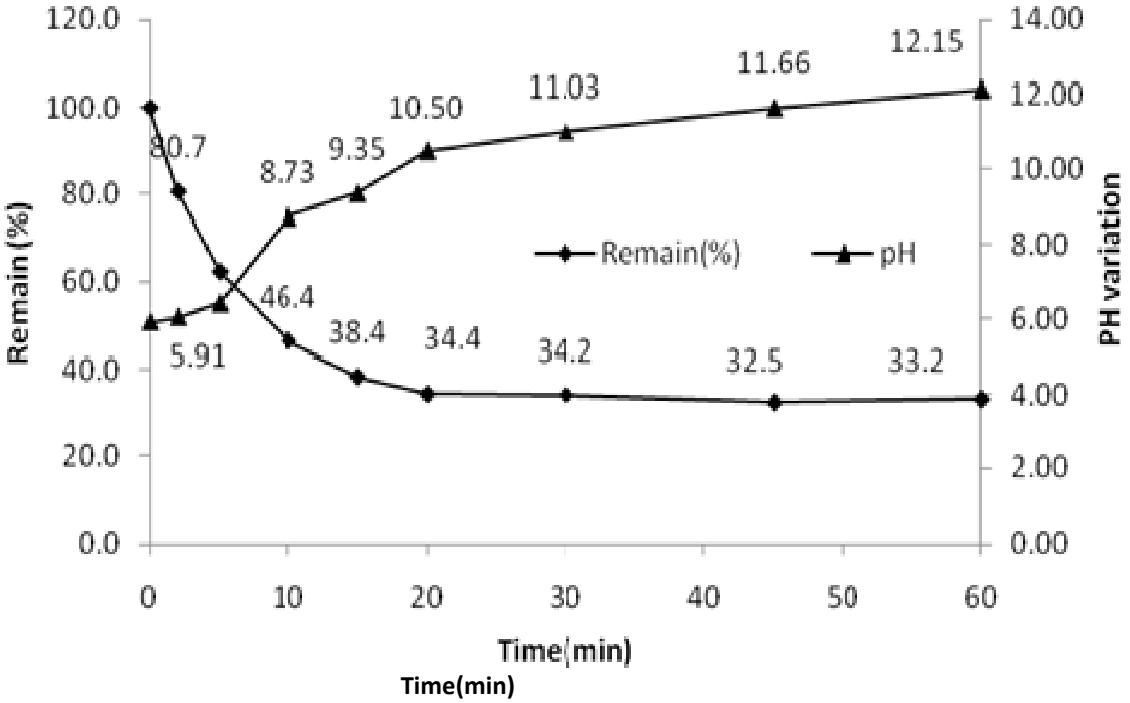

Figure (A72): Remaining percentage of p-Cresol and pH vs. time after treatment of p-Cresol by using stainless steel electrode with (30) seconds polarity time and current density of 15mA/cm2

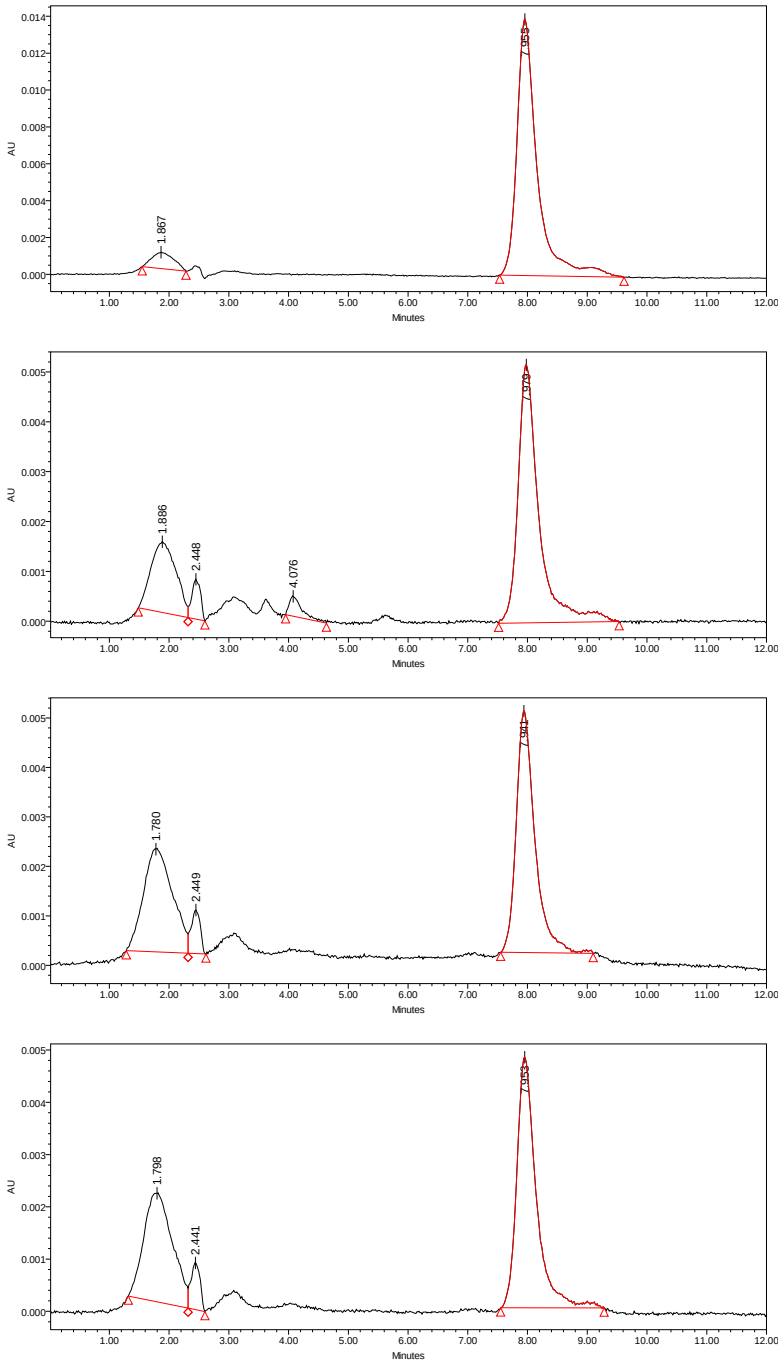

Figure (A73): HPLC chromatogram of p-Cresol for sample treated at 0, 15, 45, and 60minutes interval time by using stainless steel electrode at current density of 15mA/cm2with (30) seconds polarity time

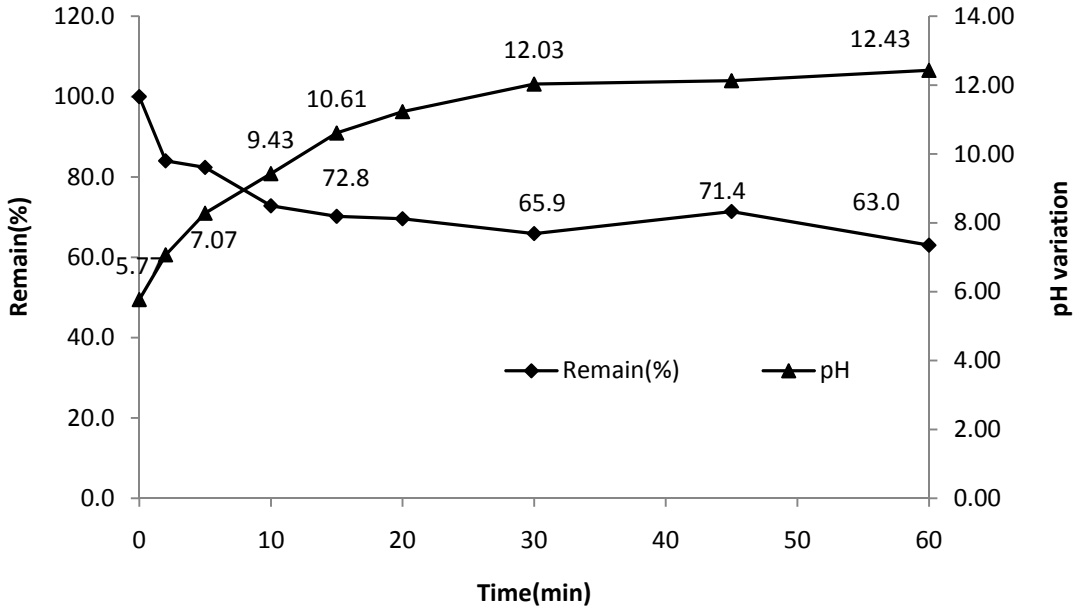

Figure (A74): Remaining percentage of p-Cresol and pH vs. time after treatment of p-Cresol by using stainless steel electrode with (45) seconds polarity time and current density of 15mA/cm2

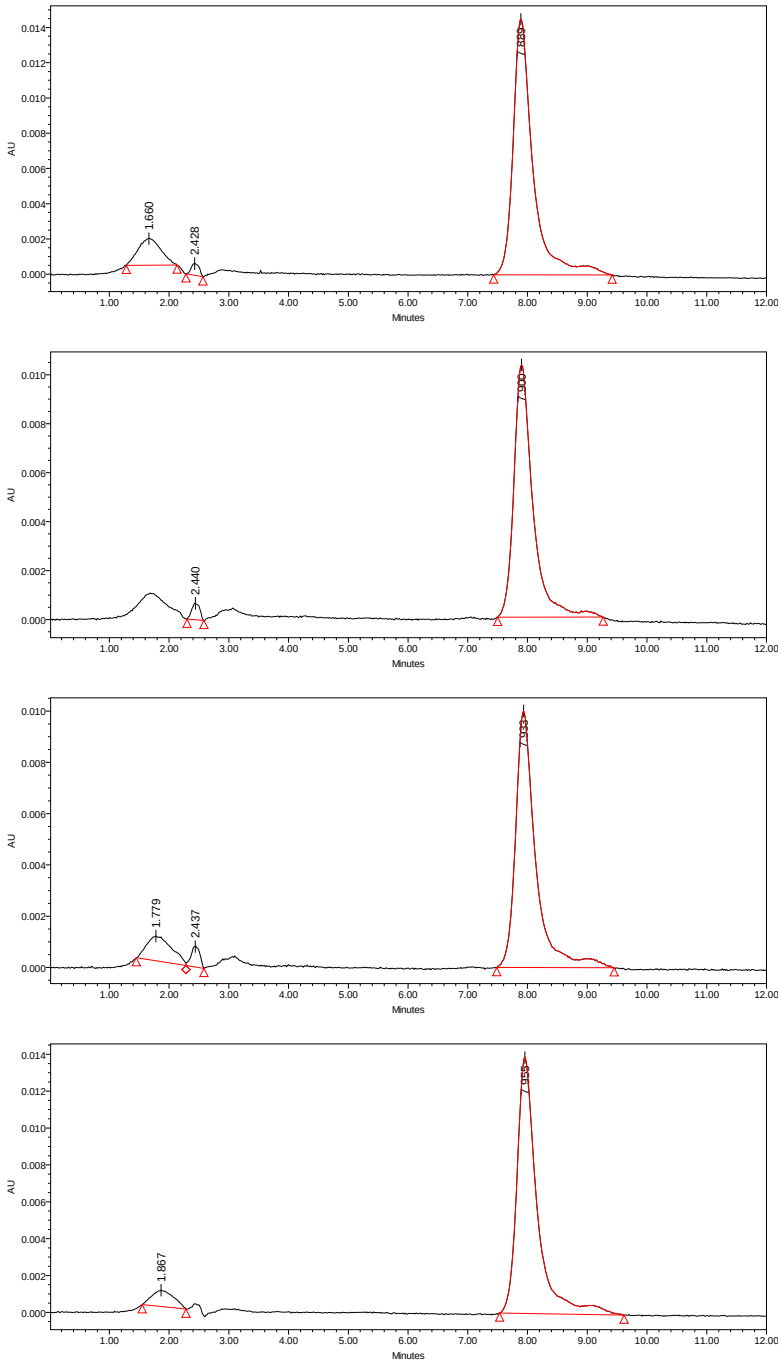

Figure (A75): HPLC chromatogram of p-Cresol for sample treated at 0, 15, 45, and 60minutes interval time by using stainless steel electrode at current density of 15mA/cm2 with polarity time 45 seconds

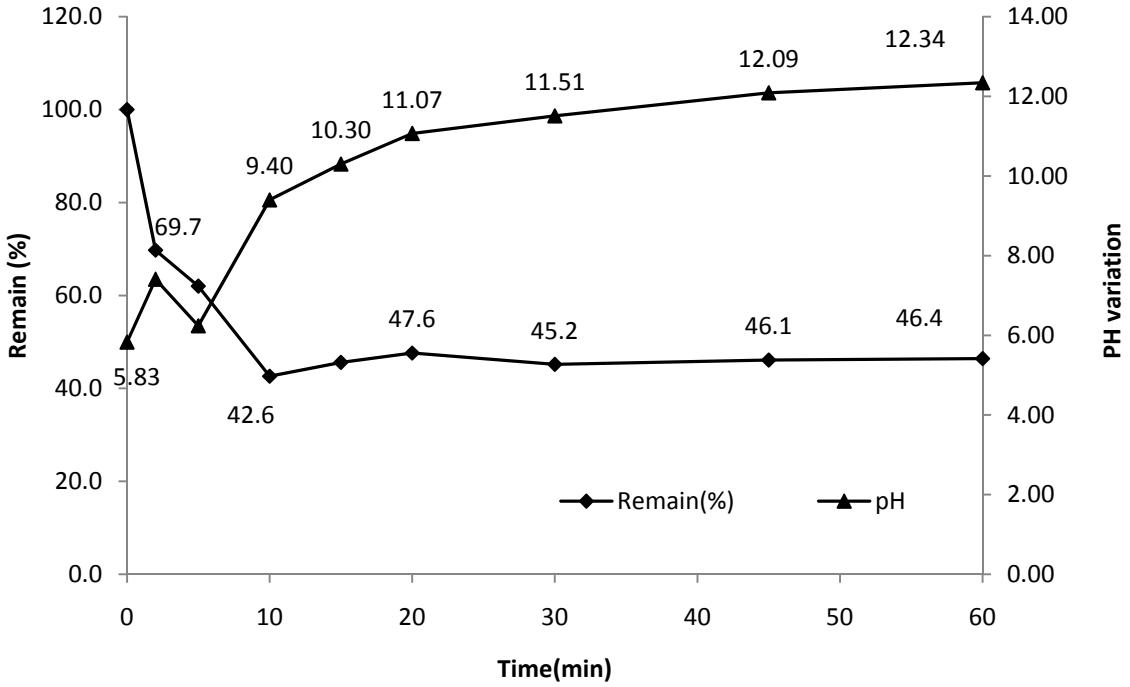

Figure (A76): Remaining percentage of p-Cresol and pH vs. time after treatment of p-Cresol by using stainless steel electrode with (60) seconds polarity time and current density of 15mA/cm2

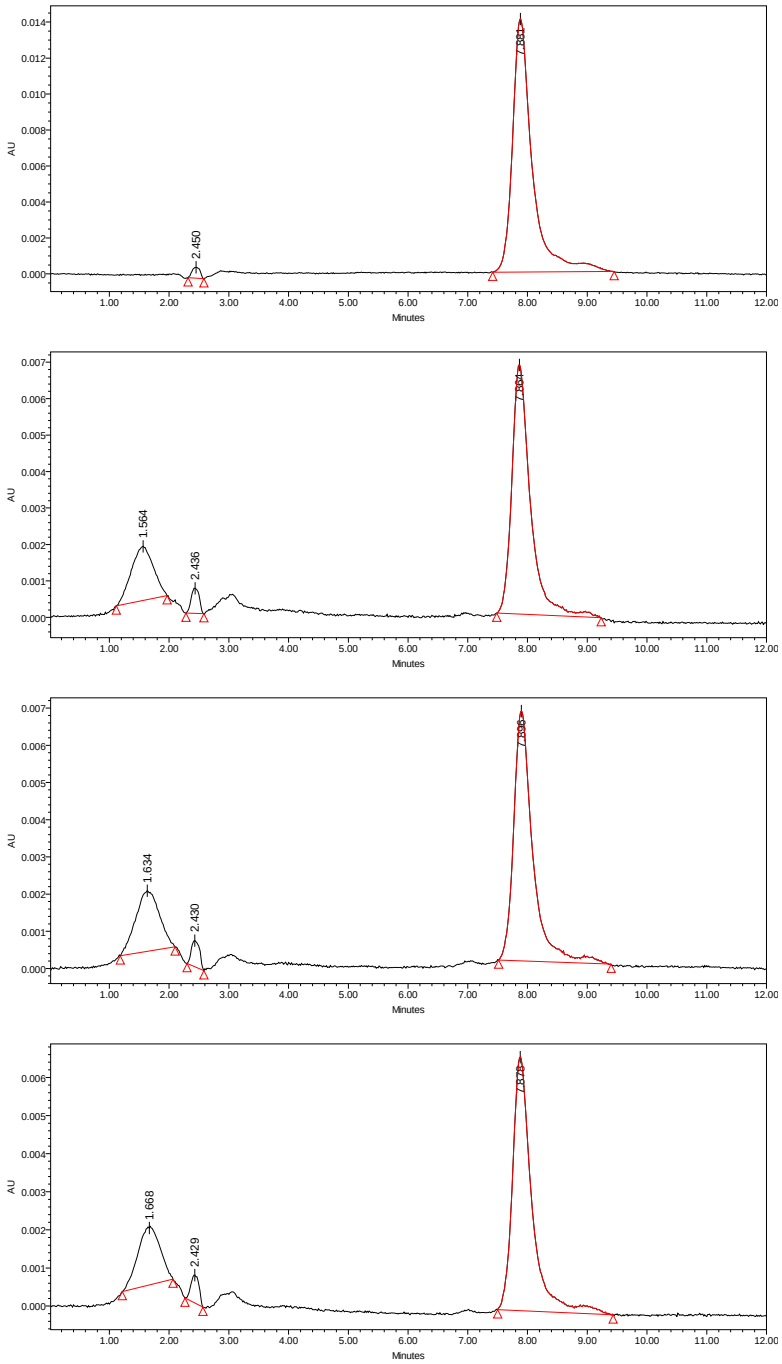

Figure (A77): HPLC chromatogram of p-Cresol for sample treated at 0, 15, 45, and 60minutes interval time by using stainless steel electrode at current density of 15mA/cm2 with polarity time60 seconds

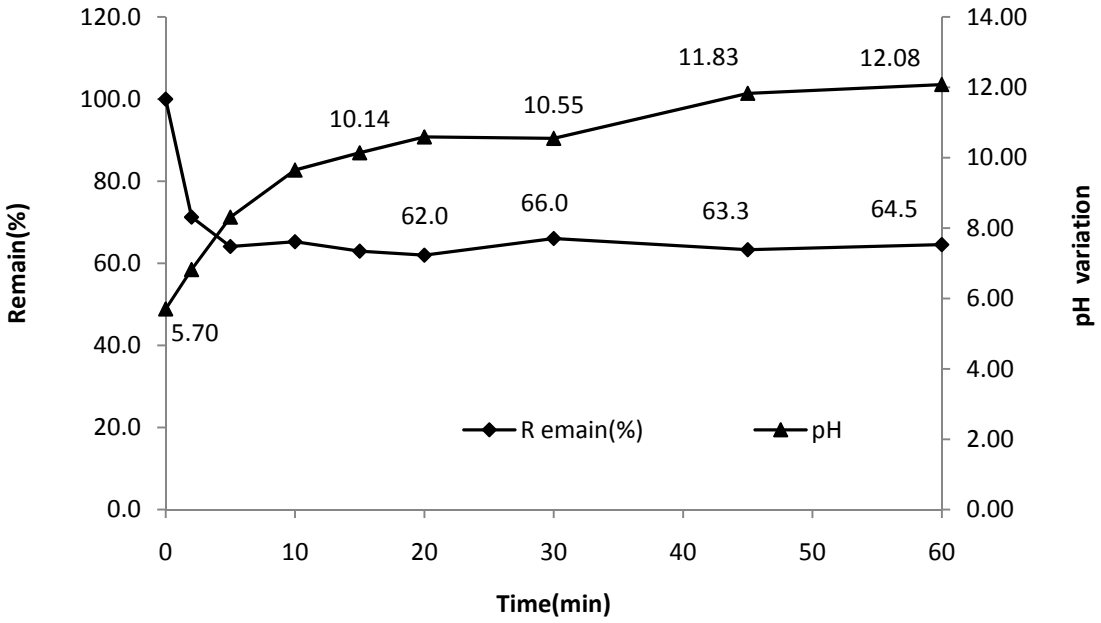

Figure (A78): Remaining percentage of p-Cresol and pH vs. time after treatment of p-Cresol by using same stainless steel anode for first time and current density of 15mA/cm2

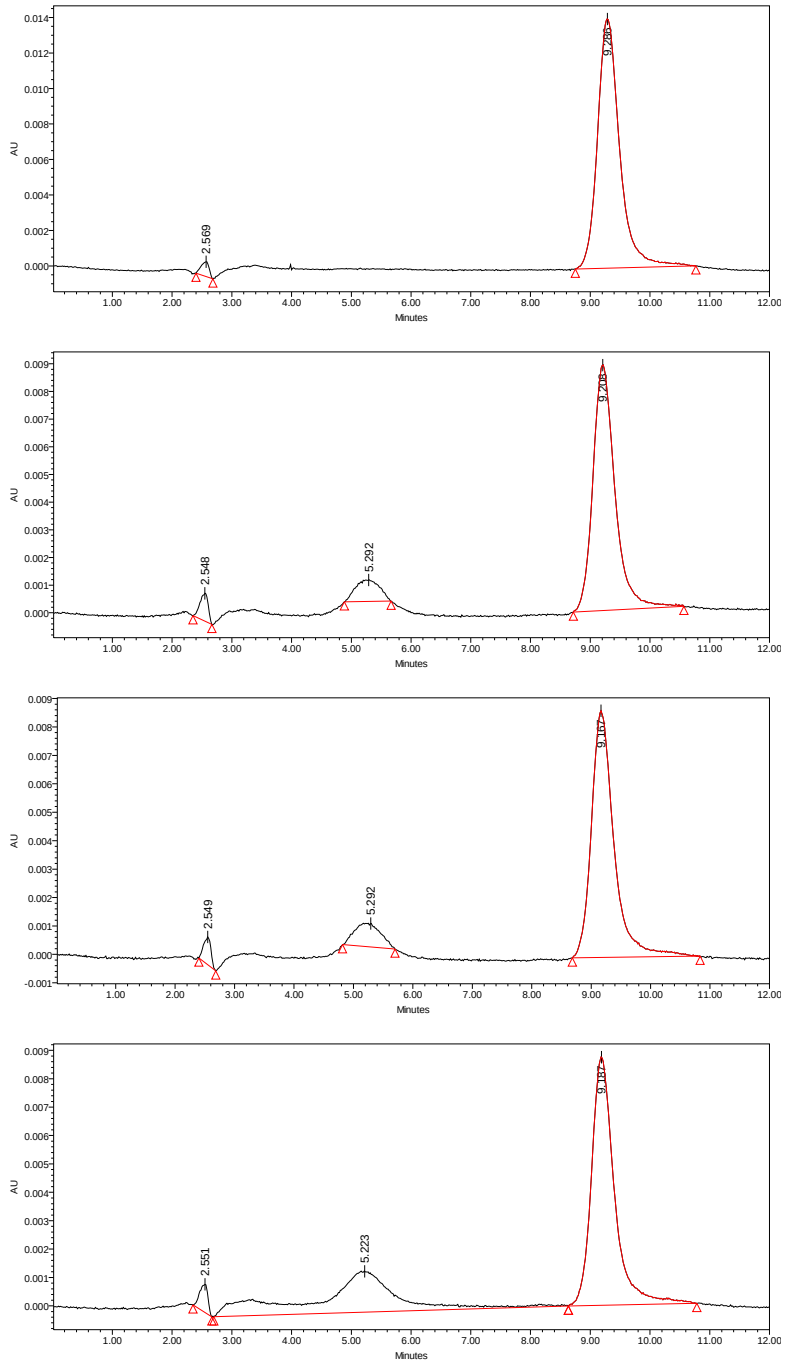

FIGURE (A79): HPLC chromatogram of p-Cresol for sample treated at 0, 15, 45, and 60minutes interval time by using stainless steel (SS-304L) electrode at current density of 15mA/cm2 for in the first experiment

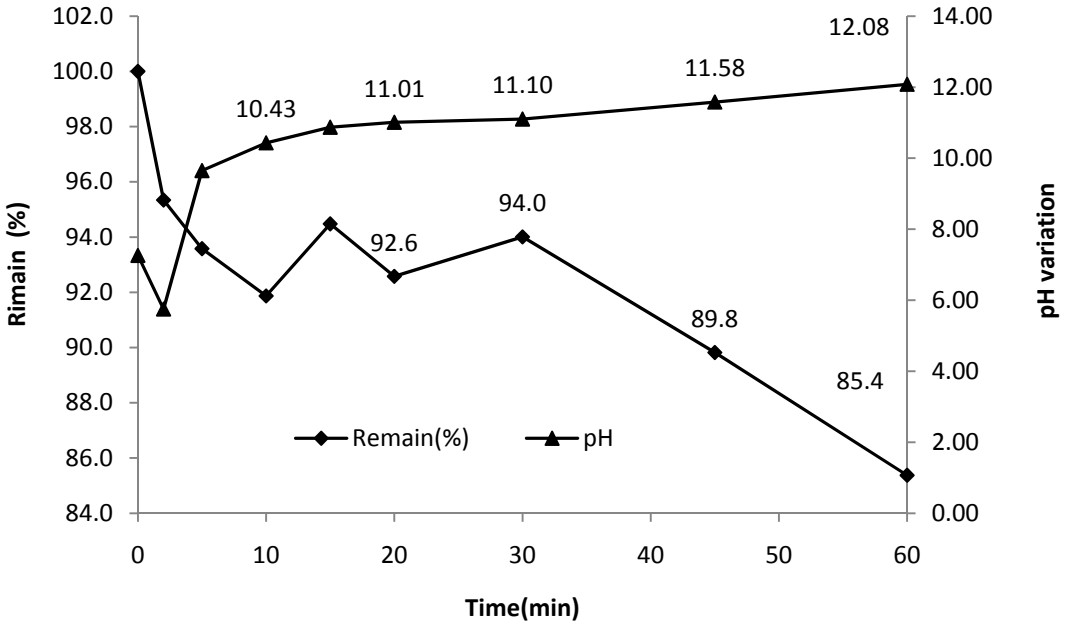

Figure (A80): Remaining percentage of p-Cresol and pH vs. time after treatment of p-Cresol by using same stainless steel anode for second time after cleaning its surface and with current density of 15mA/cm2

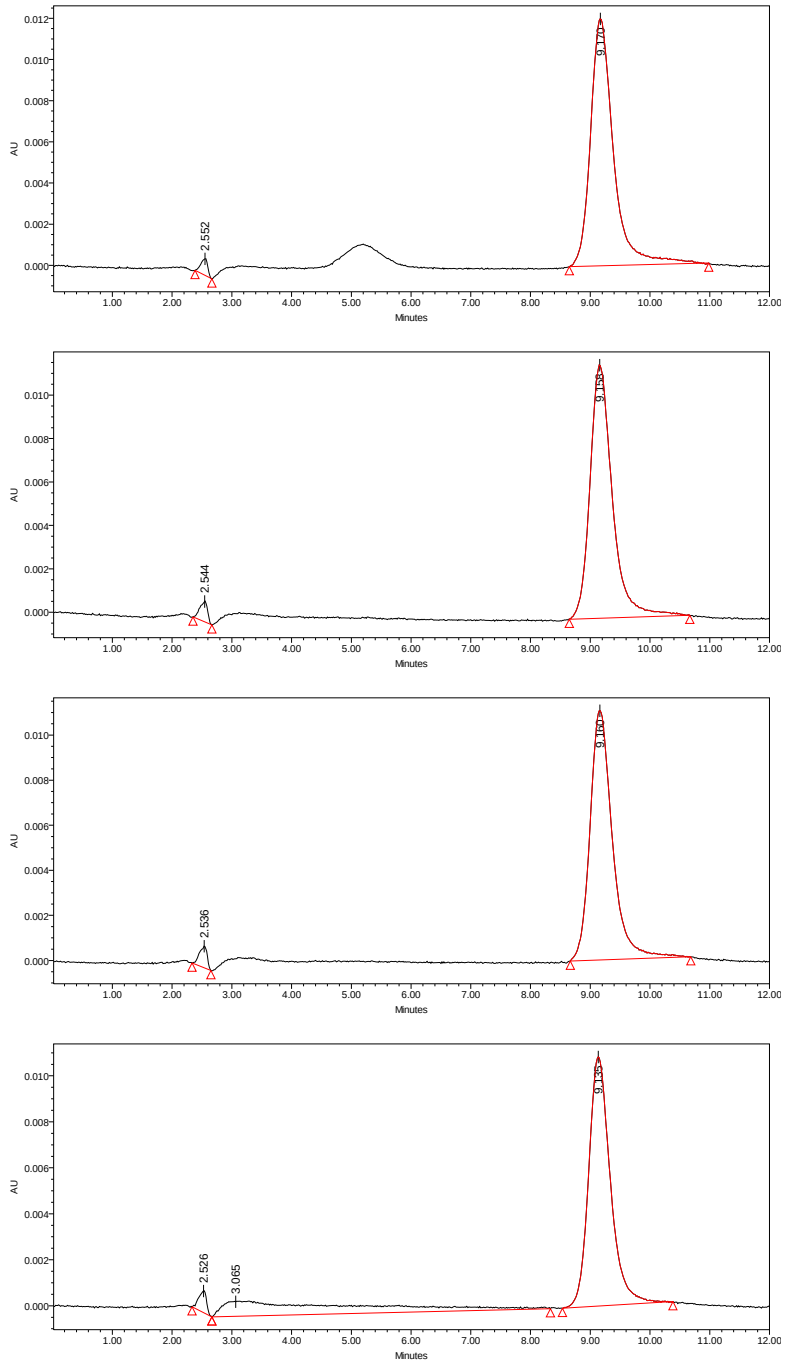

Figure (A81): HPLC chromatogram of p-Cresol for sample treated at 0, 15, 45, and 60minutes interval time by using stainless steel (SS-304L) electrode at current density of 15mA/cm2 for in the second experiment

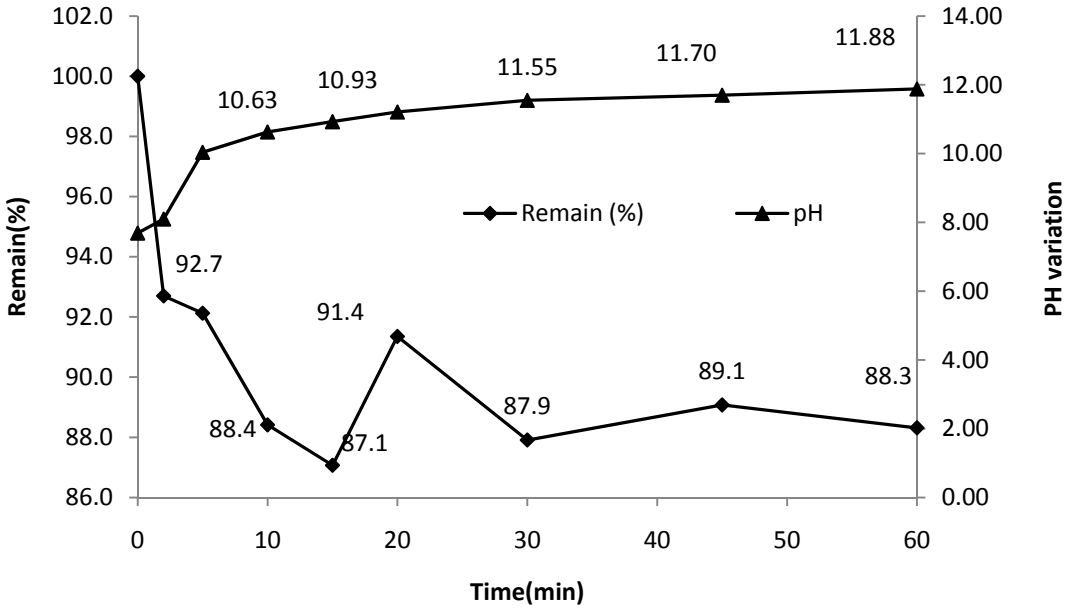

Figure (A82): Remaining percentage of p-Cresol and pH vs. time after treatment of p-Cresol by using same stainless steel anode for third time after cleaning its surface and with current density of 15mA/cm2

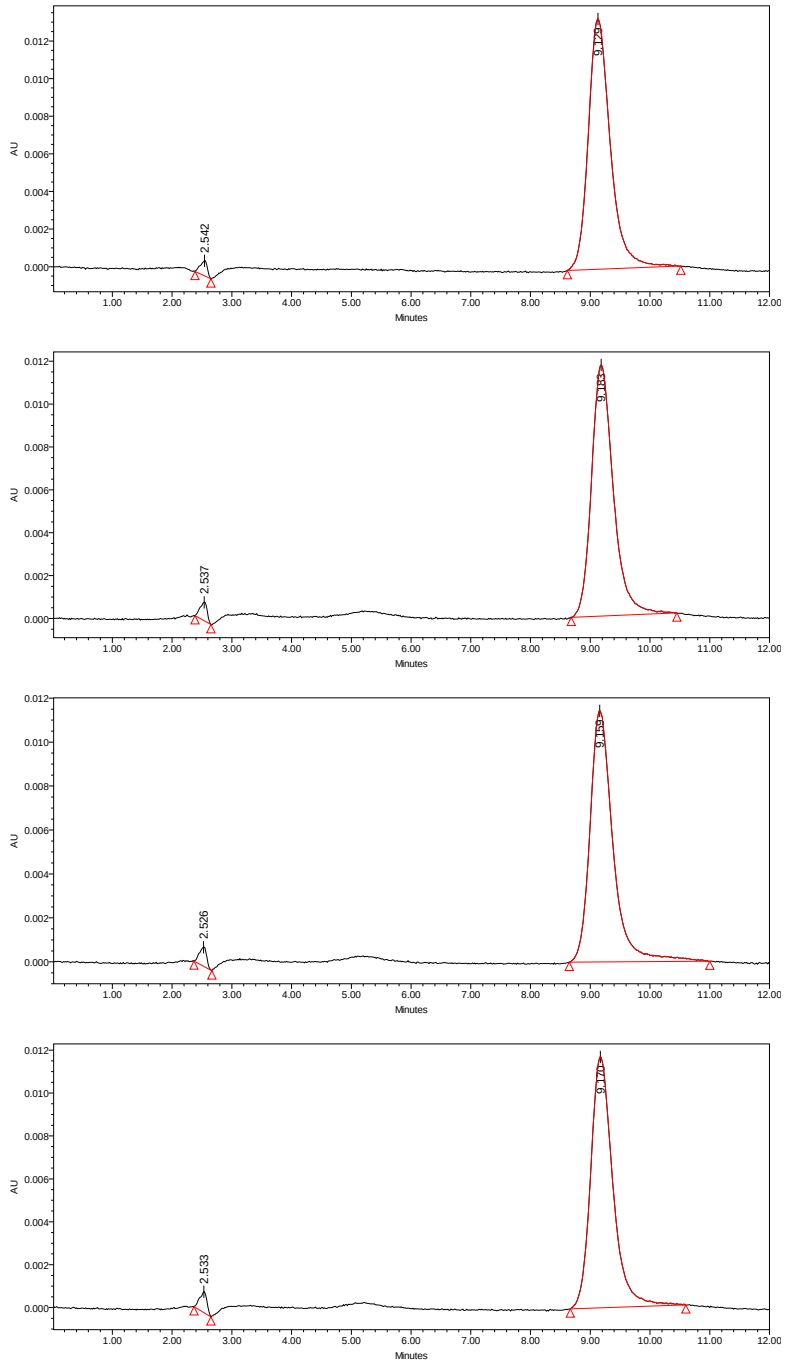

Figure (A83): HPLC chromatogram of p-Cresol for sample treated at 0, 15, 45, and 60minutes interval time by using stainless steel (SS-304L) electrode at current density of 15mA/cm2 for in the third experiment

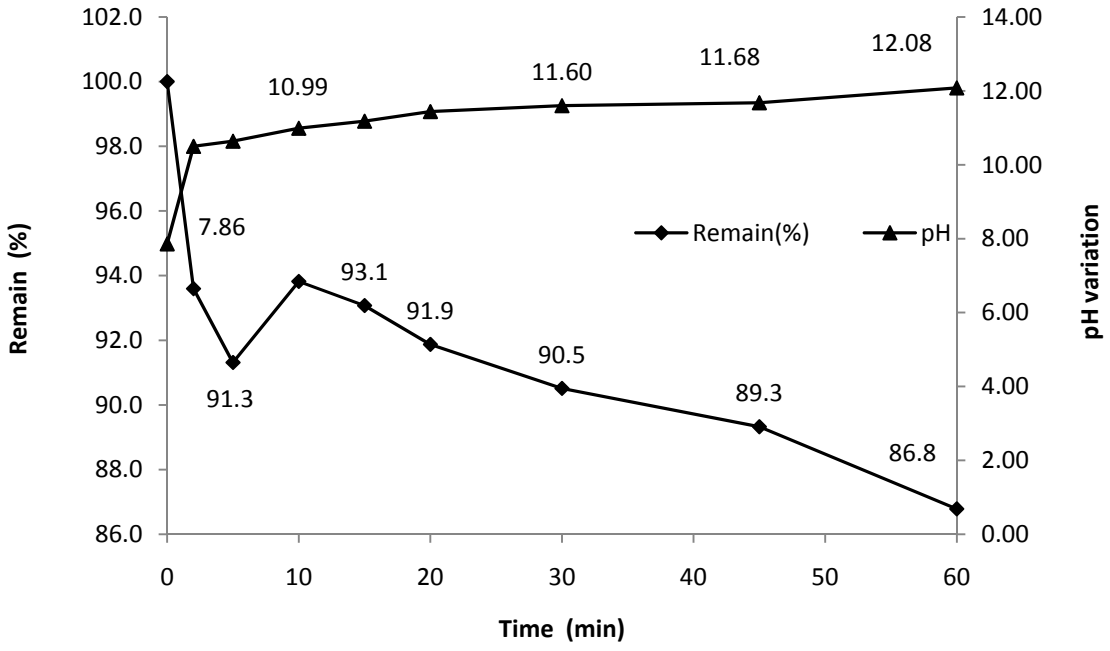

Figure (A84): Remaining percentage of p-Cresol and pH vs. time after treatment of p-Cresol by using same stainless steel anode for fourth time after cleaning its surface and with current density of 15mA/cm2

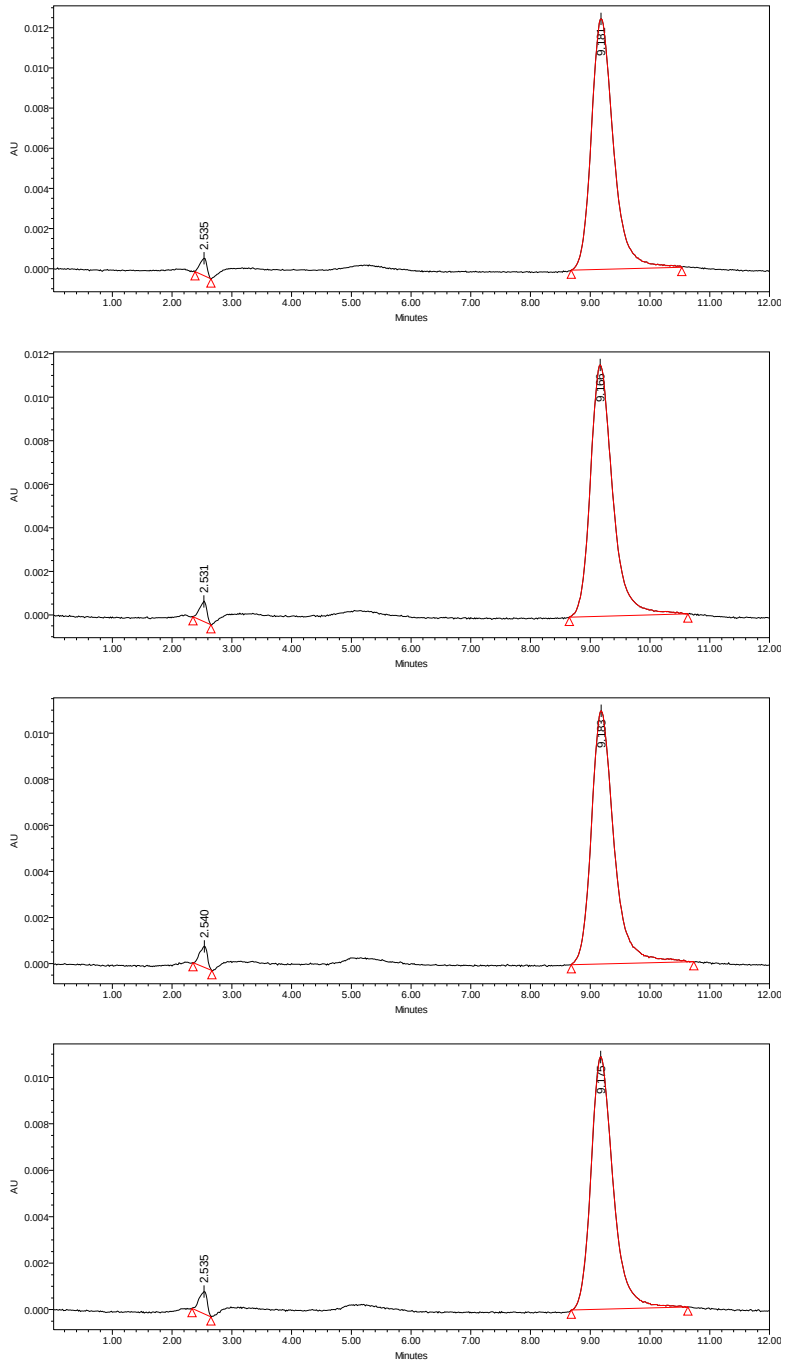

Figure (A85): HPLC chromatogram of p-Cresol for sample treated at 0, 15, 45, and 60minutes interval time by using stainless steel (SS-304L) electrode at current density of 15mA/cm2 for in the fourth experiment

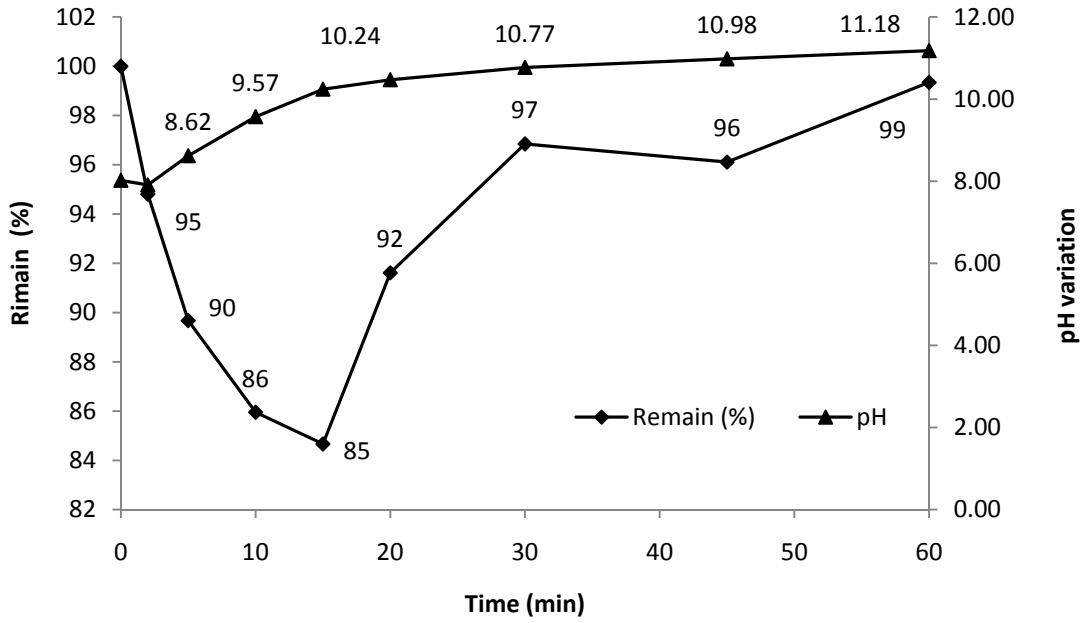

Figure (A86): Remaining percentage of p-Cresol and pH vs. time after treatment of p-Cresol by using same stainless steel anode in fifth experiment time after cleaning its surface and with current density of 15mA/cm2

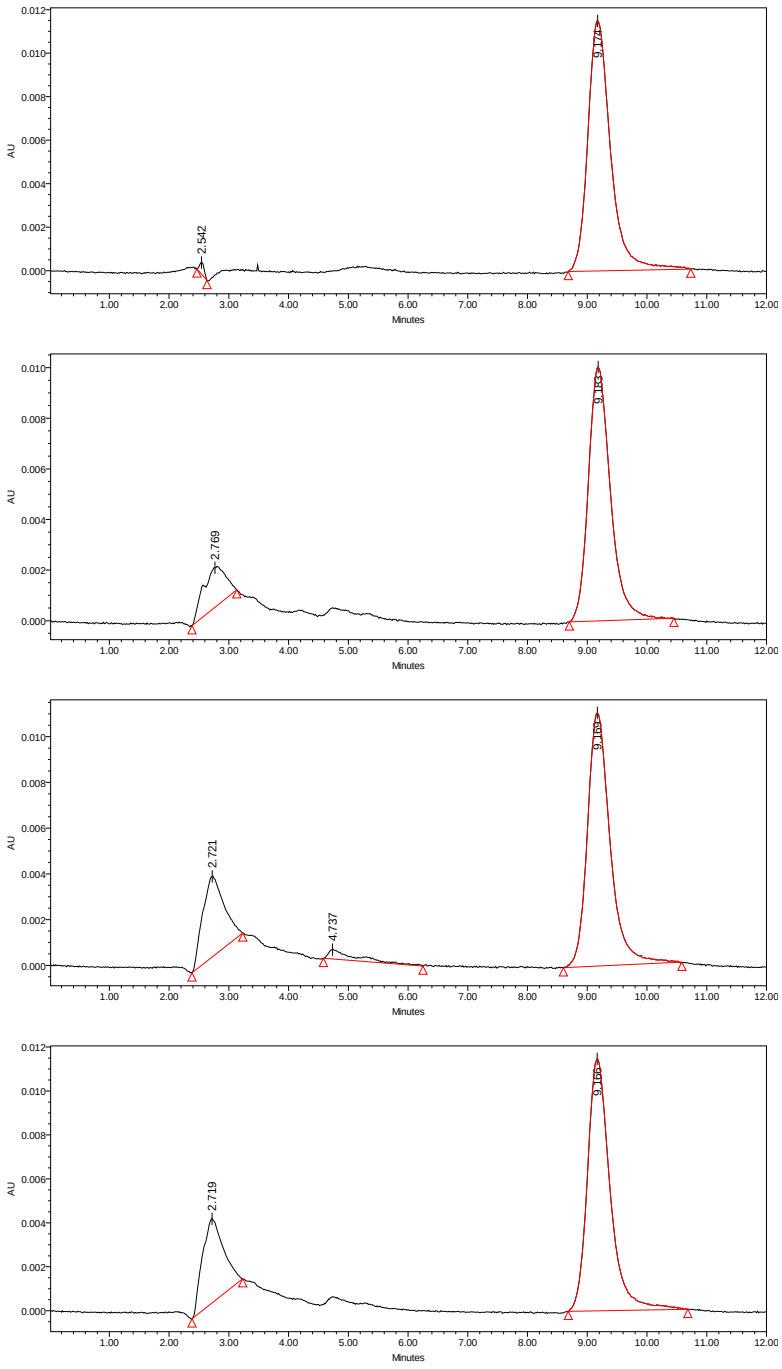

Figure (A87): HPLC chromatogram of p-Cresol for sample treated at 0, 15, 45, and 60minutes interval time by using stainless steel (SS-304L) electrode at current density of 15mA/cm2 for in the fifth experiment

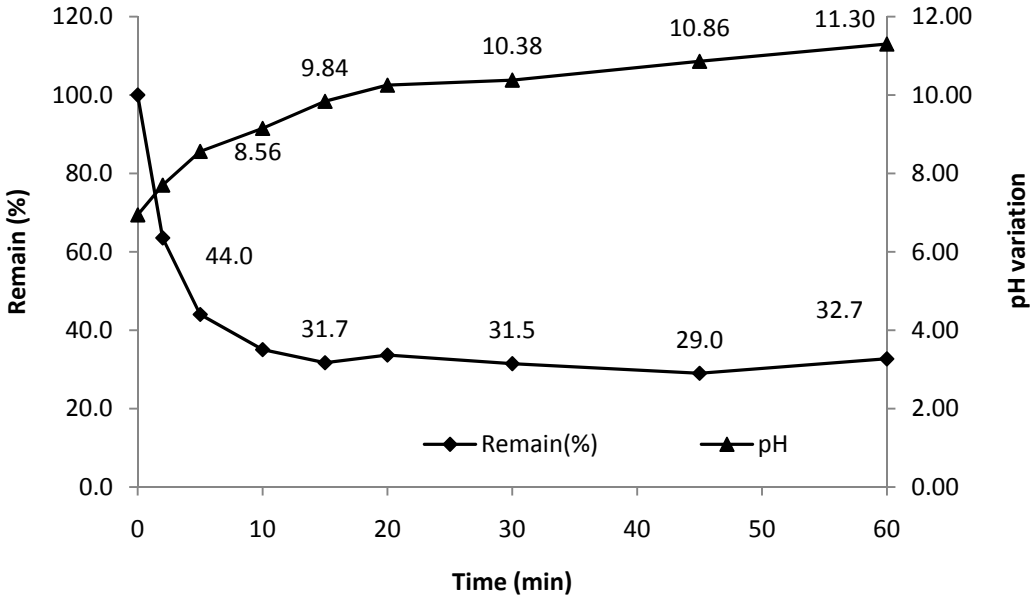

Figure (A88): Remaining percentage of p-Cresol and pH vs. time after treatment of p-Cresol by using same stainless steel (SS-304L) electrode and with current density of 15mA/cm2

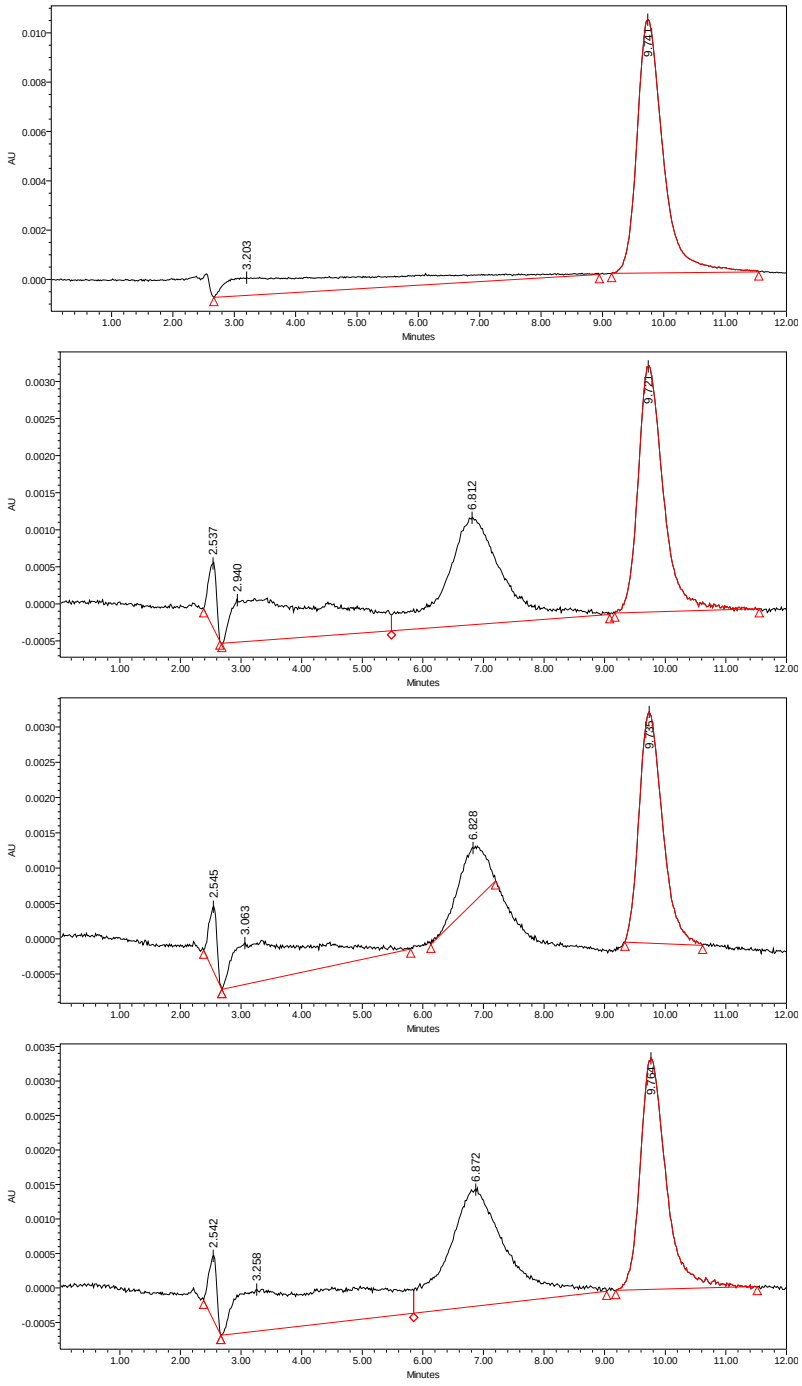

Figure (A89): HPLC chromatogram of p-Cresol for sample treated at 0, 15, 45, and 60minutes interval time by using stainless steel (SS-304L) electrode at current density of 15mA/cm2

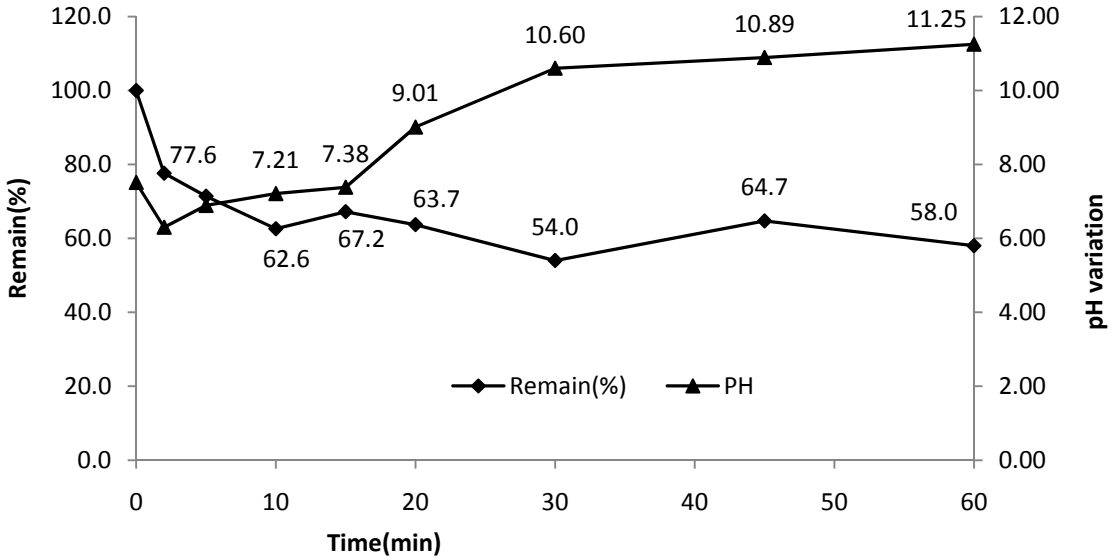

Figure (A90): Remaining percentage of p-Cresol and pH vs. time after treatment of p-Cresol by using same stainless steel (SS-316L) electrode and with current density of 15mA/cm2

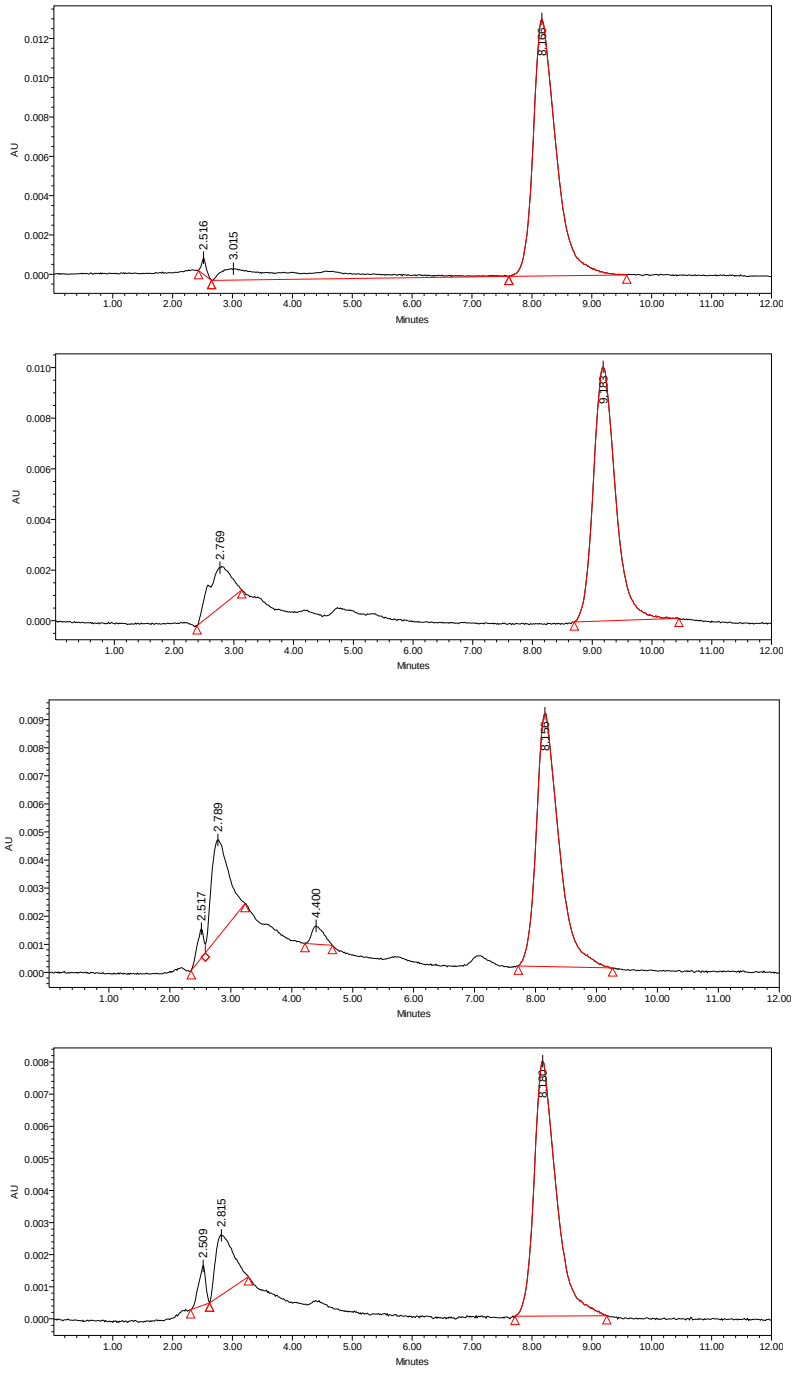

Figure (A91): HPLC chromatogram of p-Cresol for sample treated at 0, 15, 45, and 60minutes interval time by using stainless steel (SS-316L) electrode at current density of 15mA/cm2

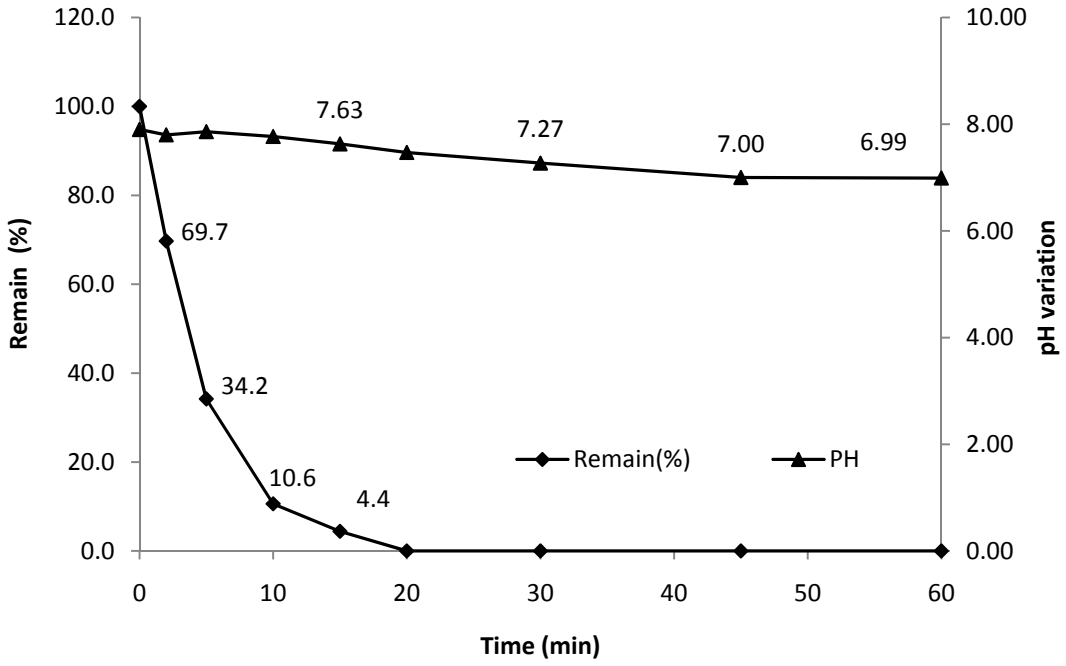

Figure (A92): Remaining percentage of p-Cresol and pH vs. time after treatment of p-Cresol by using same grapHite electrode with raw water and current density of 20mA/cm2

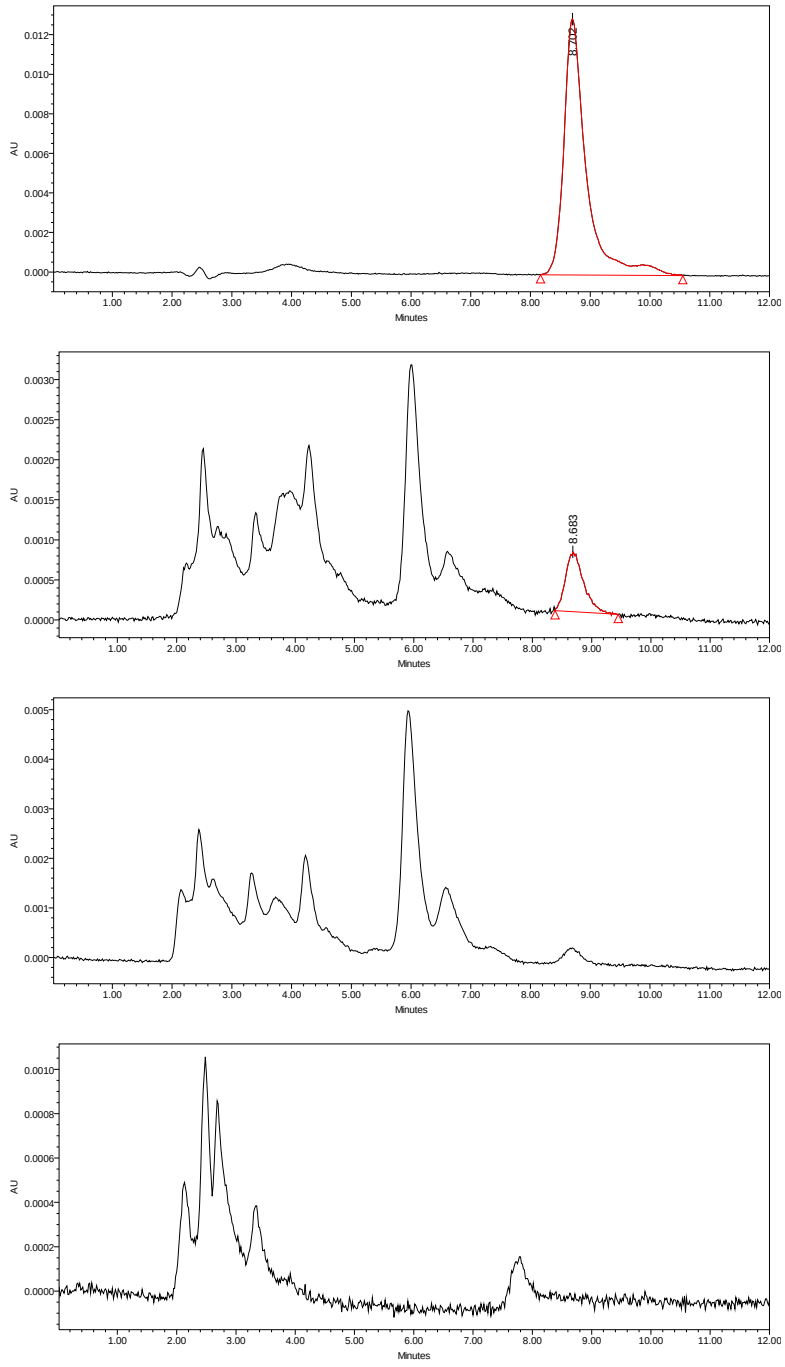

Figure (A93): HPLC chromatogram of p-Cresol for sample treated at 0, 15, 45, and 60minutes interval time by using grapHite electrode at current density of 20mA/cm2with raw water

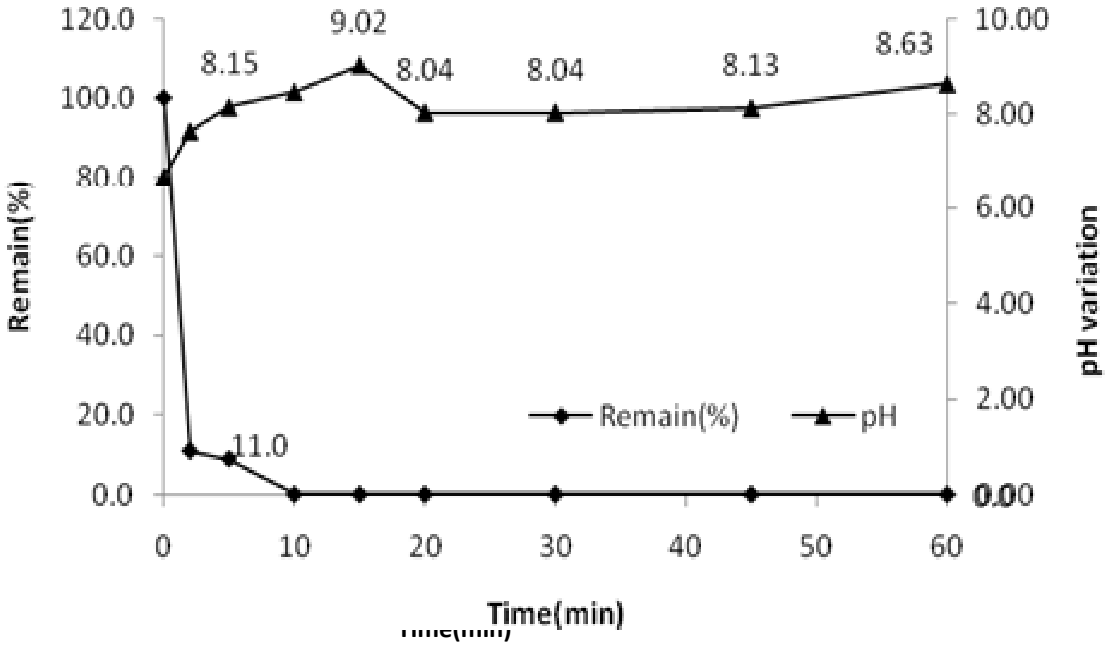

Figure (A94): Remaining percentage of p-Cresol and pH vs. time after treatment of p-Cresol by using same diamond electrode with raw water and current density of 20mA/cm2

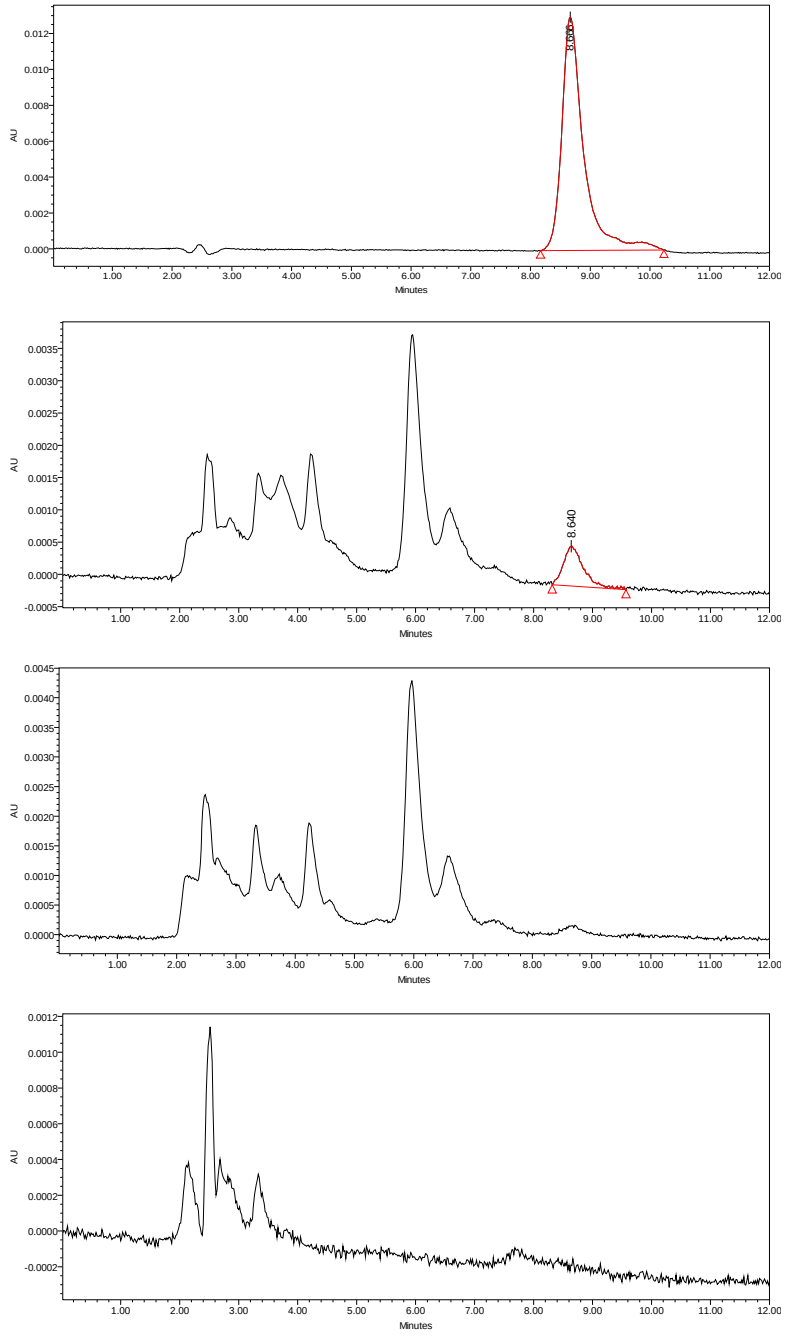

Figure (A95): HPLC chromatogram of p-Cresol for sample treated at 0, 15, 45, and 60minutes interval time by using diamond electrode at current density of 20mA/cm2 with raw water

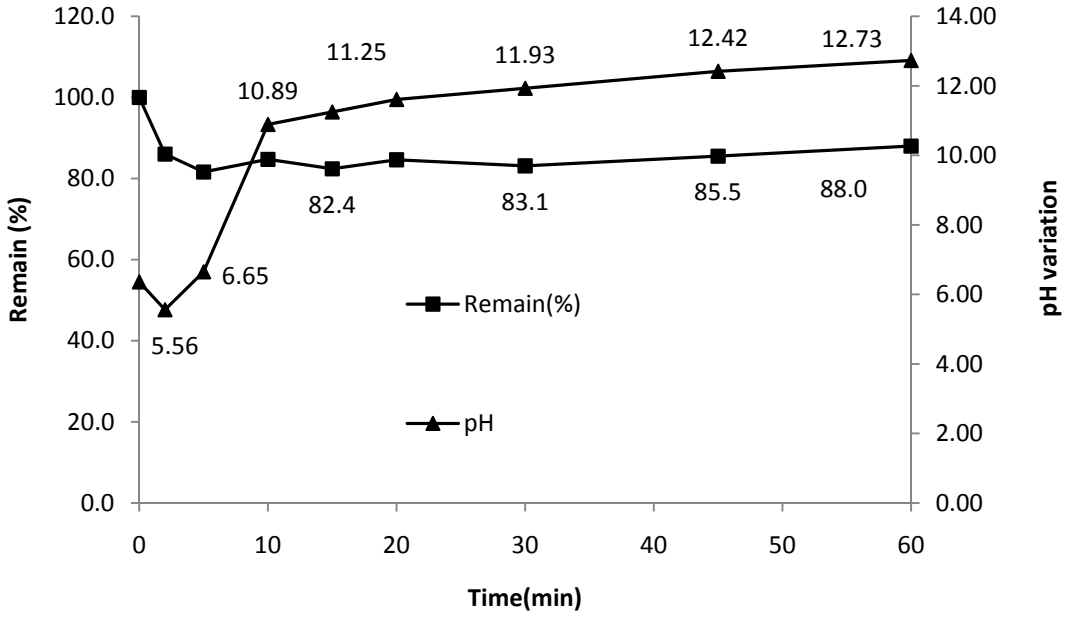

Figure (A96): Remaining percentage of p-Cresol and pH vs. time after treatment of p-Cresol by using same stainless steel electrode with raw water and current density of 20mA/cm2

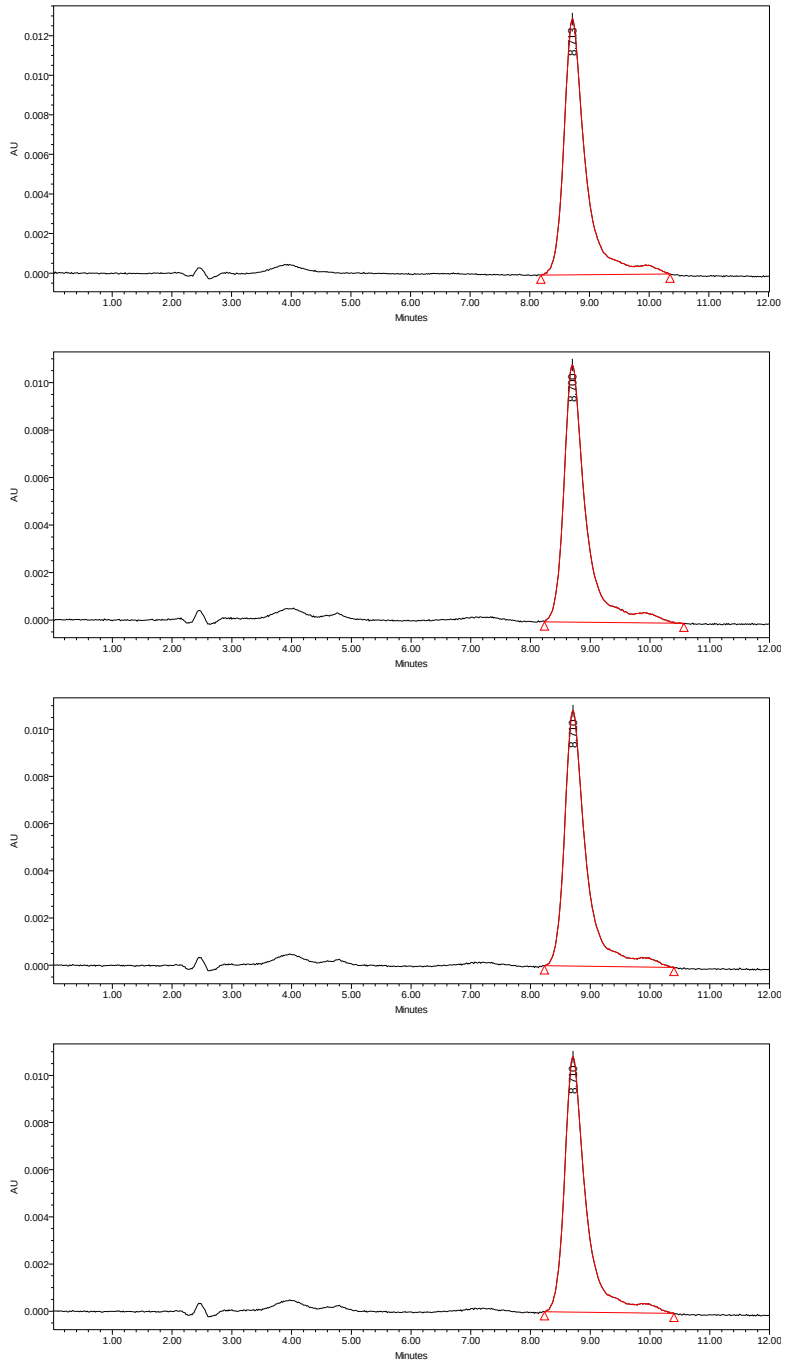

Figure (A97): HPLC chromatogram of p-Cresol for sample treated at 0, 15, 45, and 60minutes interval time by using stainless steel (SS-316L) electrode at current density of 20mA/cm2 with tap water

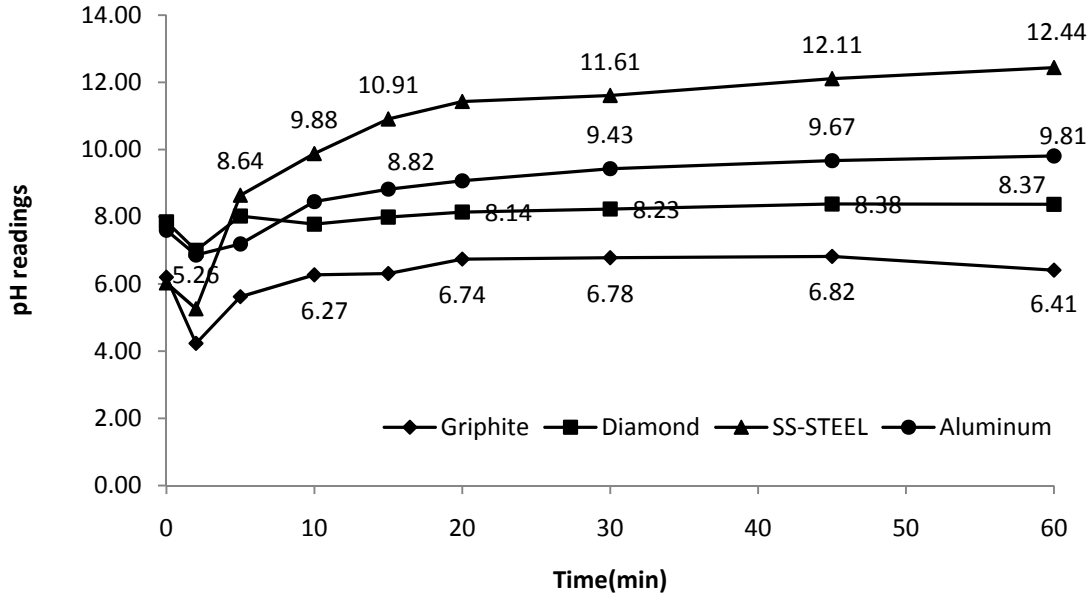

Figure (A98): pH variation verses time for different electrodes at current density of 15 mA/cm2

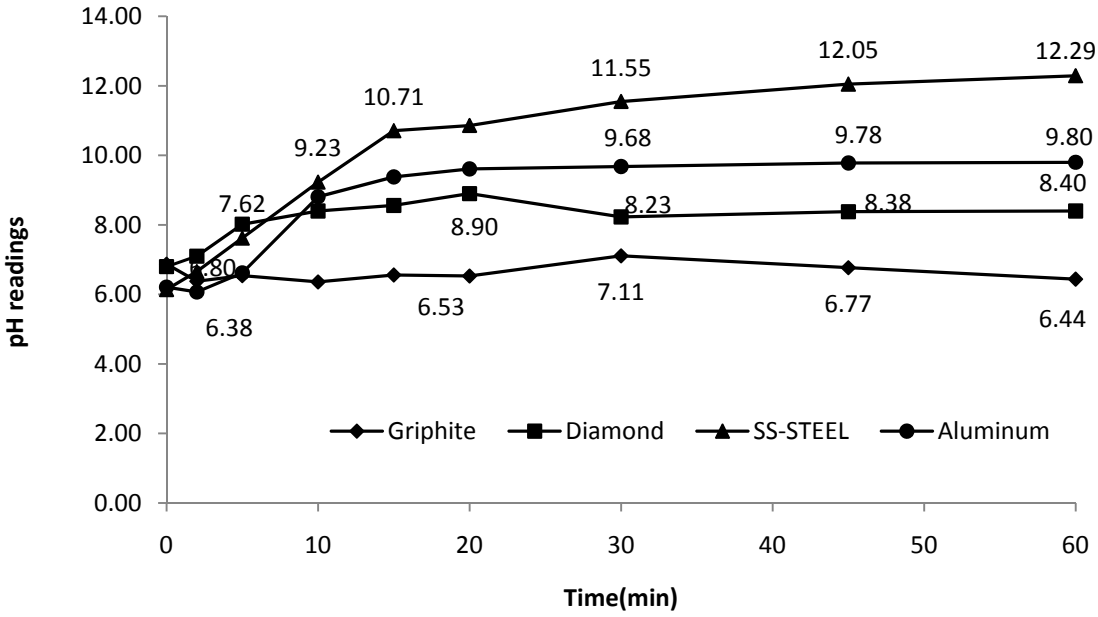

Figure (A99): pH variation verses time for different electrodes at current density of 10 mA/cm2

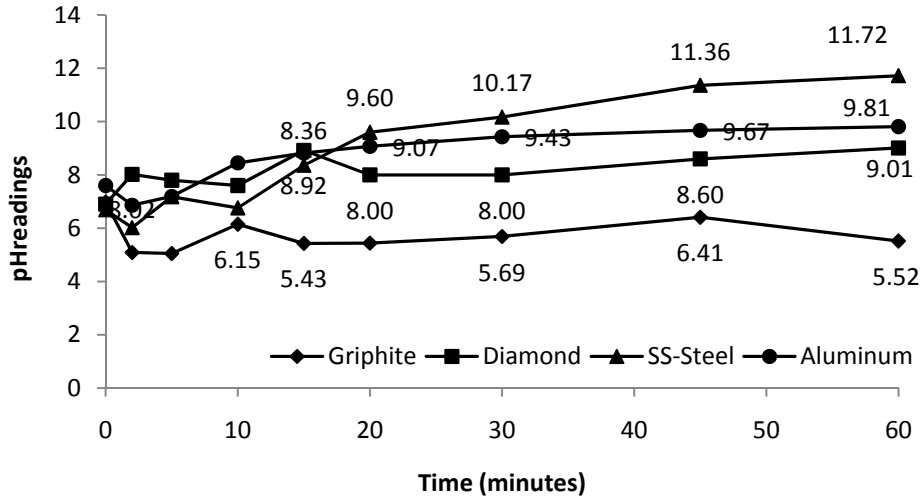

Figure (A100): pH variation verses time for different electrodes at current density of 5 mA/cm2

REFERENCES

A.M. Jirka and M.J. Carter, "Micro Semi-Automated Analysis of Surface and Wastewaters for Chemical Oxygen Demand", Analytical Chemistry, Vol. 47, p. 1397 (1975).

Abuzaid, N.S., et al., 2002, Ground Water Coagulation Using Stainless Steel Electrodes, Advances in Environmental Research, Vol. 6, P. 325 – 333.

Allen, H.L., et. al., 1990, Treatment of Phenol and Cresol Contaminated Soil, Journal of Hazardous Material, Vol. 25, P. 343 – 360.

Ameer, M.A., et al., F.E., 2004, Electrochemical Behavior of Passive Films on Molybdenum-Containing Austenitic Stainless Steel in Aqueous Solutions, Electrochimica Acta , Vol. 50, P. 43 – 49.

American Chemical Society (ACS), http://pubs.acs.org, (Visited: 2009-10-21).
Bard, A.J., Inzelt, G., and Scholz F., 2008, Electrochemical Dictionary, Berlin: Springr, pp. 723-2770.

Amin, M.A., 2005, Passivity and Passivity Breakdown of a Zinc Electrode in Aerated Neutral Sodium Nitrate Solutions, Electrochimica Acta, Vol. 50, P. 1265–1274.

Amin, Mohammed A., 2005, Passivity and Passivity Breakdown of a Zinc Electrode in Aerated Neutral Sodium Nitrate Solutions, Electrochimica Acta, Vol. 50, P. 1256 – 1274.

Anizza, M. P., Delucchi, M., and. Cerisola, G., Electrochemical degradation of anionic surfactants, *J. Appl. Electrochem.* 35 (2005), pp. 357–361.

APHA Standard Methods, 20th ed., p. 5-17, method 5220 D (1998).

Arias, C., et. al., 2005, Degradation of 4, 6-Dinitro-O-Cresol from Water by Anodic Oxidation with a Boron-Doped Diamond Electrode, Electrochimica Acta, Vol. 50, P. 3685–3692.

Arias, C., et. al., 2007, Solar Photoelectro-Fenton Degradation of Cresols Using a Flow Reactor with a Boron-Doped Diamond Anode, Applied Catalysis B: Environmental, Vol. 75, P. 17–28.

Arias, C., et. al., 2009, Electrochemical Incineration of Cresols: A Comparative Study between PbO2 and Boron-Doped Diamond Anodes, Chemosphere, Vol. 74, P. 1340–1347.

ASTM D 1252-00, Chemical Oxygen Demand (Dichromate Oxygen Demand) of Water, Test Method B.

Azni Idris and Katayon Saed, 2003, Posible Utilization of Silica gels for removal of pHenol from aqueous solutions, Journal of The Environmentalist, Vol. 23, 4, P 329-334.

Azni Idris and Katayon Saed, 2002, Degradation of Phenol in wastewater using anolyte generated from electrochemical generation of brine solution, Global Nest: The International Journal, Vol. 4, and No. 2- 3, P 39-144.

Baba, H., et al., 2002, Role of Nitrogen on the Corrosion Behavior of Austenitic Stainless Steels, Corrosion Science, Vol. 44, P. 2393 – 2407.

Baba, H., Katada, Y., 2006, Effect of Nitrogen on Crevice Corrosion in Austenitic Steel, Corrosion Science, Vol. 48, P. 2510 – 2524.

Bala Srinivasan, P., et al., 2006, An Assessment of Impact Strength and Corrosion Behavior of Shielded Metal Arc Welded Dissimilar Weldments Between UNS 31803 and IS 2062 Steels, Materials & Design, Vol. 27, P. 182 – 191.

Beaudet, R., et. al., 1999, Simultaneous Removal of Phenol, Ortho- and Para-Cresol by Mixed Anaerobic Consortia, Can. J. Microbiol, Vol. 45, No. 4, P. 318–325.

Becerik, I., et al., 1999, Effect of Temperature on the Electro oxidation of Some Organic Molecules on Pt Doped Conducting Polymer Coated Electrodes, Turk J Chem, Vol. 23, P. 353 – 359.

Betova, I., et al., 2002, Influence of the Electrolyte Composition and Temperature on the Transpassive Dissolution of Austenitic Stainless Steels in Simulated Bleaching Solutions, Electrochimica Acta, Vol. 47, P. 3335 – 3349

.

Blunt, L., Ramasawmy, H., 2002, 3D Surface Characteristic of Electropolished EDMed Surface and Quantitative Assessment of Process Variables Using Taguchi Methodology, International Journal of Machine Tools & Manufacture, Vol. 42, P. 1129 – 1133.

Bocea, G., et. al., 2005, Use of Dimensionally Stable Anodes for the Electrochemical Treatment of Textile Wastewaters, Chem. Bull. "POLITEHNICA" Univ. (Timişoara), Vol. 50, No. 64, P. 1-2.

Bonfatti, F., et al., 2000, Anodic Mineralization of Organic Substrates in Chloride-Containing Aqueous Media, Electrochimica Acta, Vol. 46, P. 305 – 314.

Brayer Y., et. al., 1988, Disturbances and Inhibitions of Biological Treatment of Wastewater from an Integrated Refinery, Wat. Sci. Tech., Vol. 20, No. 10, P. 21 – 29.

Brillas, E., et. al., 2009, Electro catalytic Properties of Diamond in the Oxidation of a Persistent Pollutant, Applied Catalysis B: Environmental, Vol. xxx, P. xxx–xxx.

Bukhari, Alaadin A., 2005, Investigation of Electrochemical Treatment Process as a novel Technology for Municipal Wastewater Reuse: A Parametric and A Kinetic Study, The Arabian Journal for Science and Engineering, Vol. 30, P. 41 – 53.

Bukhari, Alaadin A., 2007, Investigation of the Electro-Coagulation Treatment Process for the Removal of Total Suspended Solids and Turbidity from Municipal Wastewater, Bioresource Technology, Vol. xxx, P. 1 – 8.

Cabra, J.M.S., et. al.2007, Electro-Oxidation of Phenol on a New Type of Zeolite/GrapHite Biocomposite Electrode with Horseradish Peroxidase, Journal of Molecular Catalysis A: Chemical, Vol. 278, P. 47–52.

Cai,D., et.al., 2009, Preparation and Characterization of Ti/SnO2–Sb2O3–Nb2O5/PbO2 Thin Film as Electrode Material for the Degradation of Phenol, Journal of Hazardous Materials, Vol. 164, P. 367 – 373.

Cataldi, R.I., et al., 2005, Study of Cobalt-Based Surface Modified Glassy Carbon Electrode: Electro catalytic Oxidation of Sugars and Alditols, Electro analysis, Vol. 7, P. 3.5 – 311.

Chedeville, O., Tosun-Bayraktar, A., Porte, C., 2005, Modeling of Fenton Reaction for the Oxidation of Phenol in Water, Journal of Automated Methods and Management in Chemistry, Vol., 2: P. 31-36.

Chen, G., 2004, Electrochemical Technologies in Wastewater Treatment, Separation and Purification Technology, Vol. 38, P. 11–41.

Chen, G., et. al., 2009, Electrochemical Degradation of Bisphenol A on Different Anodes, Water Research, Vol. xxx, P. 1 – 9.

Chedeville, O., Tosun-Bayraktar, A., Porte, C., 2005, Modeling of Fenton Reaction for the Oxidation of Phenol in Water, Journal of Automated Methods and Management in Chemistry, Vol., 2: P. 31-36.

Chenlo, F., et al., 2006, Experimental Results and Modeling of the Osmotic Dehydration Kinetics of Chestnut with Glucose Solutions, Journal of Food Engineering, Vol. 74, P. 324 – 334.

Clements, J., Sato M., and Davis, R. H., 1987, IEEE Trans. Ind. Appl. IA-23, P. 224.

Cong, Y., Cheng, and Tian, T., 2005, Dechlorination by Combined Electrochemical Reduction and Oxidation, Journal of Zhejiang University SCIENCE, Vol. 6B (6), P. 563-568.

Cruz, M., et al., 2007, Electrochemical Properties of Electrodeposited Nicked PHospHide Thin Films in Lithium Cells, Journal of Power Sources, Vol. 171, P. 870 – 878.

Cummins, K., 1981, PHenol and Cresol.

Dane, T. Cestarolli, and Adalqisa, R. de Andrade, 2007, Electrochemical Oxidation of PHenol at Ti/Ru0.3Pb(0.7−x)TixOy Electrodes in Aqueous Media, Journal of Electrochemical Society, Vol. 154, Issue 2: P. E25-E30.

Davies, D.P., et al., 2000, Stainless Steel as a Bipolar Plate Material for Solid Polymer Fuel Cells, Journal of Power Sources, Vol. 86, P. 237 – 242.
de Lucas, P Cañizares, M A Rodrigo, and J García-Gómez, 2008.

Dermentzis, K., Ouzounis, K., 2008, Continuous Capacitive Deionization-Electro dialysis Reversal Through Electrostatic Shielding for Desalination and Deionization of Water, Electrochimica Acta, Vol. 53, P. 7123 – 7130.

Doh, S.J., et. al., Industrial Dye Waste-Water Treatment by Electrochemical Catalytic Process Using TiO_2/ITO Electrode.

Encyclopedia Britannica, 2009, Electrochemical Reaction, Encyclopedia Britannica Online, http://www.britannica.com/EBchecked/topic/183010/electrochemical-reaction, (Visited: 05 Nov. 2009).

Ernst, P., Newman, R.C., 2002, Pit Growth Studies in Stainless Steel Foils. II. Effect of Temperature, Chloride Concentration and SulpHate Addition, Corrosion Science, Vol. 44, P. 943 – 954.

Eyraud ,M., et. al., 2008, Electrochemical Determination of P-Cresol Concentration Using Zeolite-Mmodified Electrodes, C. R. Chimie, Vol. 11, P. 1063–1073.

Fortier, G., Belanger, D., 2004, Characterization of the Biochemical Behavior of Glucose Oxidize Entrapped in a Polypyrrole Film, Biotechnology and Bioengineering, Vol. 37, P. 854 – 858.

Fryda, M., et. al., Electrochemical Advanced Oxidation Process for Water Treatment.

Giangiacomo, R., 2006, Study of Water-Sugar Interactions at Increasing Sugar Concentration by NIR Spectroscopy, Food Chemistry, Vol. 96, P. 371 – 379.

Girija, S., et al., 2005, Determination of Corrosion Types for AISI Type 304L Stainless Steel Using Electrochemical Noise Method, Materials Science & Engineering A, Vol. 407, P. 188 – 195.

Gonzalez, I., et. al. , 2007, Electrochemical Incineration of P-Cresol and O-Cresol in the Filter-Press-Type FM01-LC Electrochemical Cell Using BDD Electrodes in Sulfate Media at pH 0, Electrochimica Acta, Vol. 52, P. 3229–3235.

Guo, Y.B., Hong, F.C., 2003, Adhesion Improvements for Diamond-like Carbon Films on Polycarbonate and Polymethylmethacrylate Substances by Ion Plating with Inductively Coupled Plasma, Diamond and Related Materials, Vol. 12, P. 946 – 952.

Herrero, A., et. al., 2001, Soft Calibration in a Flow System with Electrochemical Detection Application to the Determination of PHenolic Compounds, Analytica Chimica Acta, Vol. 446, P. 269–279.

Hocking, M.G., Moussa, S.O., 2001, The PHoto-Inhibition of Localized Corrosion of 304 Stainless Steel in Sodium Chloride Environment, Corrosion Science, Vol. 43, P. 2037 – 2047.

Hsien, Tzu-yang, Lin, Yen-Hui, 2005, Biodegradation of PHenolic Wastewater in a Fixed Biofilm Reactor, Chemical Engineering Journal, Vol. 27: P. 95–103.

J.A. Winters, "Method Research Study 3, Demand Analysis, An Evaluation of Analytical Methods for Water and Wastewater," USEPA (1971).

Jiang, Y., Wen, J.P., Li, H.M., Yang, S.L., Hu, Z.D., 2005, The Biodegradation of PHenol at High Concentration by the yeast Candida tropicalis, Biochem. Een. J. Vol. 24: P. 243–247.

Jiazhen, Z. et. al., 2007, Experimental and Simulation Study on the Extraction of P-Cresol Using Centrifugal Extractors, Chin. J. Chem. Eng., Vol. 15, No. 2, P. 209-214.

Joshi, A., Locke, B., Arce, P., and Finney W., 2006, Hazard Waste Hazard Mater, Vol. 41: P. 3.

Kavitha V., Palanivelu K., 2005, Destruction of Cresols by Fenton Oxidation Process, Water Research, Vol. 39, P. 3062–3072.

Kim, H.J., et al., Remote Voltage Generation Through Sono- Electrochemical Process on Platinum Surface, Electrochemistry Communications, Vol. 8, P. 801 – 806.

Kish, J.R., et al., 2003, Anodic Behavior of Stainless Steel S43000 in Concentrated Solutions of SulpHuric Acid, Corrosion Science, Vol. 45, P. 1571 – 1594.

Laborde, J.L., et. al., 2008, Sonoelectro-Fenton Process: A Novel Hybrid Technique for the Destruction of Organic Pollutants in Water, Journal of Electro analytical Chemistry, Vol. 624, P. 329–332.

Le Bozac, N., et al., 2001, Influence of Stainless Steel Surface Treatment on the Oxygen Reduction Reaction in Seawater, Corrosion Science, Vol. 43, P. 765 – 786.

Li X.Y., Cui Y.H., Feng Y.J., Xie, Z.M., Gu J.D., 2005, Reaction Pathways and Mechanisms of the Electrochemical Degradation of PHenol on Different Electrodes, Water Research, Vol 39: P. 1972-1981.

Liu, D., et al., 2007, Elecro-Spark Deposition of Fe-Based AmorpHous Alloy Coatings, Materials Letters, Vol. 61, P. 165 – 167.

Luo, J.L., Yang, Q., 2001, Effects of Hydrogen and Tensile Stress on the Breakdown of Passive Films on Type 304 Stainless Steel, Electrochimica Acta, Vol. 46, P. 851 – 859.

N.B. Tahar and A. Savall, 1998, Mechanistic Aspects of PHenol Electrochemical Degradation by Oxidation on a Ta/PbO2 Anode, Journal of the Electrochemical Society, Vol. 145 (10), P. 3427-3434.

N.B. Tahar and A. Savall, 1999, J. Appl. Electrochem., Vol. 29, P. 277.

Ochoa , F.G., et. al. 2006, Wet Oxidation of PHenol, Cresols and NitropHenols Catalyzed by Activated Carbon in Acid and Basic Media, Applied Catalysis B: Environmental, Vol. 65, P. 269–281.

Ozyilmaz, A.T., et al., 2006, The Corrosion Behaviours of Polyaniline Coated Stainless Steel in Acidic Solutions, Thin Solid Films, Vol. 496, P. 431 – 437.

Pacheco, M. J., Mor˜ao, A., Lopes, A., Cir´ıaco, L., Goncalves, I., 2007, Degradation of PHenols Using Boron-doped Diamond Electrodes: A method for quantifying the extent of combustion, Electrochimica Acta, Vol. 53: P. 629–636.

Palanivelu, K., Rajkumar, D., 2003, Electrochemical Degradation of Cresols for Wastewater Treatment, Ind. Eng. Chem. Res., Vol. 42, No.9, P. 1833–1839.

Palanivelu, K., Rajkumar, D., 2004, Electrochemical Treatment of Industrial Wastewater, Journal of Hazardous Materials, Vol. B113, P. 123–129.

Palanivelu, K., Rajkumar, D., 2005, Destruction of Cresols by Fenton Oxidation Process, Water Research, Vol. 39, P. 3062–3072.

Pasic, A., et al., 2006, Fiber-Optic Flow-Through Sensor for Online Monitoring of Glucose, Analytical & Bioanalytical Chemistry, Vol. 326, P. 1618 – 2642.

Piccardo, P., et al., 2007, ASR Evaluation of Different Kinds of Coatings on a Ferritic Stainless Steel as SOFG Interconnects, Surface & Coatings Technology, Vol. 202, P. 1221 – 1225.

Pontolio, J.O., et al., 2005, Preparation and Characterization of Electrochemically Modified Electrodes Containing the Metal Complexion Moiety Quinolin-8-ol Anchored to the Polymeric Film, Journal of Electro analytical Chemistry, Vol. 584, P. 124 – 130.

Prasad, G.R., et al., 2005, PECVD of Biocompatible Coatings on 316L Stainless Steel, Surface & Coatings Technology, Vol. 200, P. 1031 – 1035.

Ren, Y.J., Zeng, C.L., 2008, Effect of Conducting Composite Polpyrrole/Polyaniline Coating on the Corrosion Resistance of Type 304 Stainless Steel for Bipolar Plates of Proton-Exchange Membrane Fuel Cells, Journal of Power Sources, Vol. 182, P. 524 – 530.

Rico, V., et al., 2006, Effect of Visible Light on the Water Contact Angles on Illuminated Oxide Semiconductors other than TiO2, Solar Energy Materials & Solar Cells, Vol. 90, P. 2944 – 2949.

Rubin, A., et al., 2008, Impedance Characterization of the Electrochemical Environment Under a Polymer Film Artificially delaminated, Electrochimica Acta, Vol. 53, P. 6484 – 6488.

Rucinskiene, A., et al., 2002, Magnetic Field Effect on Stainless Steel Corrosion in FeCl3 Solution, Electrochemistry Communications, Vol. 4, P. 86 – 91.

Shumyantseva, V.V., et al., 2006, A New Format o Electrodes for the Electrochemical Reduction of Cytochromes P450, Journal of Inorganic Biochemistry, Vol. 100, P. 1353 – 1357.

Siddiqui, M., A., 2006, Treatment of Simulated Petrochemical Wastewater by Means of Continuous Electrocoagulation-Ultrefiltration Process, M. S. Thesis, Civil Engineering Department, King Fahd University of Petroleum & Minerals.

Tezuka, M., Tomizawa, S., 2006, Oxidative Degradation of Aqueous Cresols Induced by Gaseous Plasma with Contact Glow Discharge Electrolysis, Plasma Chemistry and Plasma Processing, Vol. 26, No. 1, P. 43 – 52.

USEPA Methods for Analysis of Waters & Wastes , method 410.4 (1983).

Van Hege, K., e al., 2004, Electrode-Oxidative Abatement of Low-Salinity Reverse Osmosis Membrane Concentrates, Water Research, Vol. 38, P. 1550 – 1558.

Wang, J., and Farrell, J., 2004, Electrochemical Inactivation of Triclosan with Boron Doped Diamond Film Electrodes, Department of Chemical and Environmental Engineering, University of Arizona, Environmental Science & Technology, Vol. 38: NO. 19, P. 5232-5237.

Wilde, C.P., Zhang, M., 1992, Oxidation of Glucose at Electrodeposited Platinum Electrodes, Journal of Electro analytical Chemistry, Vol. 340, P. 241 – 255.

Xuejun Chen1, Zhemin Shen1*, Xiaolong Zhu2, Yaobo Fan2, and Wenhua Wang1, 2005, Advanced treatment of textile wastewater for reuse using electrochemical oxidation and membrane filtration, Journal of Water SA, Vol. 31 No. 1, P. 0378-4738.

Y.H. Wanga, K.Y. Chana, X.Y. Lib, and S.K. Soc, 2006, Electrochemical degradation of 4-chloropHenol at nickel–antimony doped tin oxide electrode, Journal of ChemospHere, Vol. 65, Issue 7, P. 1087-1093.

Yagan, A., et al., 2008, Poly (N-Ethyl aniline) Coatings on 304 Stainless Steel for Corrosion Protection in Aqueous HCI and NaCL Solutions, Electrochimica Acta, Vol. 53, P. 2474 – 2482.

Yan, M., Tsair, F., Chih, H., Jui, C., Feng, M. H., 2007, Degradation of PHenol and TCE using Suspended and Chitosan-Bead Immobilized Pseudomonas Putida, Journal of Hazardous Materials, Vol. 148: P. 660–670.

Yao, S., et al., 1974, De-ureation by Oxidation, Bioelectrochemistry and Bioenergetics, Vol. 1, P. 180 – 186.

You, T., et al., 2002, Characterization and Electrochemical Properties of High Dispersed Copper Oxide/Hydroxide Nanoparticles in GrapHite-like Carbon Films Prepared by RF Sputtering Method, Electrochemistry Communications, Vol. 4, P. 468 – 471.

Zhang, H., and George A., S., 2005, Electrochemical Process for Oxidative Destruction of 4-ChloropHenol, Civil & Environmental Engineering, University of Cincinnati.

Zhao, L., et al., 2007, Analysis of SEI Formed with Cyano-Containing Imidazolium-Based Ionic Liquid Electrolyte in Lithium Secondary Batteries, Journal of Power Sources, Vol. 174, P. 352 – 358.

Zhong, L., et al., 2006, A Passivation Mechanism of Doped Polyaniline on 410 Stainless Steel in Deaerated H2SO4 Solution, Electrochimica Acta, Vol. 51, P. 5494 – 5501.

Zhu, H., et al., 2004, Accelerating Effect and Mechanism of Passivation of Polyniline on Ferrous Metals, Electrochimica Acta, Vol. 49, P. 5161 – 5166.

Zou, Y., et al., An Electroless Plating Film of Palladium on 304 Stainless Steel and its Excellent Corrosion Resistance, Thin Solid Films, Vol. 516, P. 7565 – 7570.

Zou, Y., et al., An Electroless Plating Film of Palladium on 304 Stainless Steel and its Excellent Corrosion Resistance, Thin Solid Films, Vol. 516, P. 7565 – 7570.

VITA

EDUCATION

Master of Science in Civil Engineering, King Fahd University Of Petroleum & Minerals, may 2010. Dhahran, Saudi Arabia.

Major: Environmental Engineering; Minor: Water Resources

Bachelor of Science in Civil Engineering

Rome University 1980

1975 to 1980	Bachelor in civil Engineering -Transportation (December 1980) *ROME University ITALY*
1974 to 1975	University of Italian language *Perugia, Italy*
1962 to 1974	Scientific school degree(1974) *Naquora, Jordan*

PERSONAL INFORMATION & ADDRESS

Name: Mufid Abu-Eideh
Nationality: Jordan
Date of Birth: 1954
Work address: Ameron Saudi Arabia
P.O.Box 589
Dammam - 31421
Saudi Arabia
Telephone : - 0096638471500 ext/1331
Mobile : - 00966-504818925

Permanent address: Jordan-Amman
Aljubaheh –Jordan University Street
Telephone : - 0096265161217

Email :- mufidabueideh@Gmail.com